Characterizing the charm-quark showering and hadronization via charm-jet studies with ALICE

Preeti Dhankher
On behalf of the ALICE collaboration
University of California, Berkeley

BEACH 2024

06/03/2024

Jet probe a wide range of Q^2

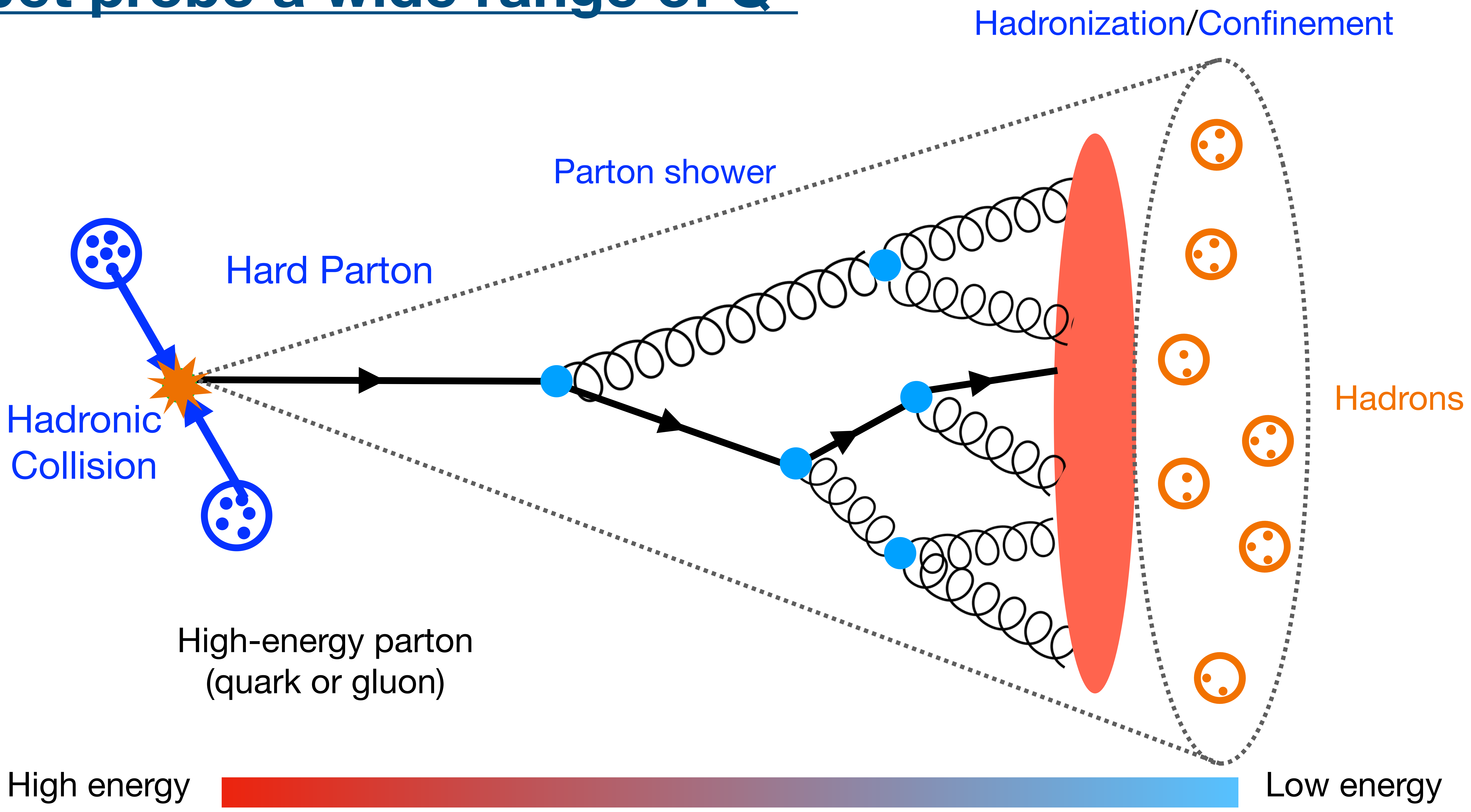

Flavor dependence in the QCD shower

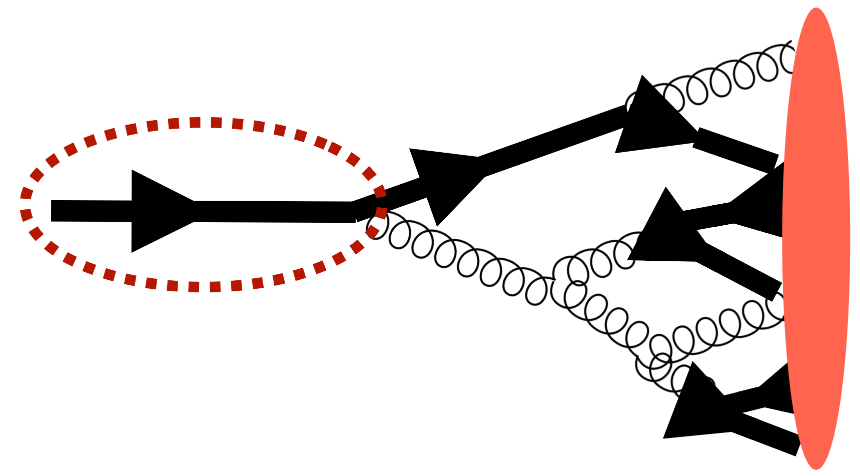

Gluon-initiated shower

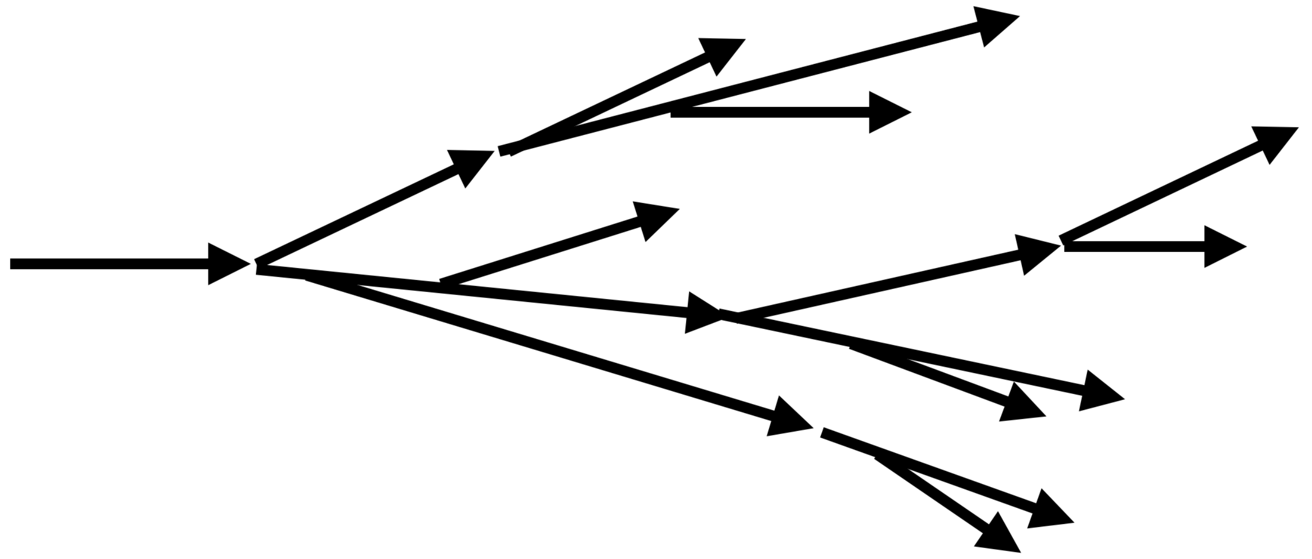

Quark-initiated shower

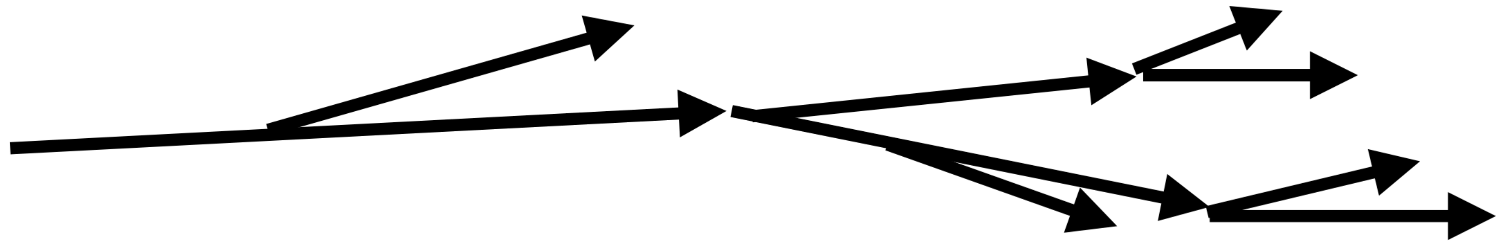

$$\frac{C_A}{C_F} = \frac{9}{4}$$

Casimir color factors

Gluon-initiated showers are expected to have a broader and softer fragmentation profile than quark-initiated showers

Flavor dependence in the QCD shower

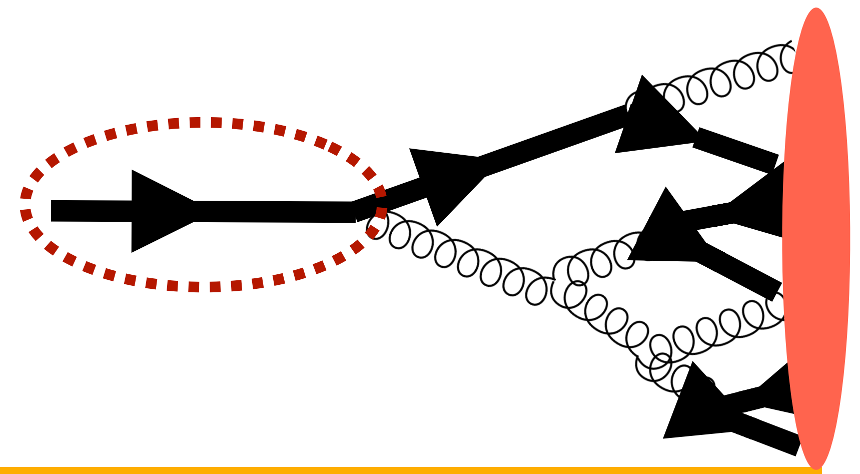

Gluon-initiated shower | **Quark-initiated shower** | **Heavy-quark-initiated shower**

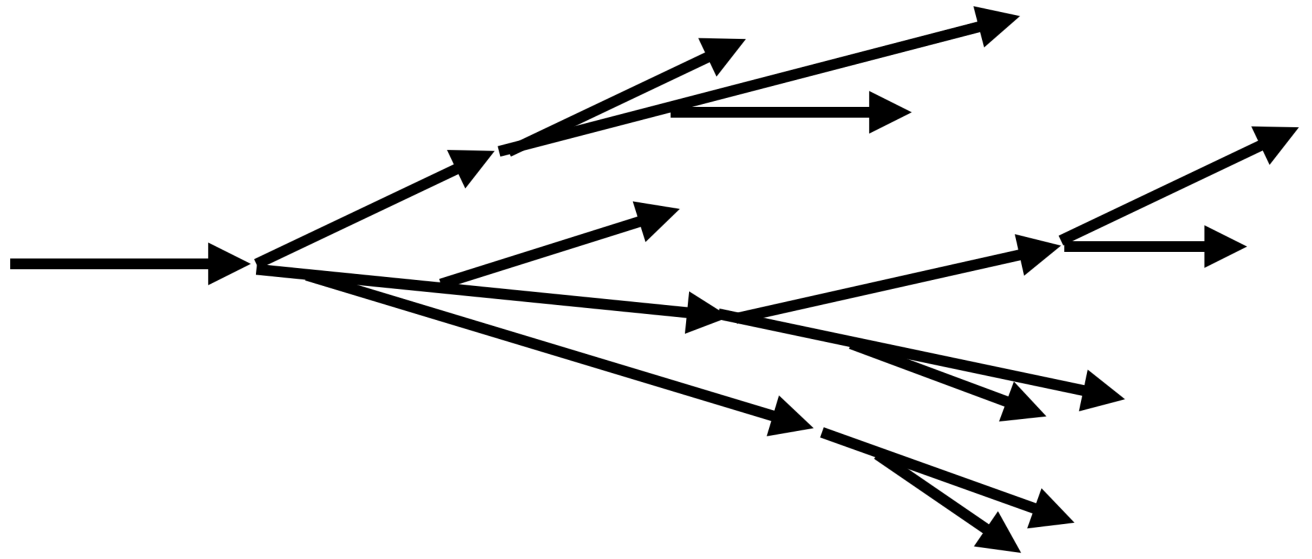

$$\frac{C_A}{C_F} = \frac{9}{4}$$

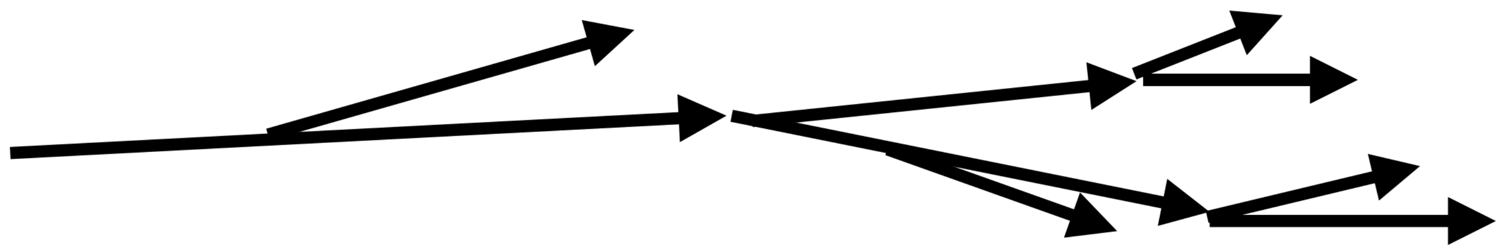

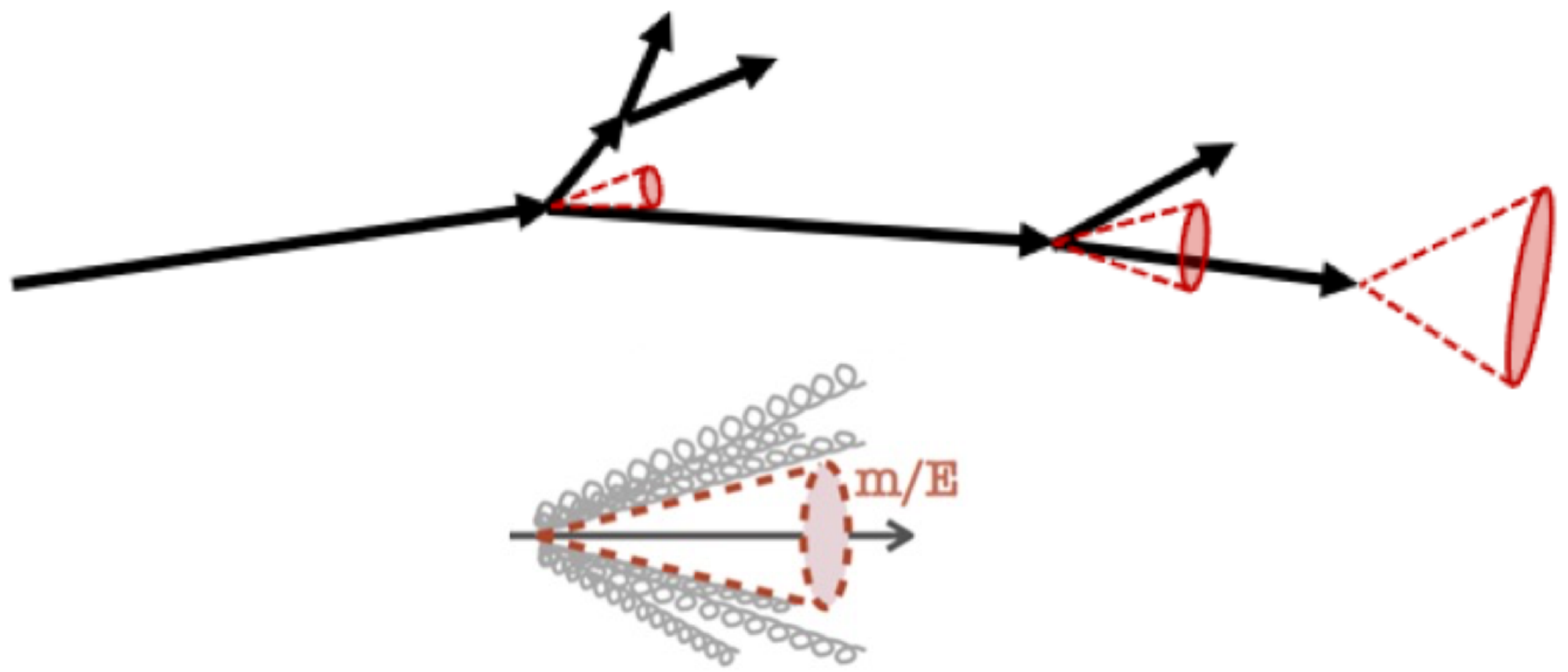

Casimir color factors

Gluon-initiated showers are expected to have a broader and softer fragmentation profile than quark-initiated showers

Mass effects

A harder fragmentation is expected in low energy heavy-quark initiated showers due to the presence of the dead-cone effect

Flavor dependence in the QCD shower

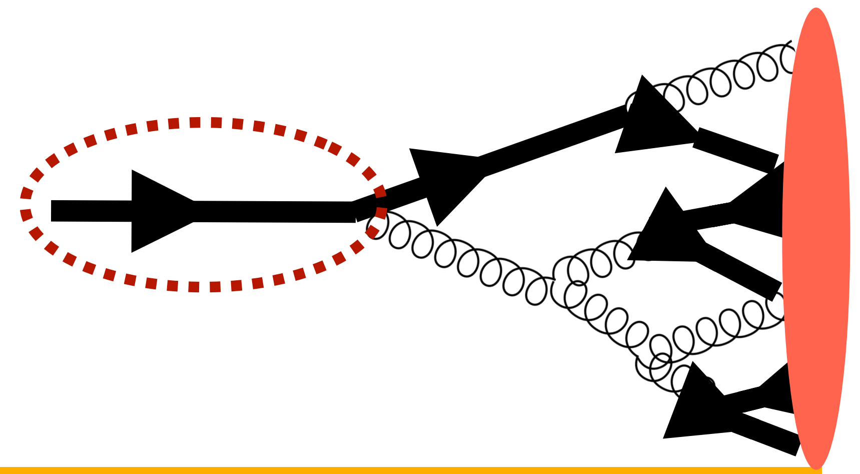

Gluon-initiated shower | **Quark-initiated shower** | **Heavy-quark-initiated shower**

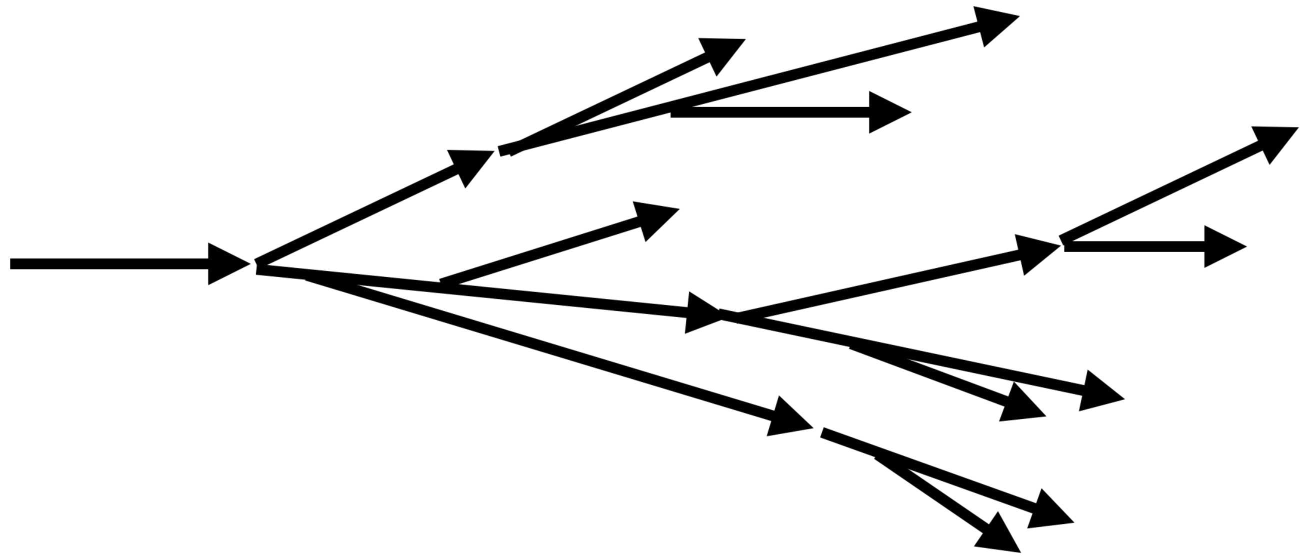

$$\frac{C_A}{C_F} = \frac{9}{4}$$

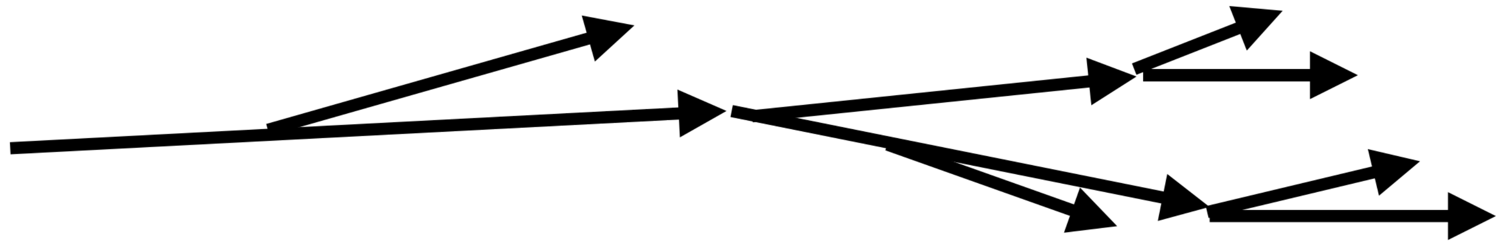

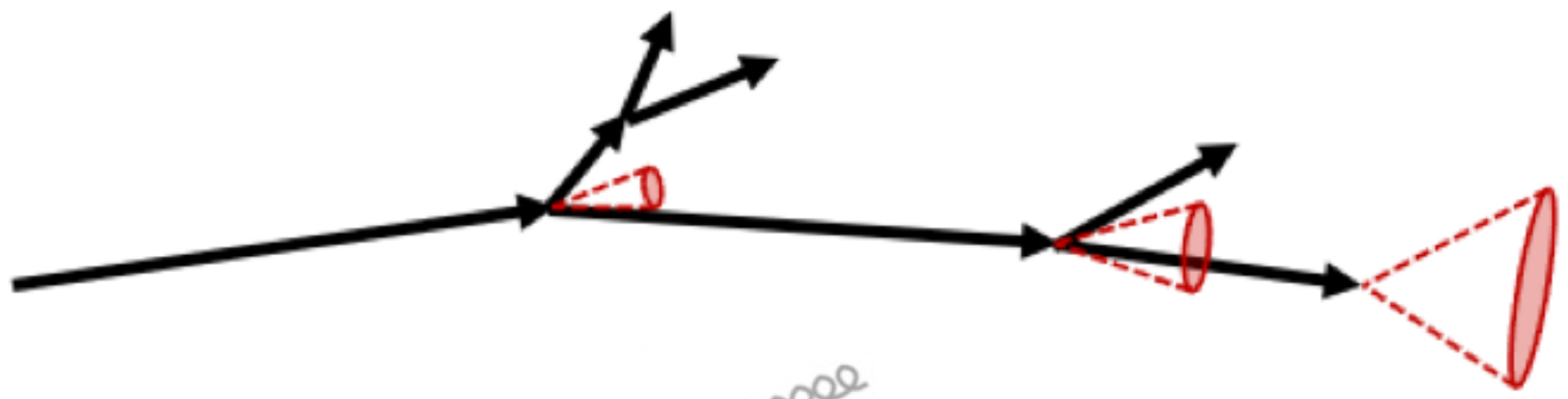

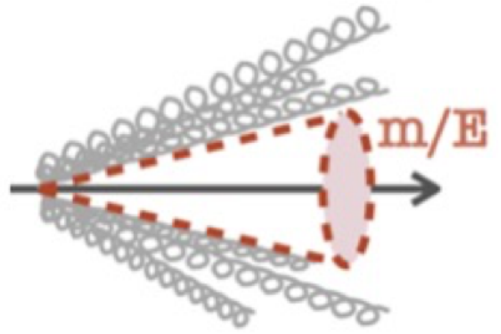

Casimir color factors

Gluon-initiated showers are expected to have a broader and softer fragmentation profile than quark-initiated showers

Mass effects

A harder fragmentation is expected in low energy heavy-quark initiated showers due to the presence of the dead-cone effect

Mass effects are dominant at low p_T

$$\theta_c \sim \frac{m_Q}{E}$$

A Large Ion Collider Experiment

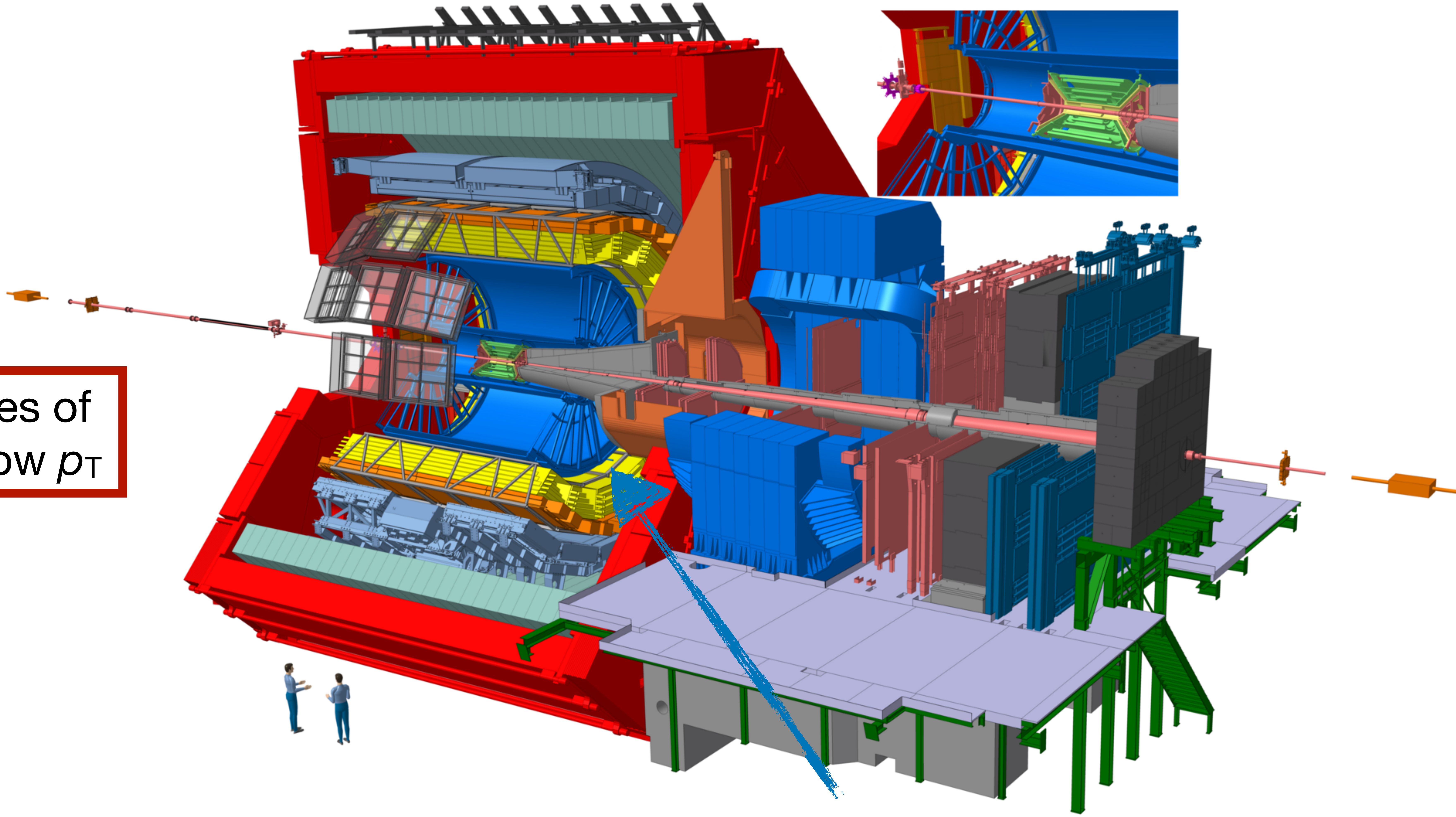

ALICE has excellent capabilities of heavy-flavor physics down at low p_T

A Large Ion Collider Experiment

Time-Of-Flight (TOF):
PID via time of flight

ALICE has excellent capabilities of heavy-flavor physics down at low p_T

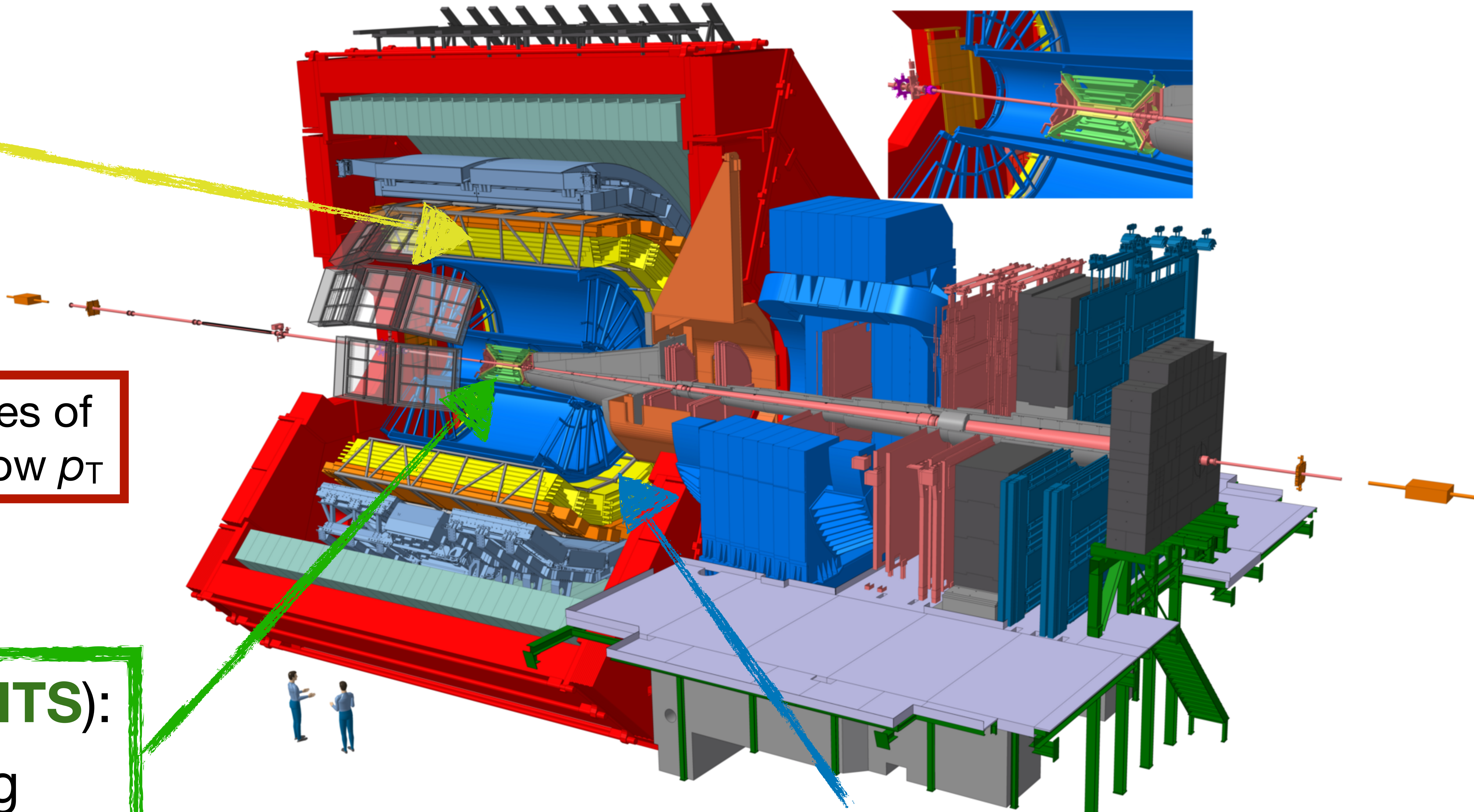

Inner Tracking System (ITS):
tracking and vertexing

Time Projection Chamber (TPC):
tracking and PID via dE/dx

Charm-jet tagging with ALICE

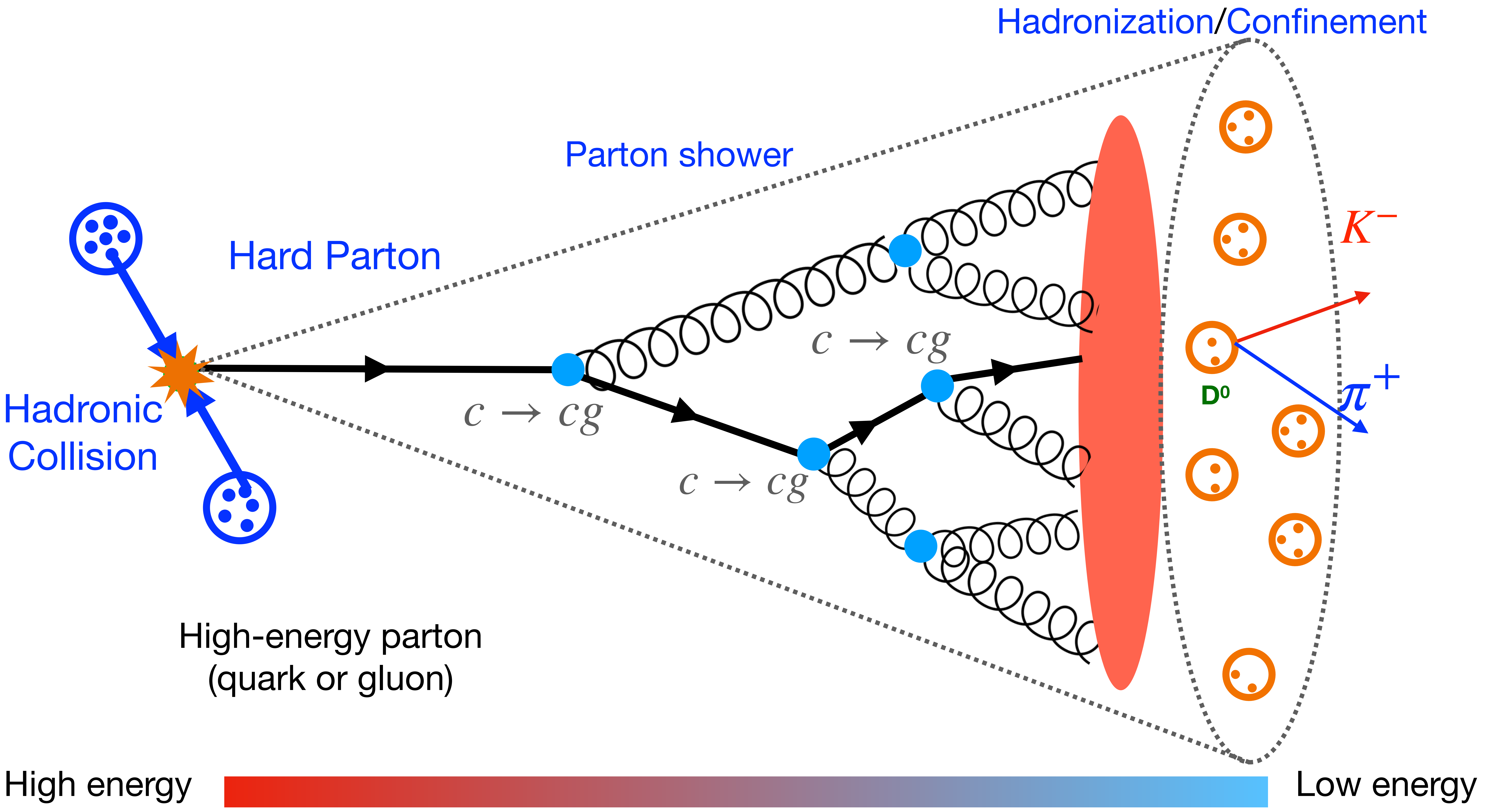

Charm-jet tagging with ALICE

1. Charm meson(D^0)/baryon(Λ_c^+) reconstruction and selection by topological cuts and PID on decay daughters.

$$D^0 \rightarrow K^- + \pi^+$$

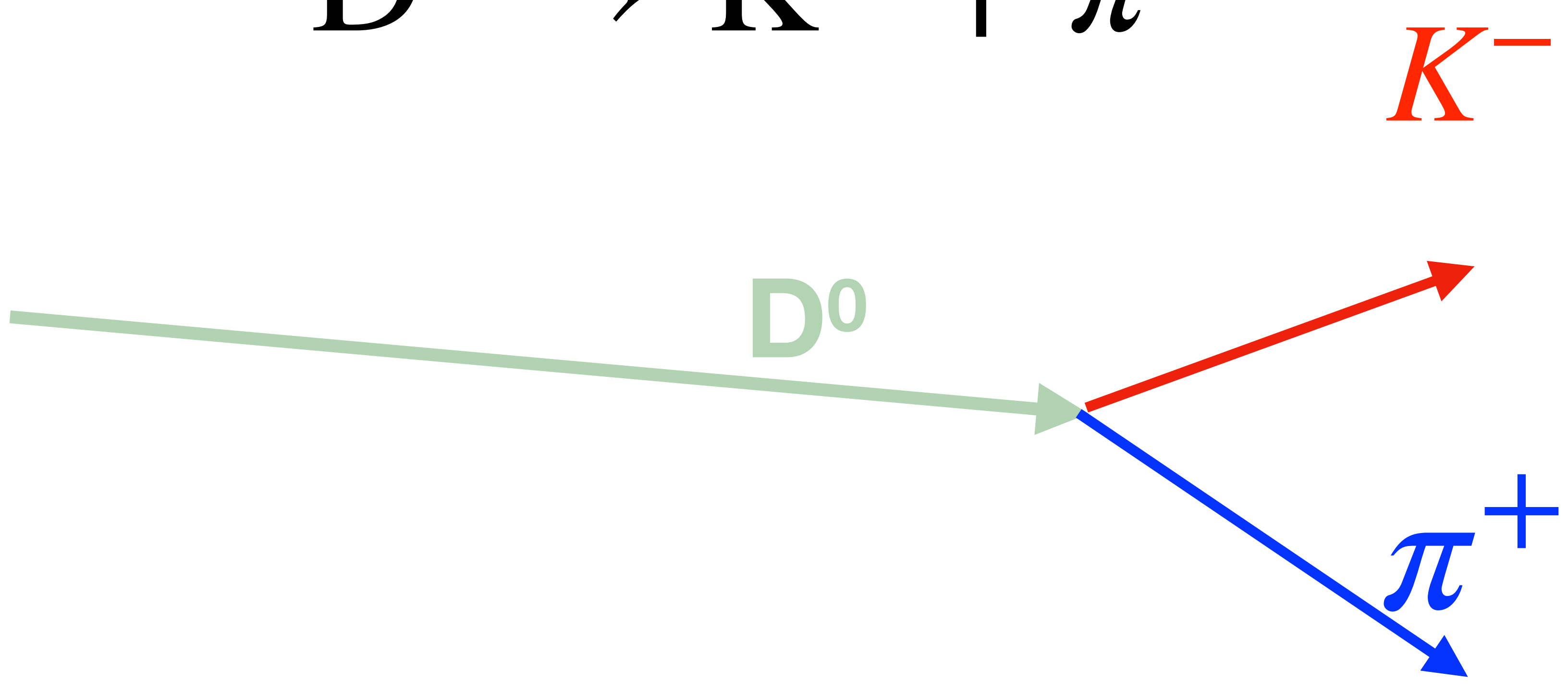

$$\Lambda_c^+ \rightarrow p + K_s^0$$

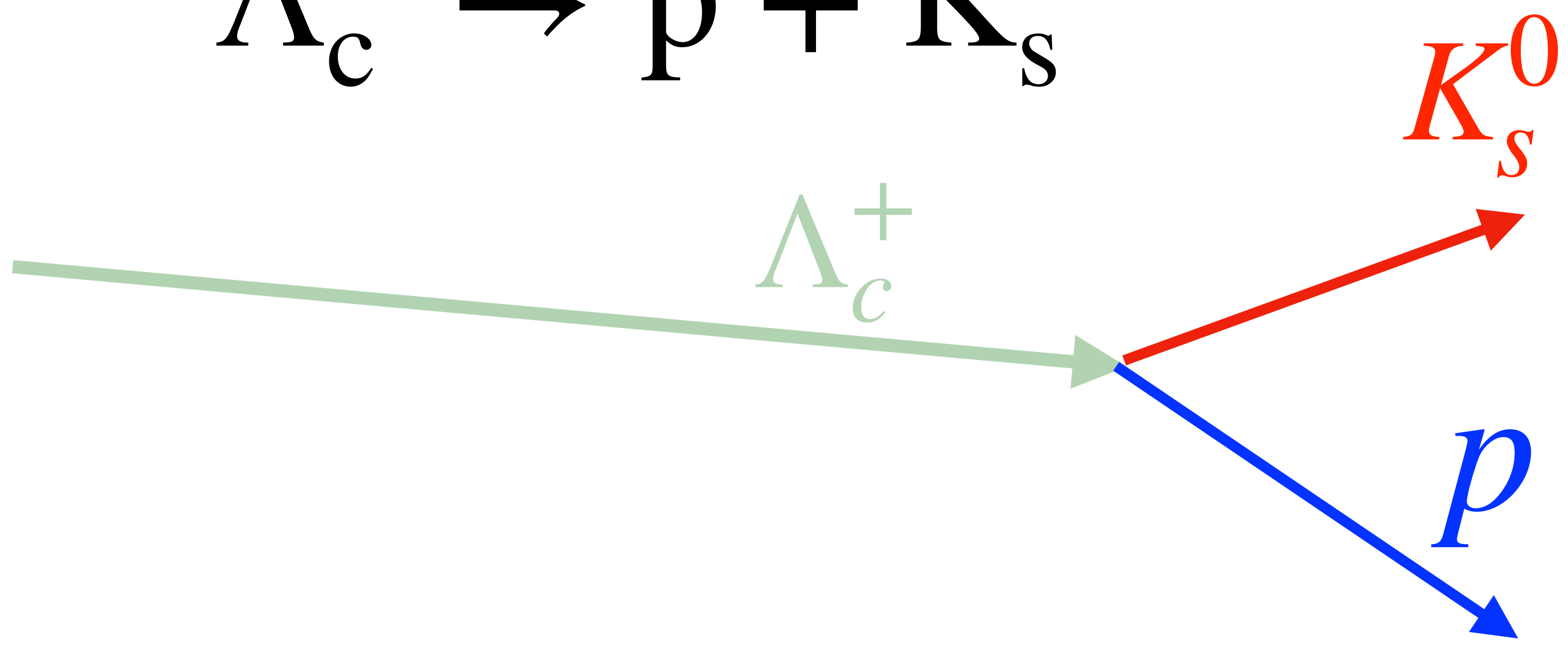

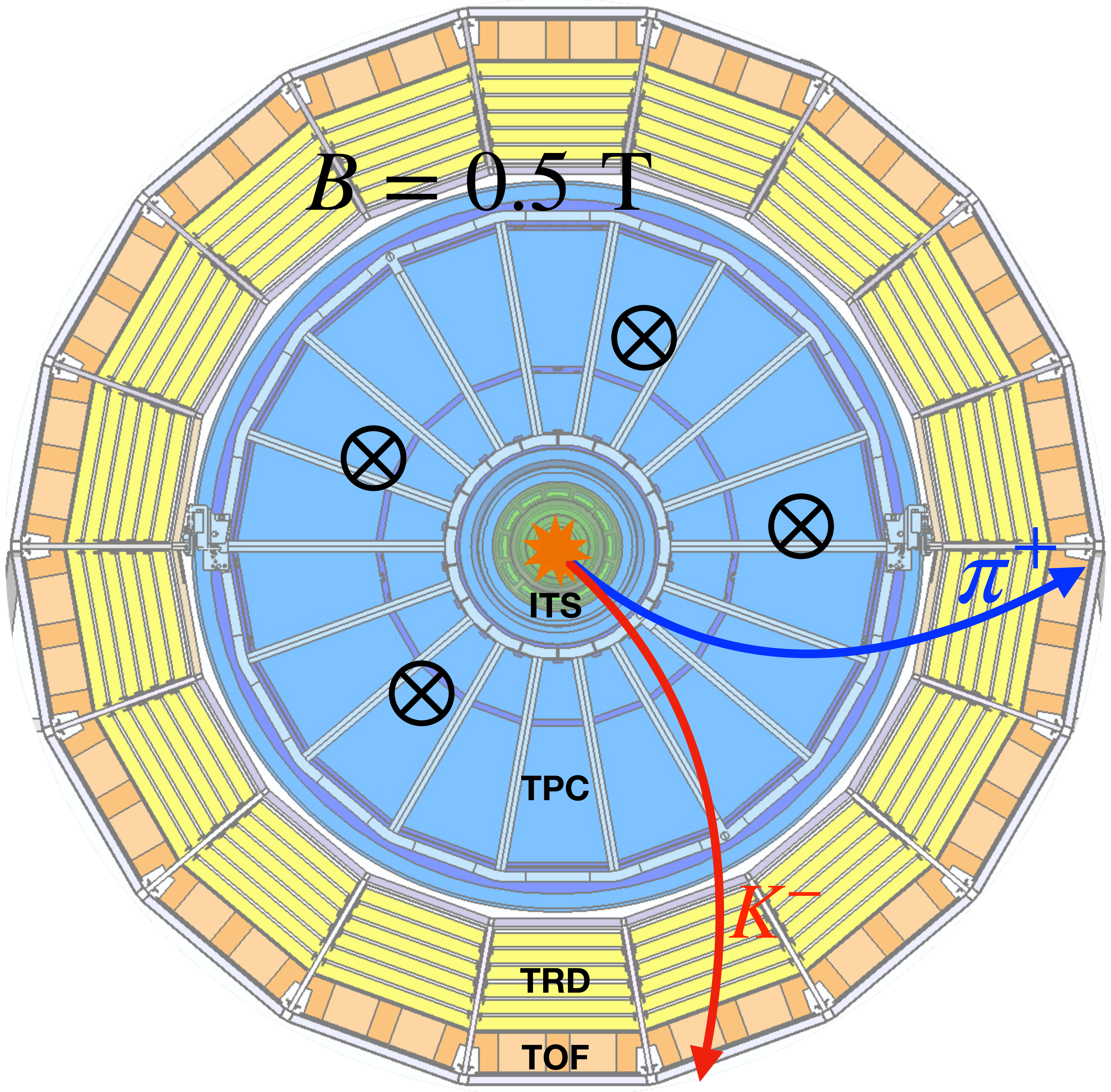

Charm-jet tagging with ALICE

1. Charm meson(D^0)/baryon(Λ_c^+) reconstruction and selection by topological cuts and PID on decay daughters.

$$D^0 \rightarrow K^- + \pi^+$$

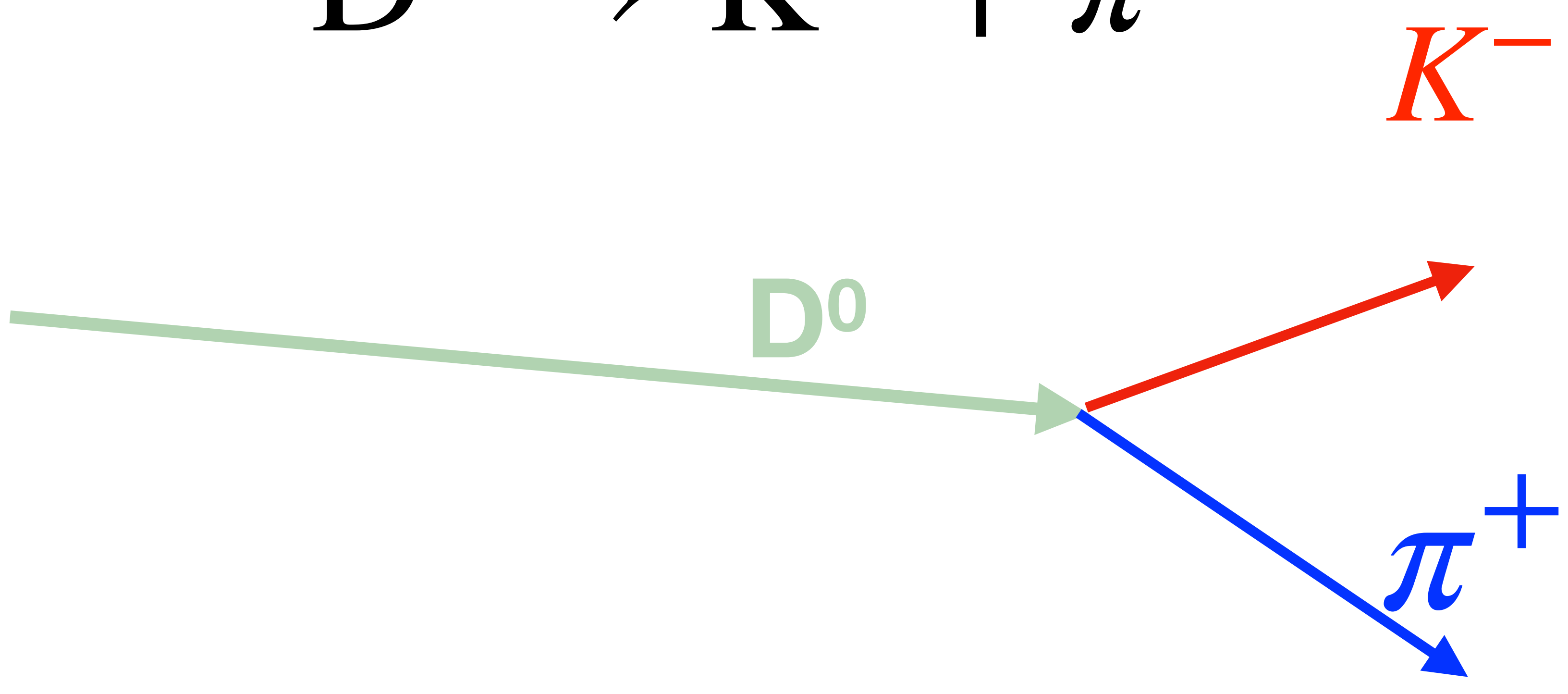

$$2 \leq p_{T,D^0} \leq 36 \text{ GeV}/c$$

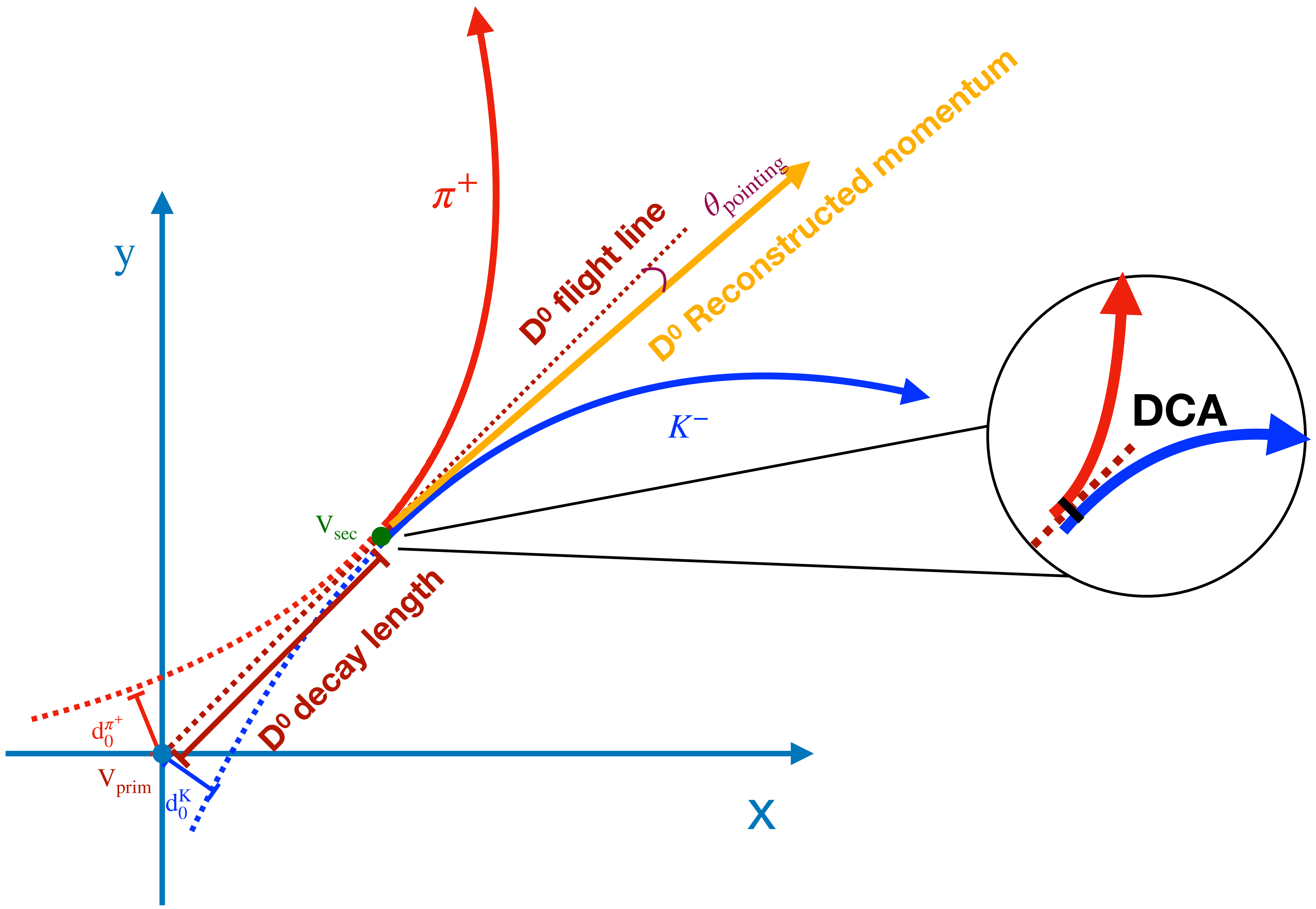

Charm-jet tagging with ALICE

1. Charm meson(D^0)/baryon(Λ_c^+) reconstruction and selection by topological cuts and PID on decay daughters.
2. Charm-tagged jet reconstruction using anti-k_T algorithm.

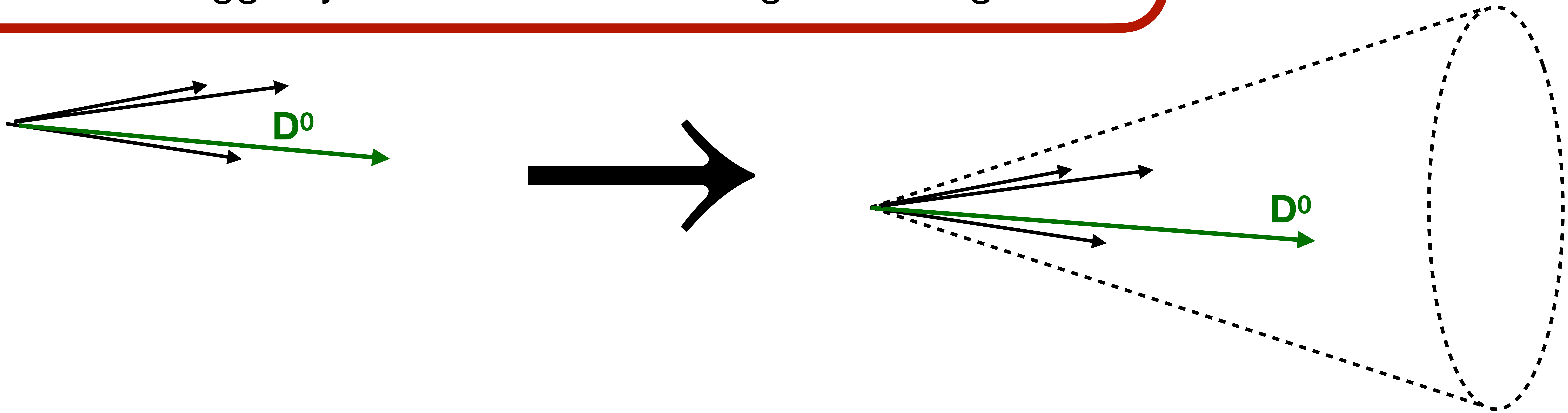

$2 \leq p_{T,D^0} \leq 36$ GeV/c

$5 \leq p_{T,\text{ch. jet}} \leq 50$ GeV/c

Charm-jet tagging with ALICE

1. Charm meson(D^0)/baryon(Λ_c^+) reconstruction and selection by topological cuts and PID on decay daughters.
2. Charm-tagged jet reconstruction using anti-k_T algorithm.
3. Subtract combinatorial background from fake daughter pairs using sideband subtraction technique in invariant mass distribution.

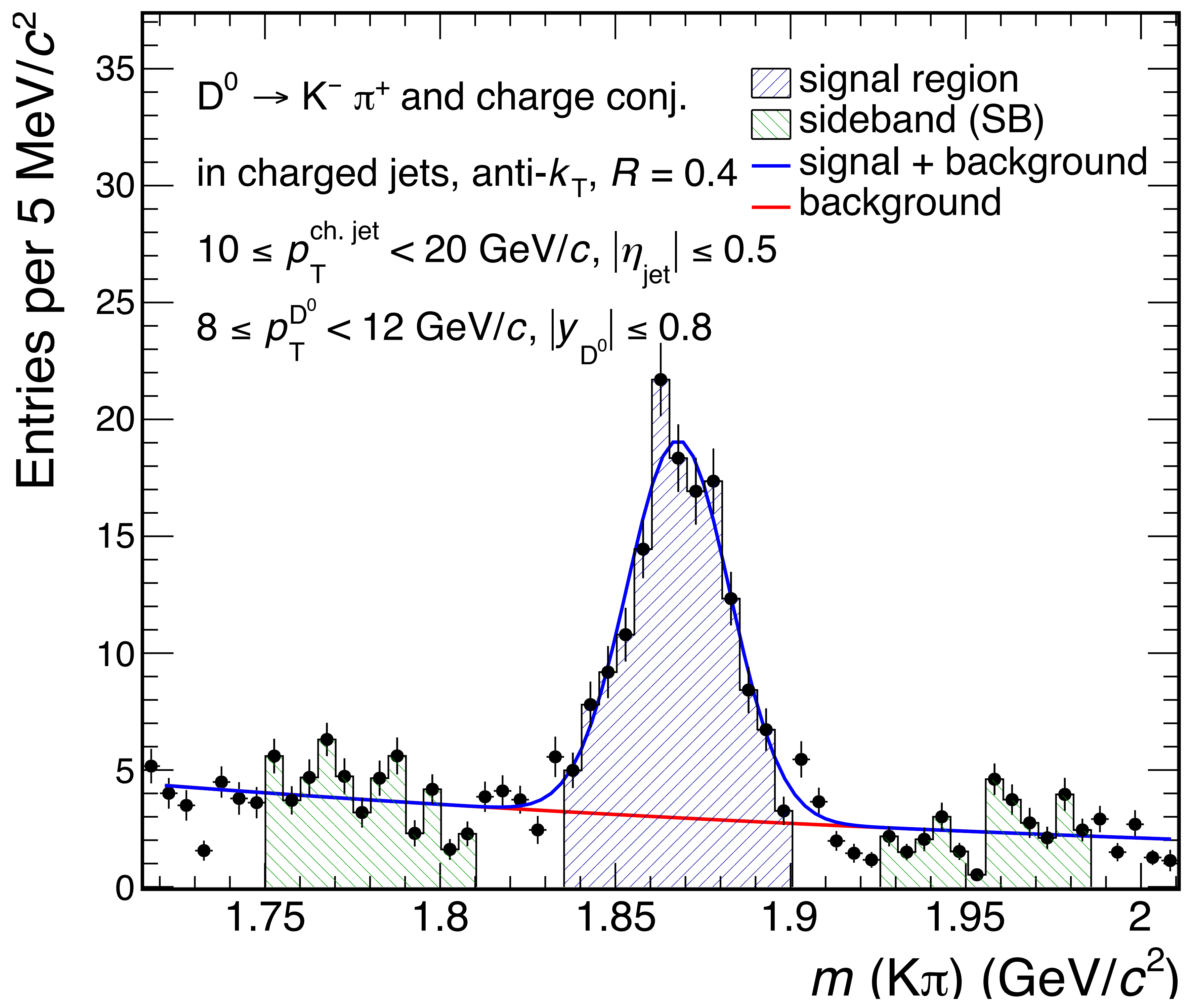

Charm-jet tagging with ALICE

1. Charm meson(D^0)/baryon(Λ_c^+) reconstruction and selection by topological cuts and PID on decay daughters.
2. Charm-tagged jet reconstruction using anti-k_T algorithm.
3. Subtract combinatorial background from fake daughter pairs using sideband subtraction technique in invariant mass distribution.

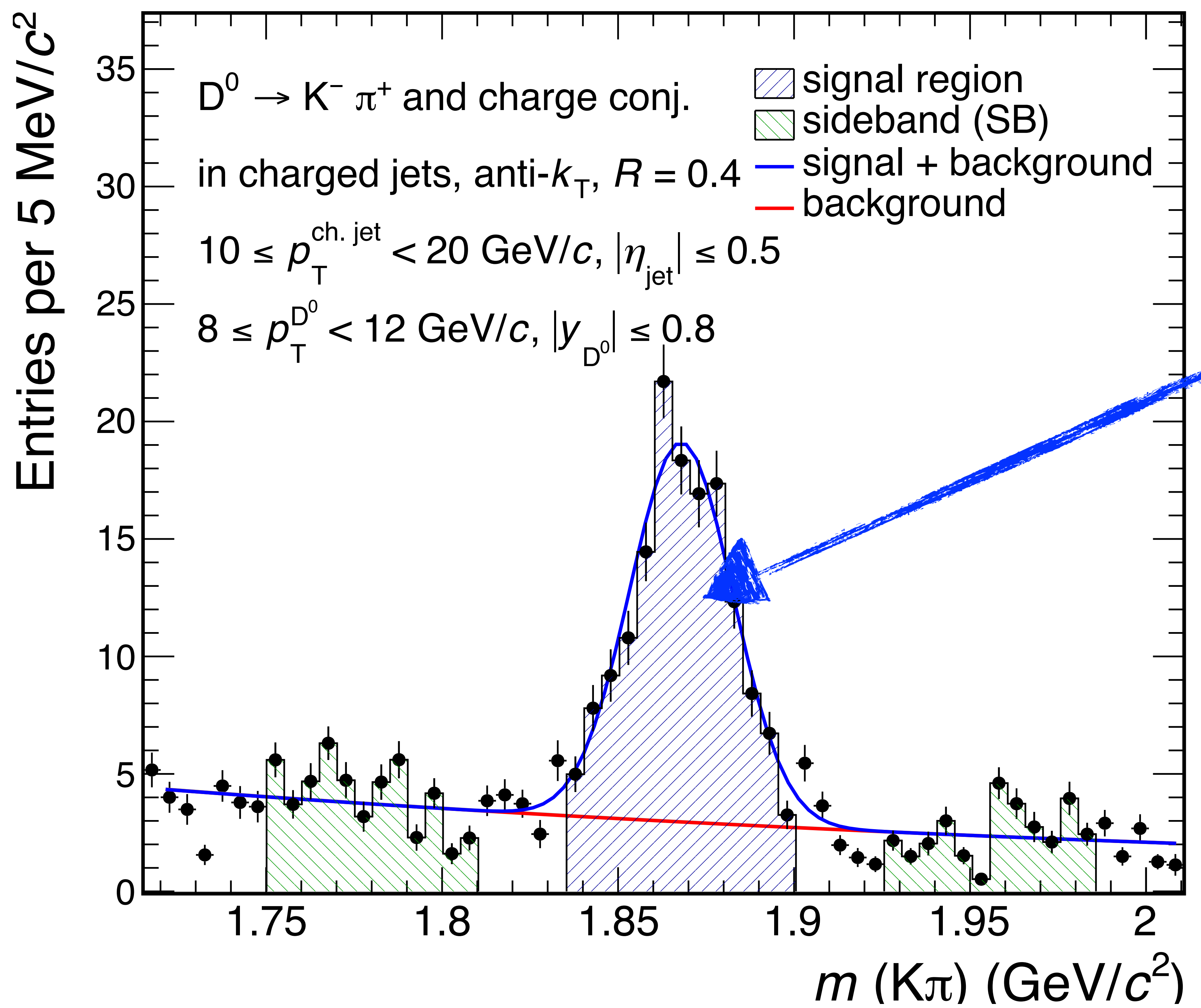

Signal region

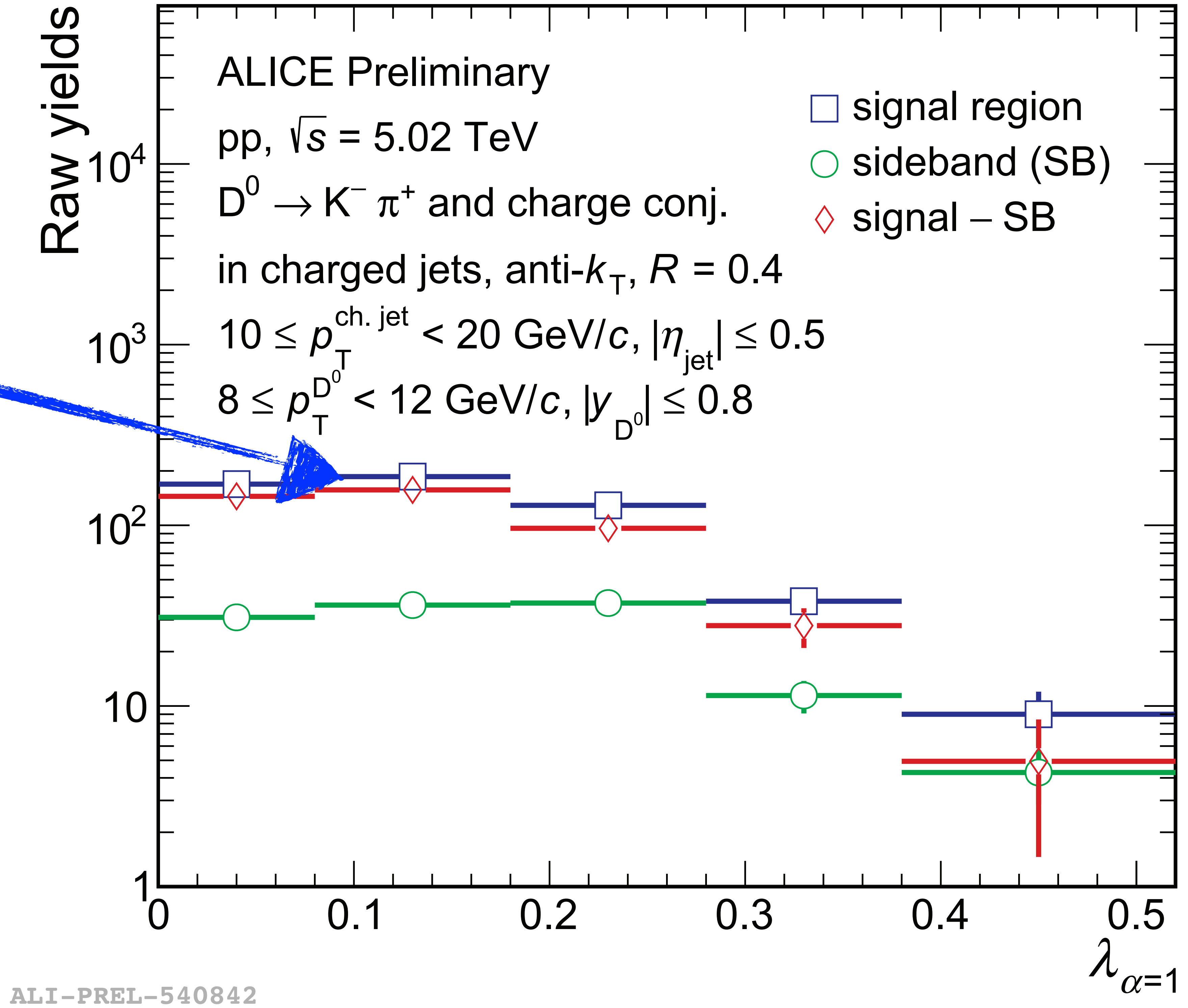

Charm-jet tagging with ALICE

1. Charm meson(D^0)/baryon(Λ_c^+) reconstruction and selection by topological cuts and PID on decay daughters.
2. Charm-tagged jet reconstruction using anti-k_T algorithm.
3. Subtract combinatorial background from fake daughter pairs using sideband subtraction technique in invariant mass distribution.

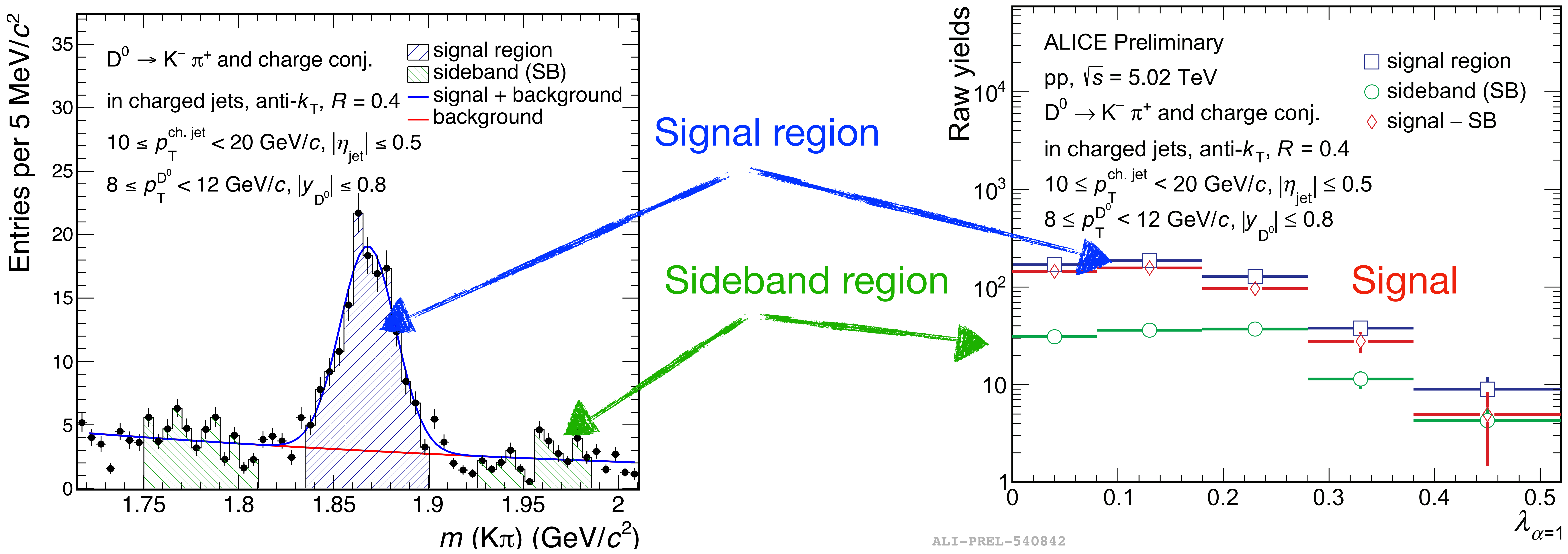

Charm-jet tagging with ALICE

1. Charm meson(D^0)/baryon(Λ_c^+) reconstruction and selection by topological cuts and PID on decay daughters.
2. Charm-tagged jet reconstruction using anti-k_T algorithm.
3. Subtract combinatorial background from fake daughter pairs using sideband subtraction technique in invariant mass distribution.
4. Efficiency correction: Charm(D^0/Λ_c^+)-tagged jet reconstruction efficiency correction

Charm-jet tagging with ALICE

1. Charm meson(D⁰)/baryon(Λ_c^+) reconstruction and sele
   and PID on decay daughters.
2. Charm-tagged jet reconstruction using anti-k_T algorith
3. Subtract combinatorial background from fake daughte
   subtraction technique in invariant mass distribution.

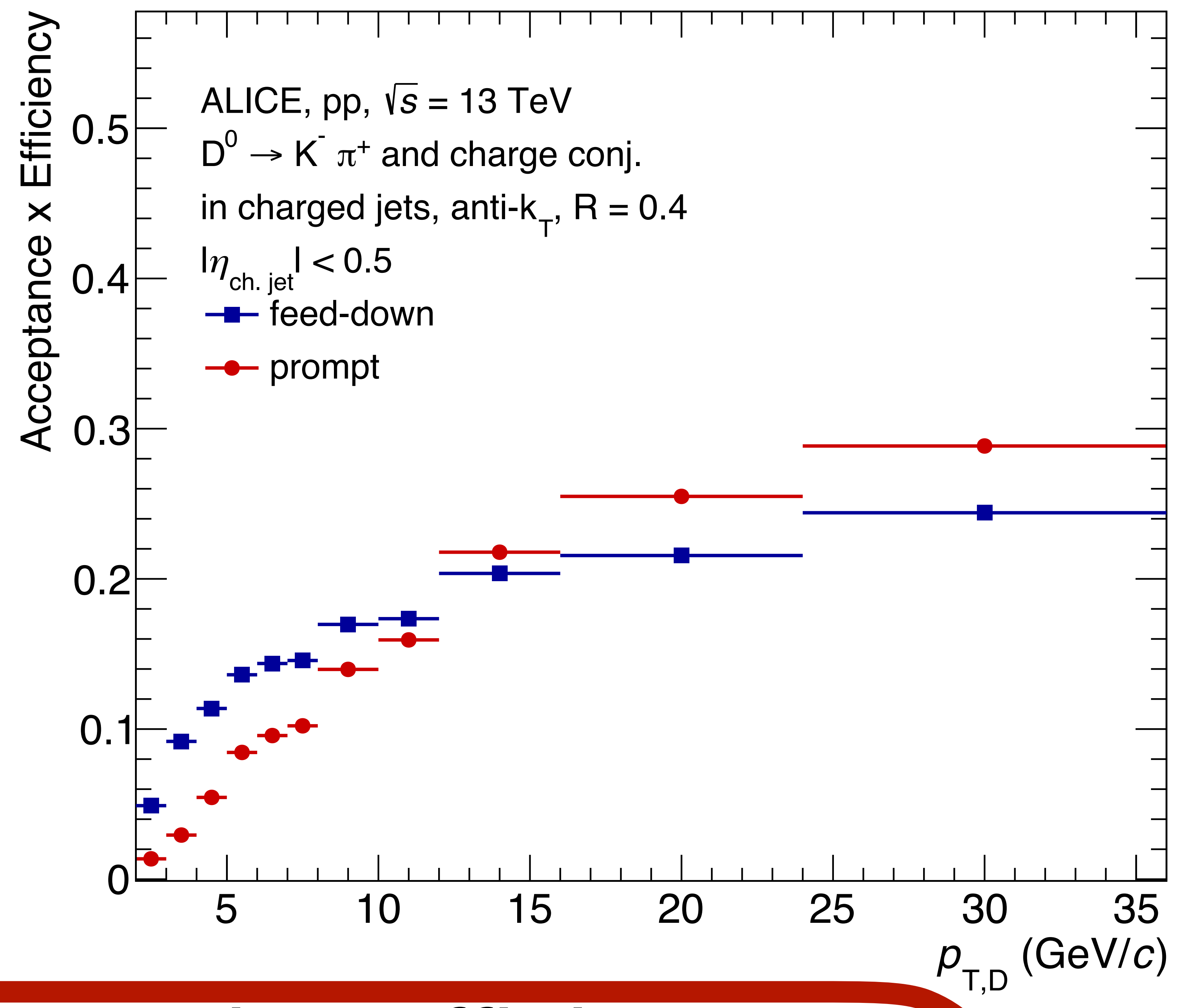

4. Efficiency correction: Charm(D^0/Λ_c^+)-tagged jet reconstruction efficiency correction

- Efficiency of the D^0 cut selections is strongly dependent on D^0-meson p_T
- sideband-subtracted distributions are corrected by the D^0 reconstruction and selection efficiency in narrow D^0 p_T intervals

Charm-jet tagging with ALICE

1. Charm meson(D^0)/baryon(Λ_c^+) reconstruction and selection by topological cuts and PID on decay daughters.
2. Charm-tagged jet reconstruction using anti-k_T algorithm.
3. Subtract combinatorial background from fake daughter pairs using sideband subtraction technique in invariant mass distribution.
4. Efficiency correction: Charm(D^0/Λ_c^+)-tagged jet reconstruction efficiency correction
5. Estimating B $\rightarrow D^0/\Lambda_c^+$ decays: Evaluate and subtract feed-down contribution using POWHEG + PYTHIA simulations

Contribution from $\mathrm{B} \rightarrow \mathrm{D}^0$ decays: Feed-down

$$N^{c\to D^0}(p_{T,ch\ jet}^{det}) = N_{raw}^{c}(p_{T,ch\ jet}^{det}) - N^{b\to D^0}(p_{T,ch\ jet}^{det})$$

Prompt D^0

Non-prompt D^0

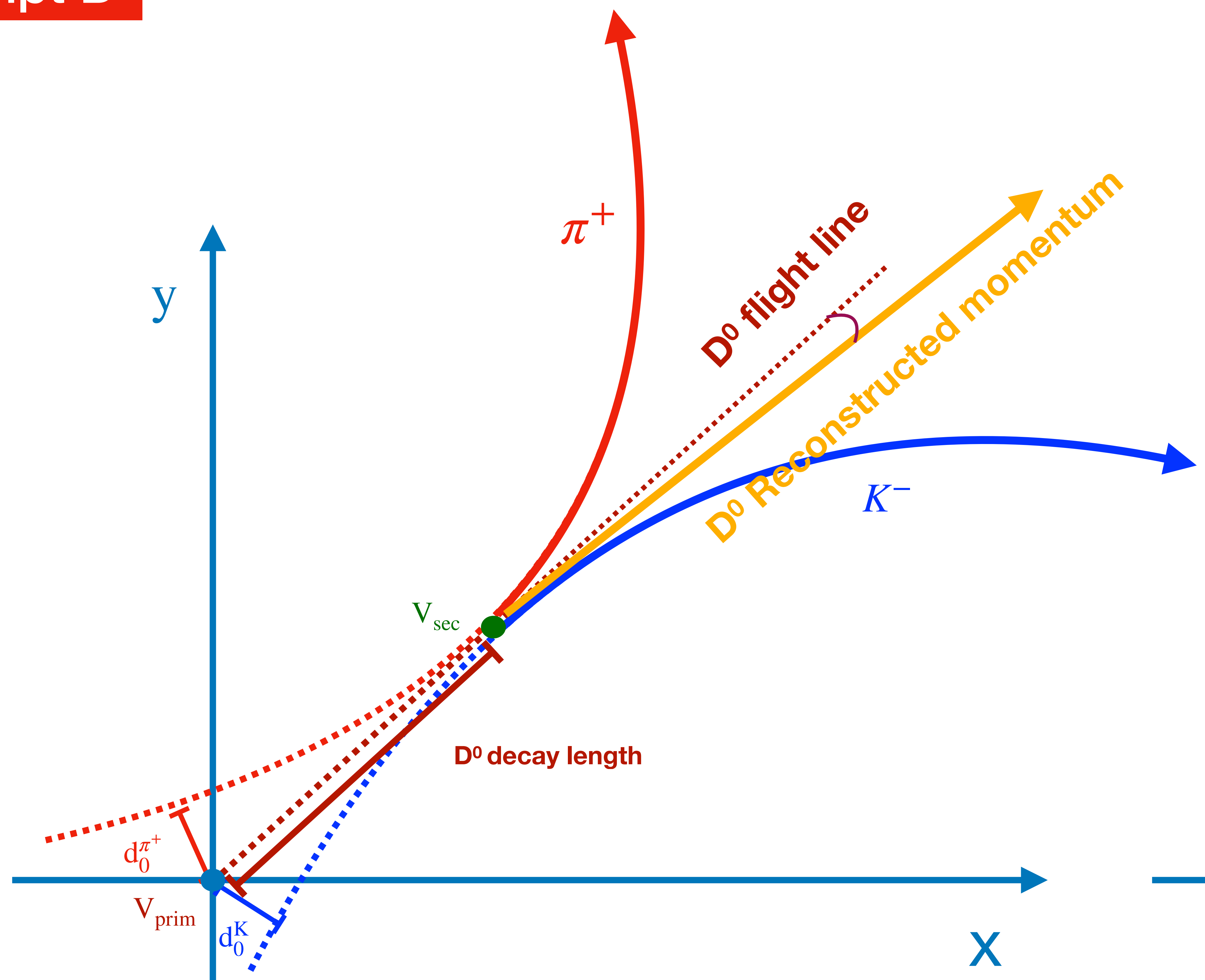

Prompt D^0 meson
(initiated by a scattered
charm quark)

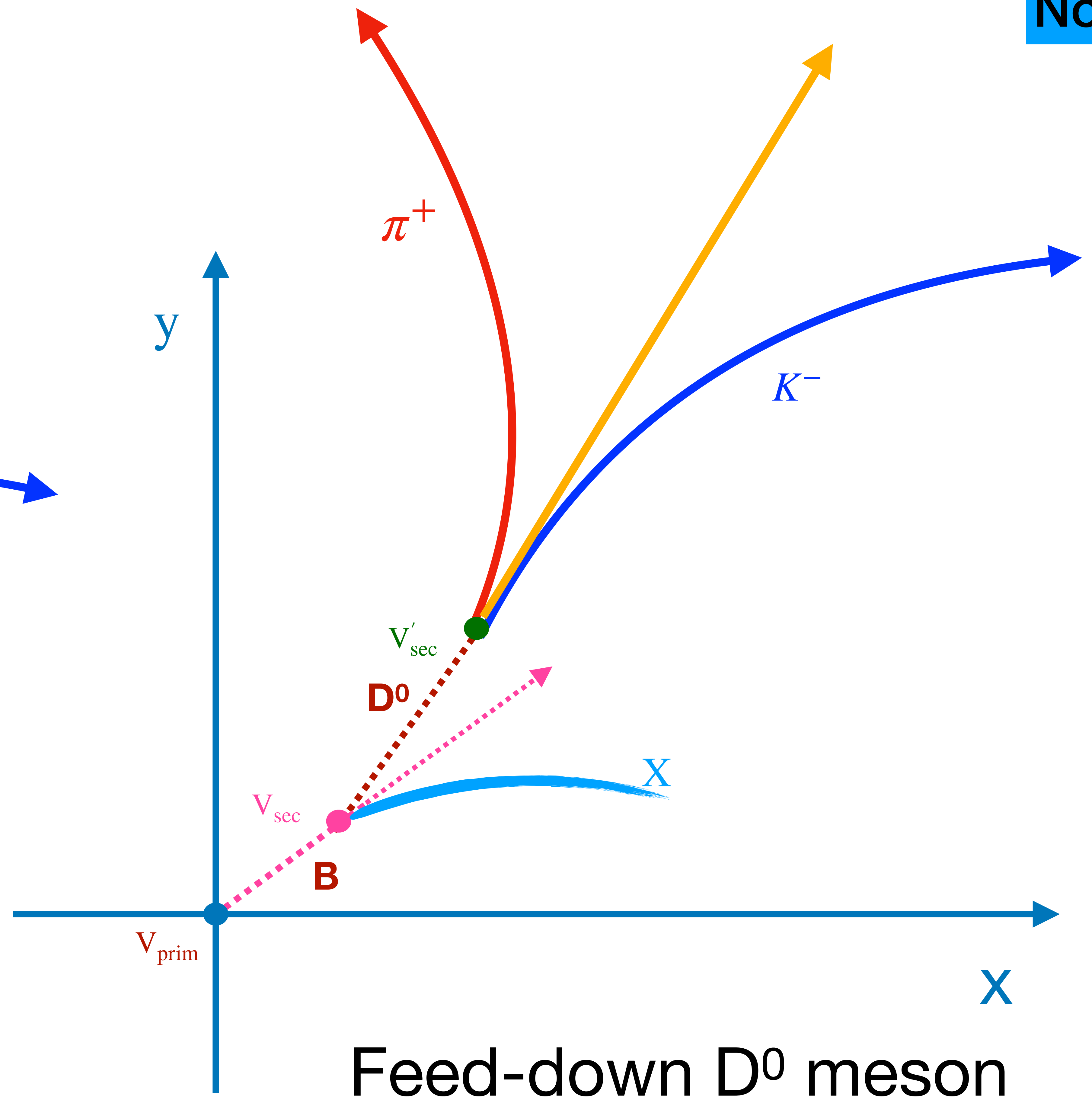

Feed-down D^0 meson
(initiated by a scattered
beauty quark)

Charm-jet tagging with ALICE

1. Charm meson(D^0)/baryon(Λ_c^+) reconstruction and selection by topological cuts and PID on decay daughters.
2. Charm-tagged jet reconstruction using anti-k_T algorithm.
3. Subtract combinatorial background from fake daughter pairs using sideband subtraction technique in invariant mass distribution.
4. Efficiency correction: Charm(D^0/Λ_c^+)-tagged jet reconstruction efficiency correction
5. Estimating $B \rightarrow D^0/\Lambda_c^+$ decays: Evaluate and subtract feed-down contribution using POWHEG + PYTHIA simulations
6. Detector effects correction: Correcting for detector effects using unfolding

Results

Jet axes distribution

Jet Angularities

Groomed z_g and R_g

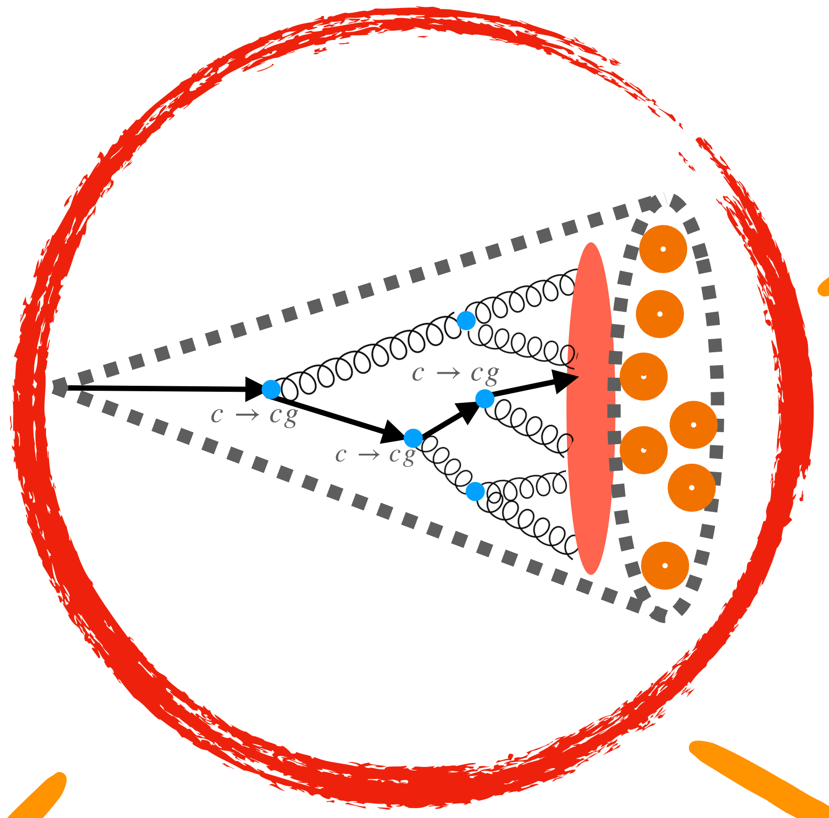

Dead-Cone Effect

Fragmentation function $z_{\parallel}$

Results

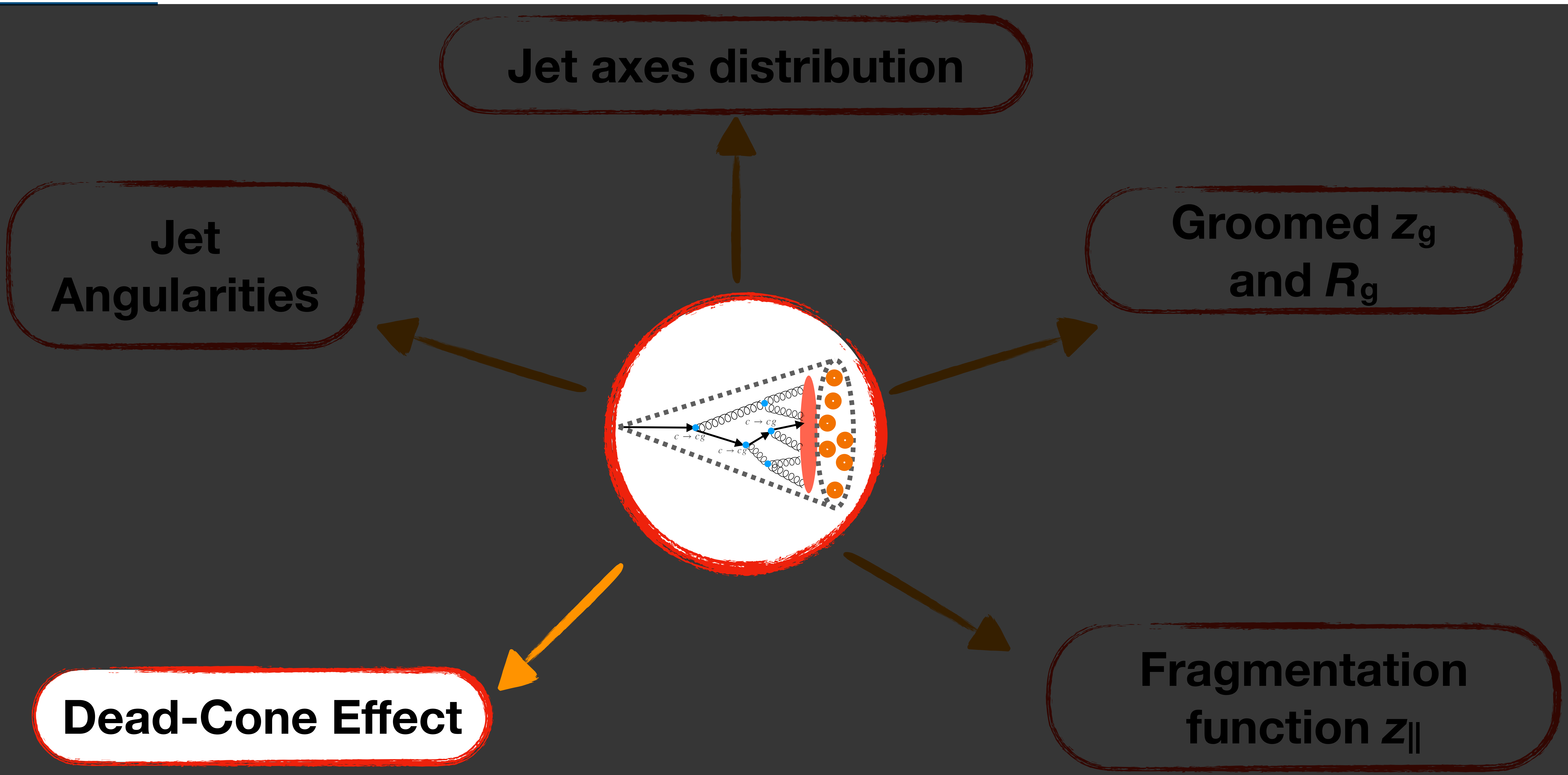

Jet axes distribution
Jet Angularities
Groomed z_g and R_g
Dead-Cone Effect
Fragmentation function $z_{||}$

First direct observation of dead-cone effect

Challenges of Measurement:

- Determining the dynamic direction of heavy-quark throughout the shower

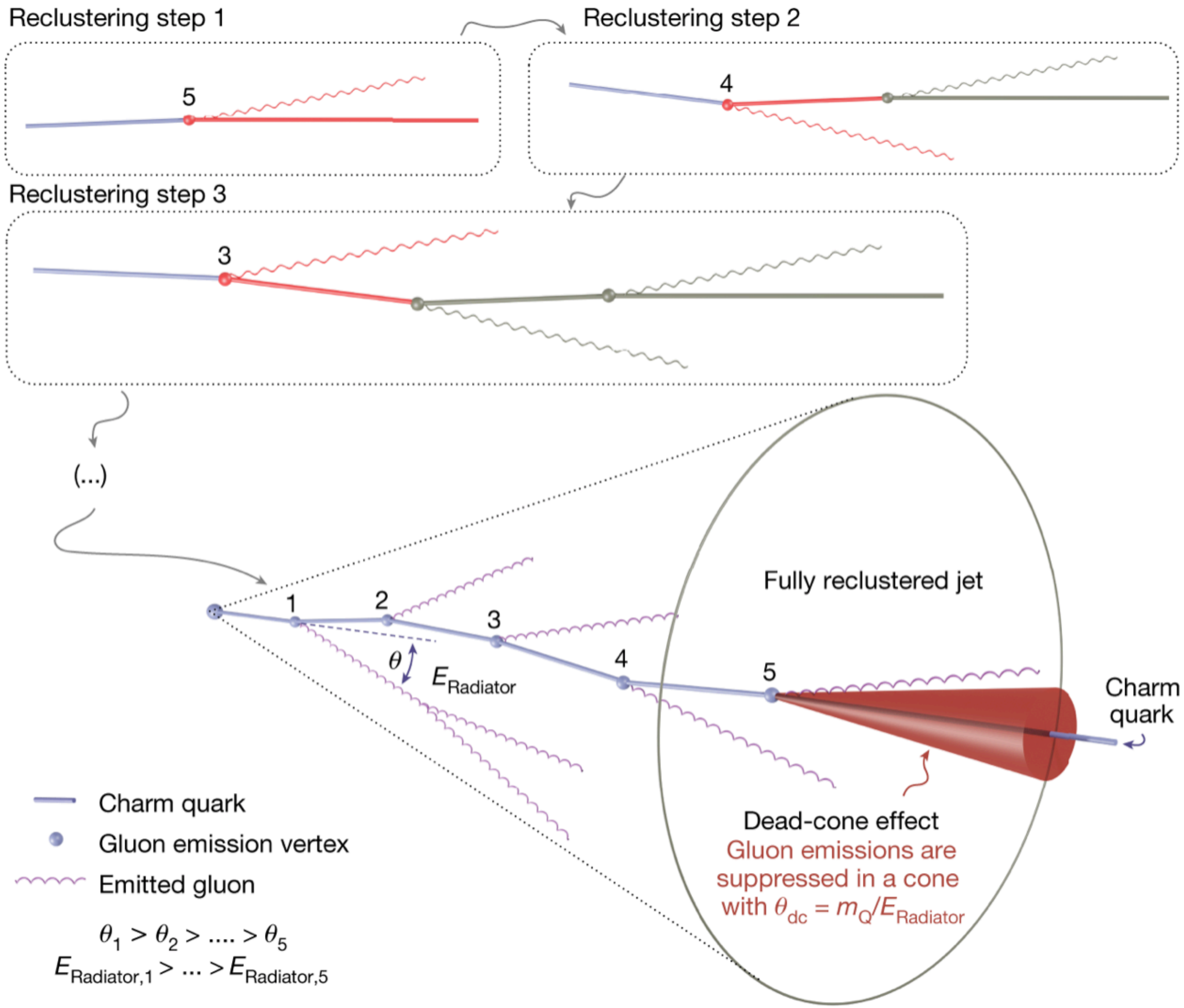

First direct observation of dead-cone effect

Challenges of Measurement:

- Determining the dynamic direction of heavy-quark throughout the shower

Solution:

- use declustering procedure with Cambridge/Aachen algorithm

.

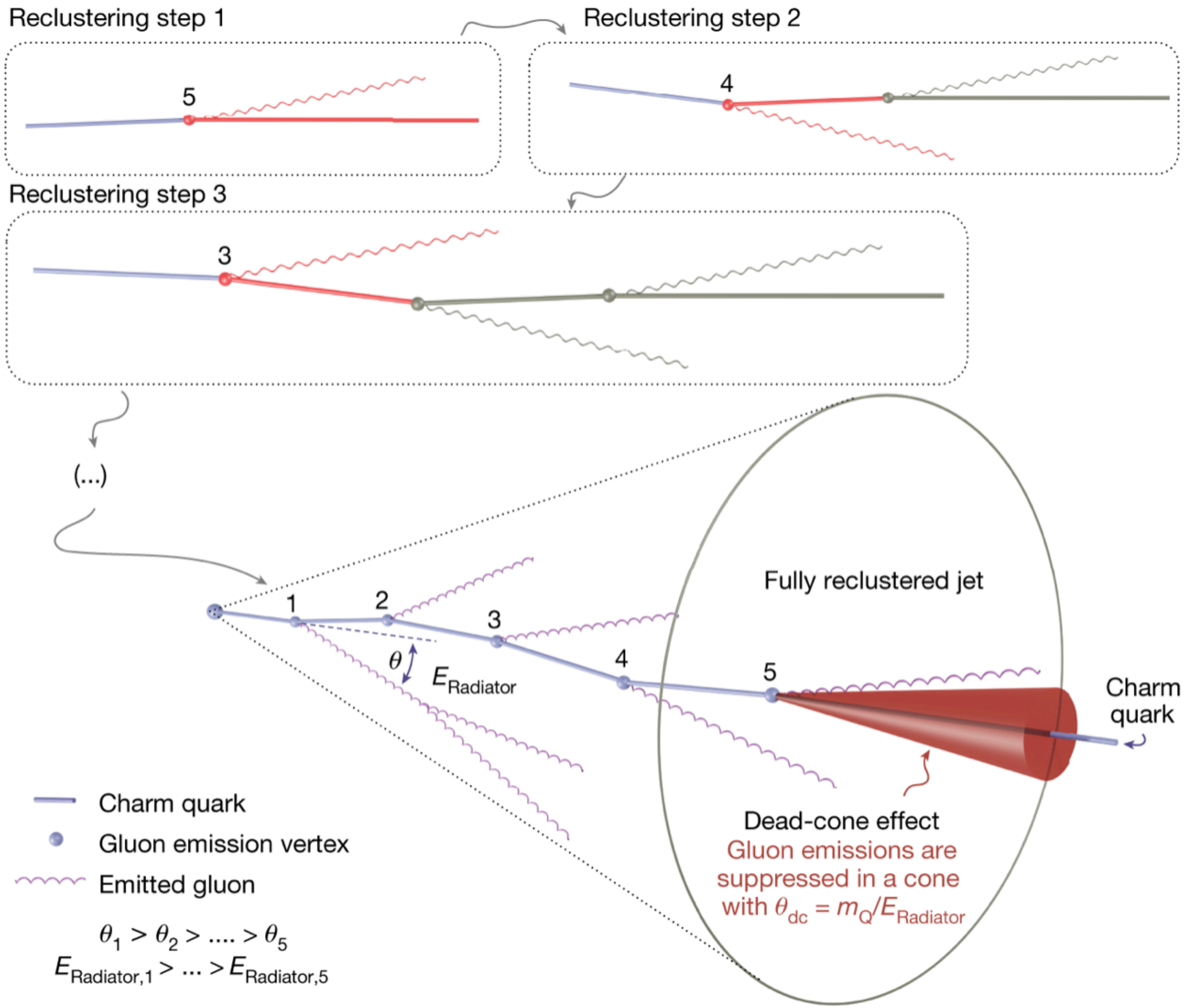

First direct observation of dead-cone effect

Challenges of Measurement:

- Determining the dynamic direction of heavy-quark throughout the shower

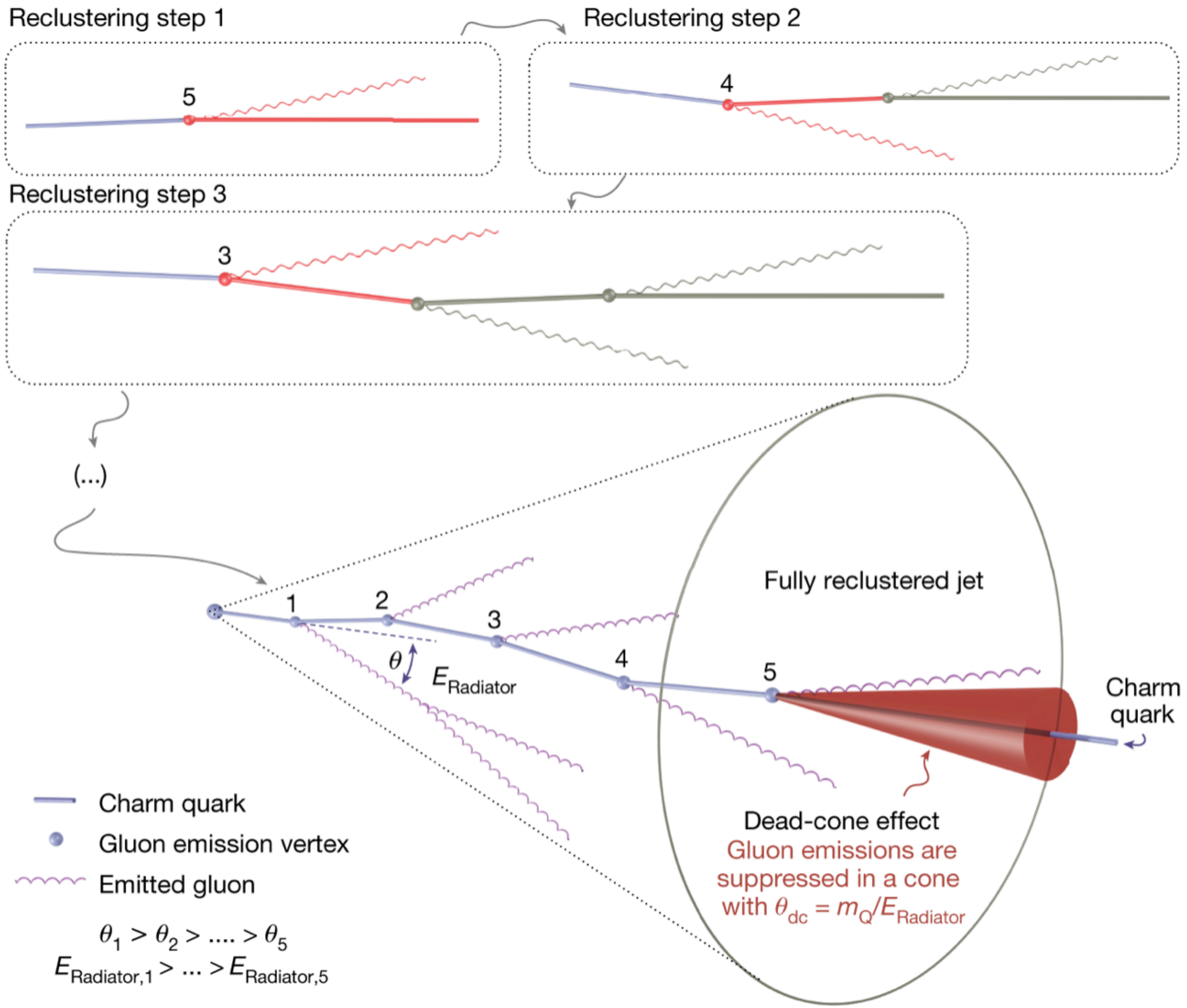

Solution:

- use declustering procedure with Cambridge/Aachen algorithm

Cambridge/Aachen clusters constituents based solely on their angular distance from one another

→ matches QCD

First direct observation of dead-cone effect

Challenges of Measurement:

- Determining the dynamic direction of heavy-quark throughout the shower

Solution:

- use declustering procedure with Cambridge/Aachen algorithm

Cambridge/Aachen clusters constituents based solely on their angular distance from one another

→ matches QCD

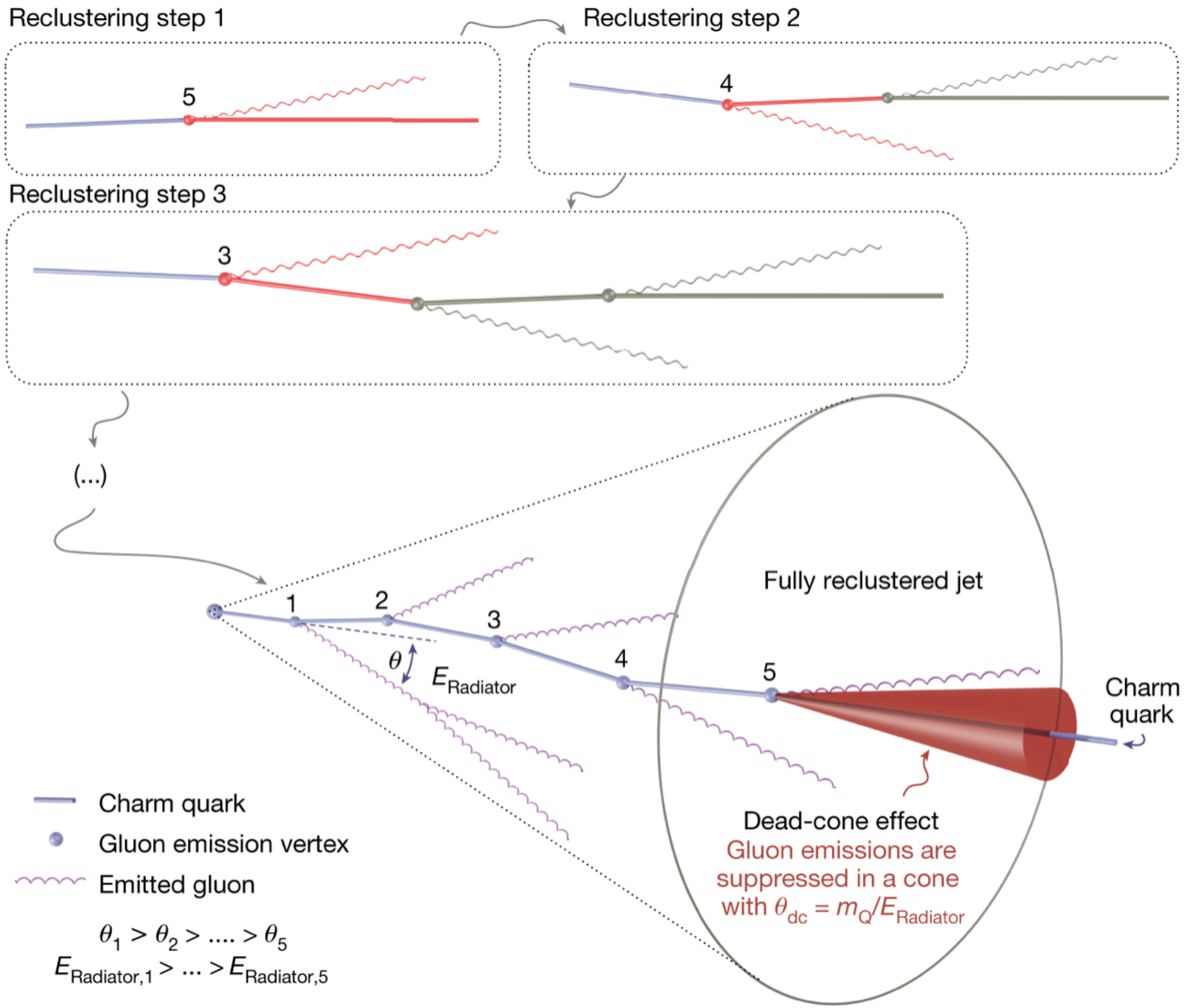

Declustring: Follow the branch with the D meson to identify the c-branch

First direct observation of dead-cone effect

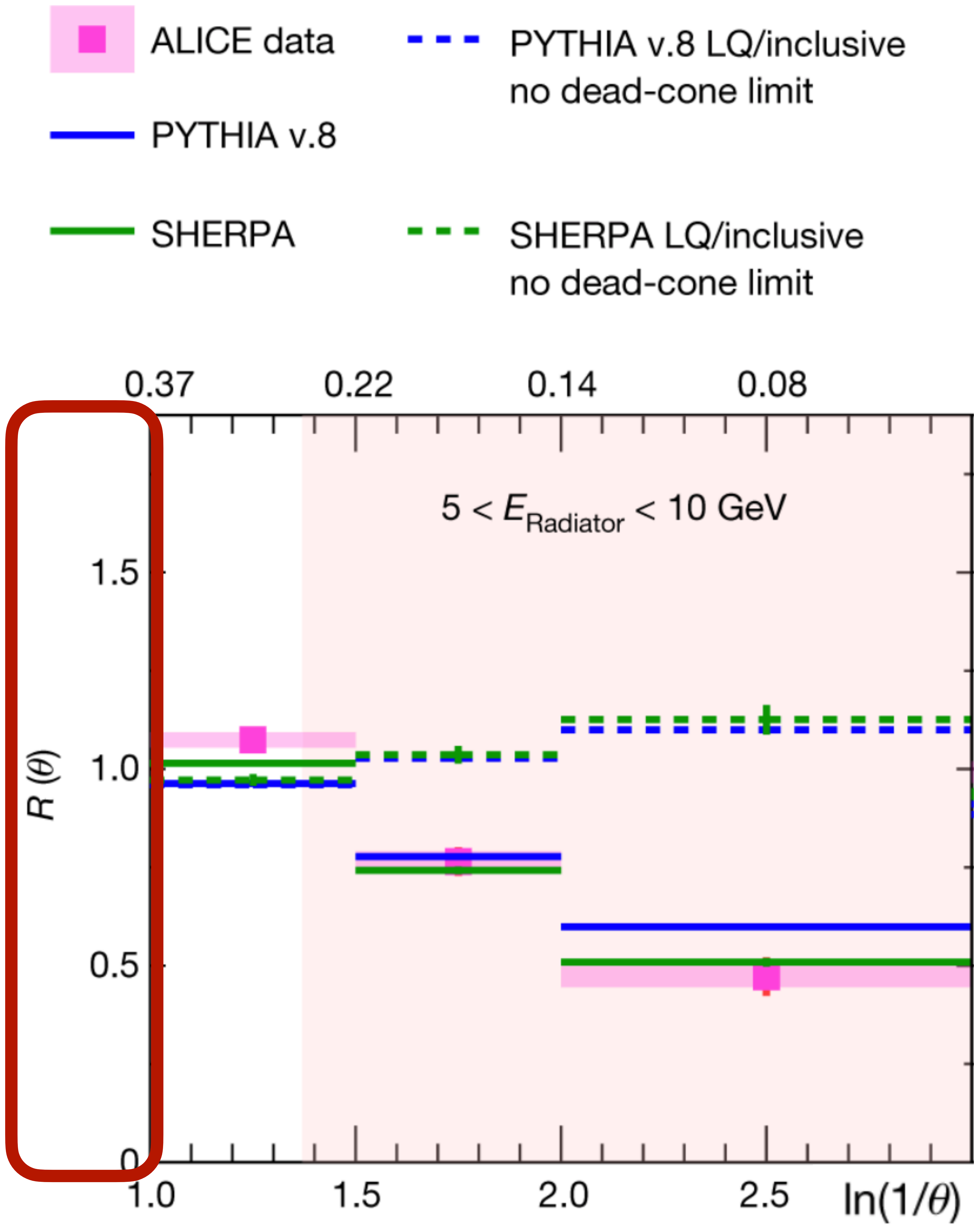

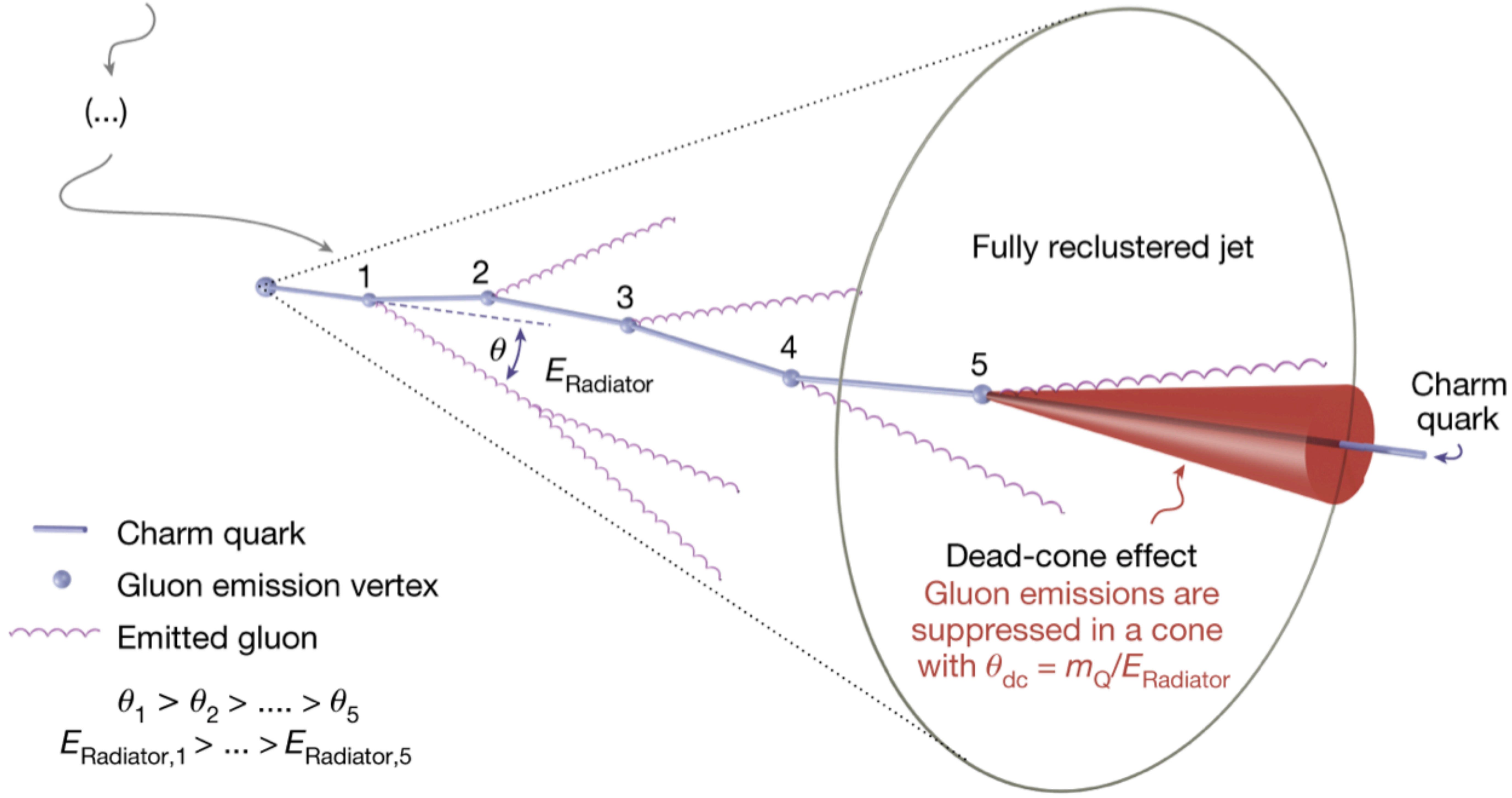

ratio of the splitting angle (θ) distribution for D^0-tagged vs. inclusive jets, vs. E_{Radiator}

$$R(\theta) = \frac{1}{N^{\text{D}^0\text{jets}}} \frac{\mathrm{d}n^{\text{D}^0\text{jets}}}{\mathrm{d}\ln(1/\theta)} / \frac{1}{N^{\text{inclusive jets}}} \frac{\mathrm{d}n^{\text{inclusive jets}}}{\mathrm{d}\ln(1/\theta)} \Big|_{k_{\text{T}},E_{\text{Radiator}}}$$

First direct observation of dead-cone effect

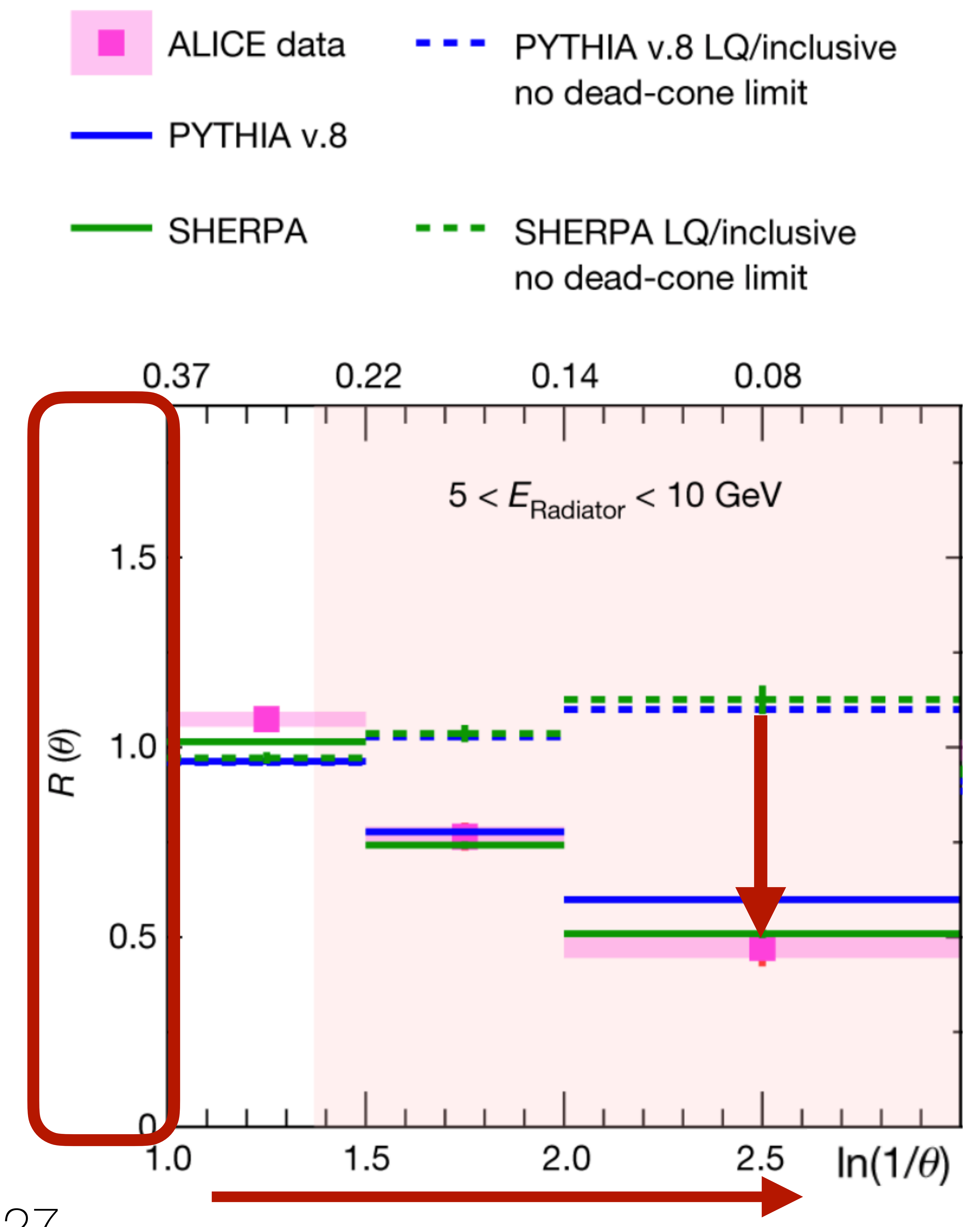

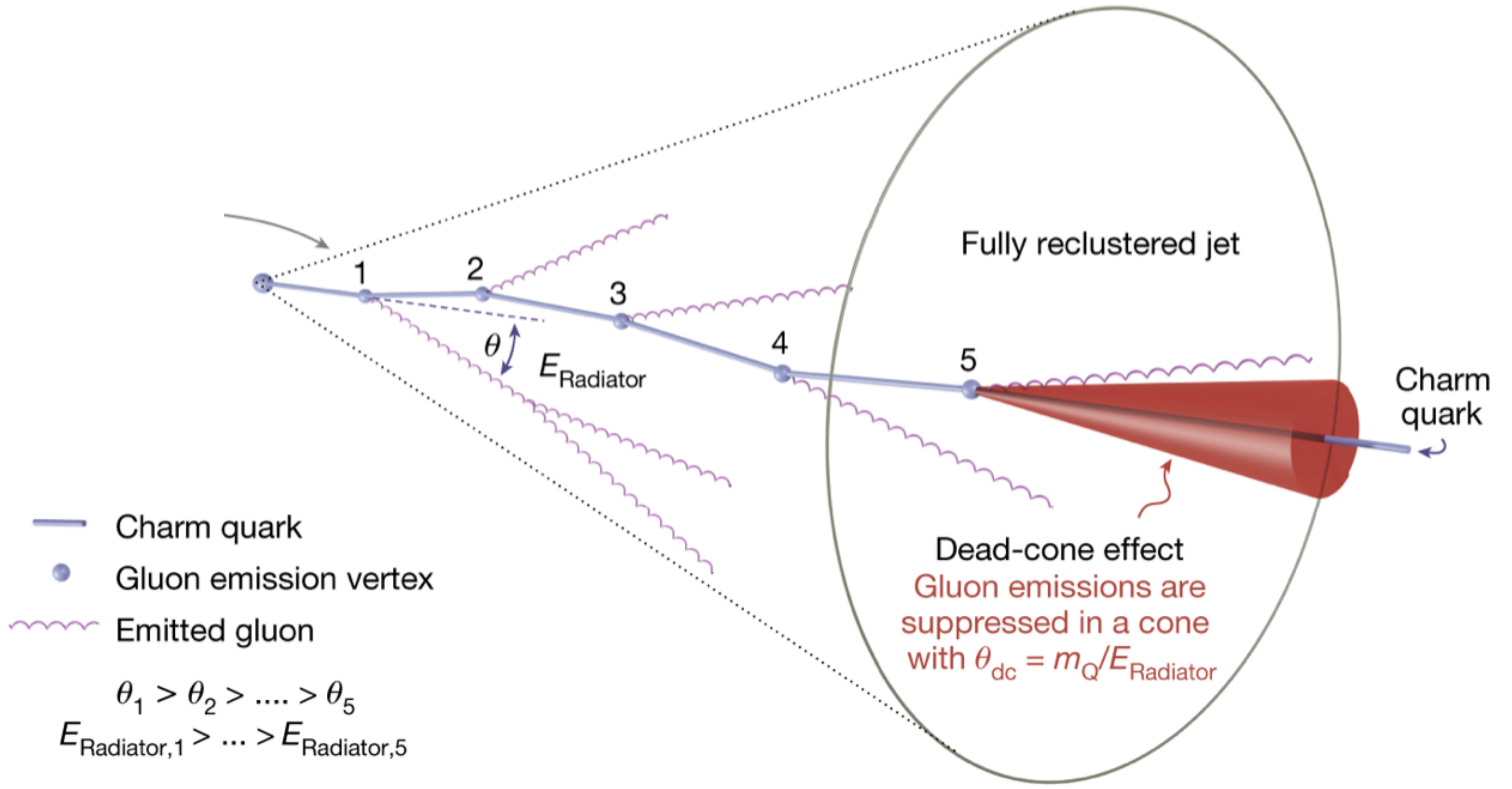

ratio of the splitting angle (θ) distribution for D^0-tagged vs. inclusive jets, vs. E_{Radiator}

$$R(\theta) = \frac{1}{N^{\mathrm{D^0 jets}}} \frac{\mathrm{d}n^{\mathrm{D^0 jets}}}{\mathrm{d}\ln(1/\theta)} \Big/ \frac{1}{N^{\mathrm{inclusive\ jets}}} \frac{\mathrm{d}n^{\mathrm{inclusive\ jets}}}{\mathrm{d}\ln(1/\theta)} \Big|_{k_{\mathrm{T}}, E_{\mathrm{Radiator}}}$$

significant suppression of small-angle emissions

First direct observation of dead-cone effect

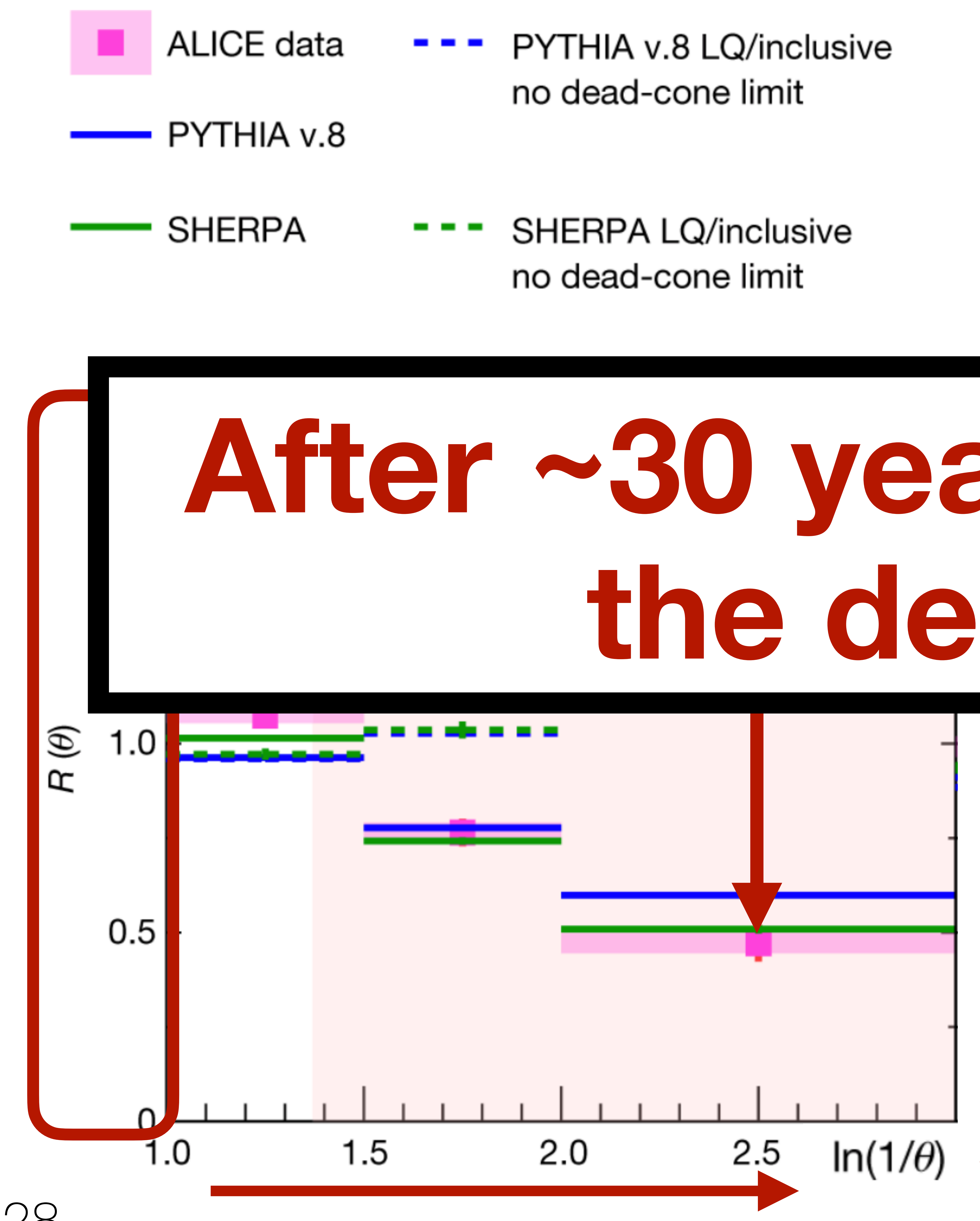

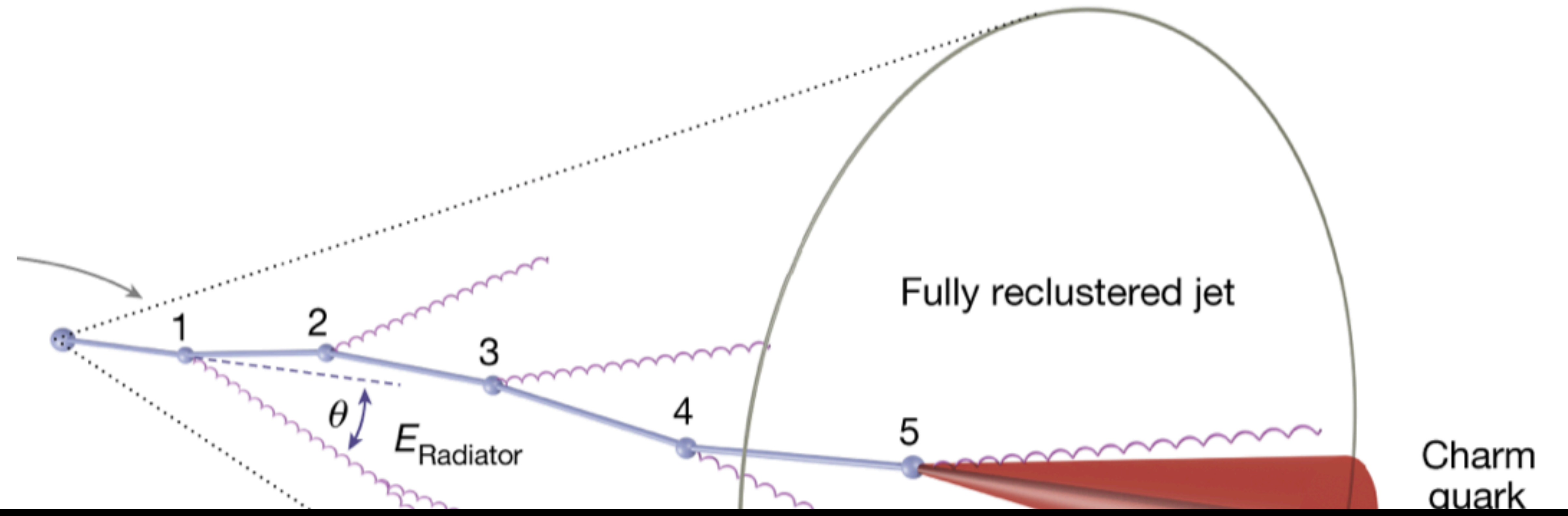

After ~30 years, directly measured the dead-cone effect!

Smaller angles

ratio of the splitting angle (θ) distribution for D^0-tagged vs. inclusive jets, vs. E_{Radiator}

$$R(\theta) = \frac{1}{N^{\mathrm{D^0 jets}}} \frac{\mathrm{d}n^{\mathrm{D^0 jets}}}{\mathrm{d}\ln(1/\theta)} \Bigg/ \frac{1}{N^{\mathrm{inclusive\ jets}}} \frac{\mathrm{d}n^{\mathrm{inclusive\ jets}}}{\mathrm{d}\ln(1/\theta)} \Bigg|_{k_{\mathrm{T}}, E_{\mathrm{Radiator}}}$$

significant suppression of small-angle emissions

Results

Jet axes distribution

Jet Angularities

Groomed z_g and R_g

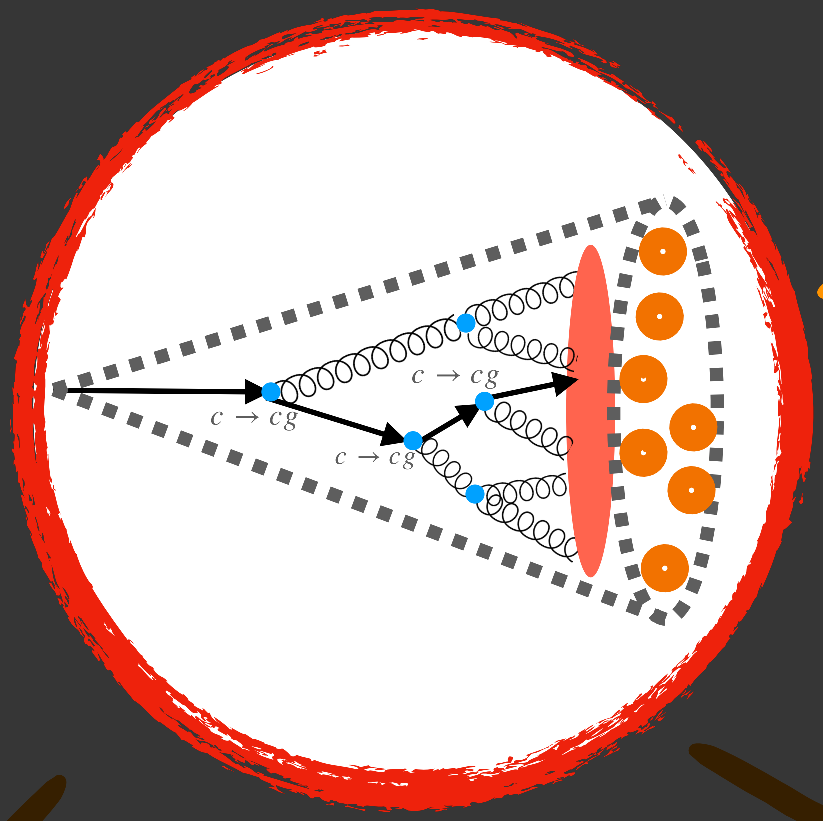

Dead-Cone Effect

Fragmentation function $z_{\parallel}$

Accessing the c→cg splitting function

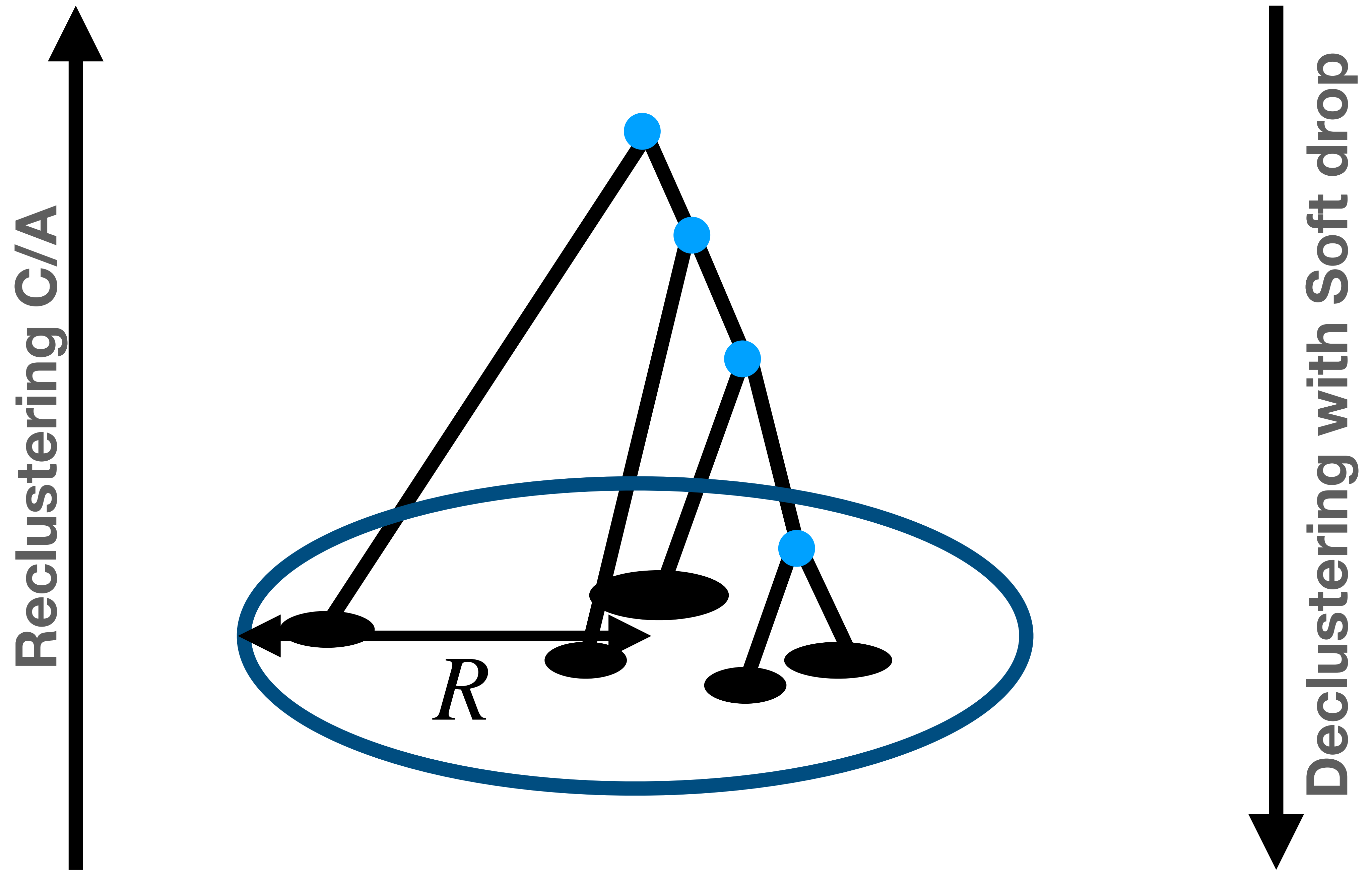

Groomed jet with the Soft Drop (SD) algorithm.

$$\frac{min(p_{T_1}, p_{T_2})}{p_{T_1} + p_{T_2}} > z_{\text{cut}} \left(\frac{\Delta R_{12}}{R} \right)^{\beta}$$

A. J. Larkoski et al. , JHEP 1405 (2014) 146

Accessing the c→cg splitting function

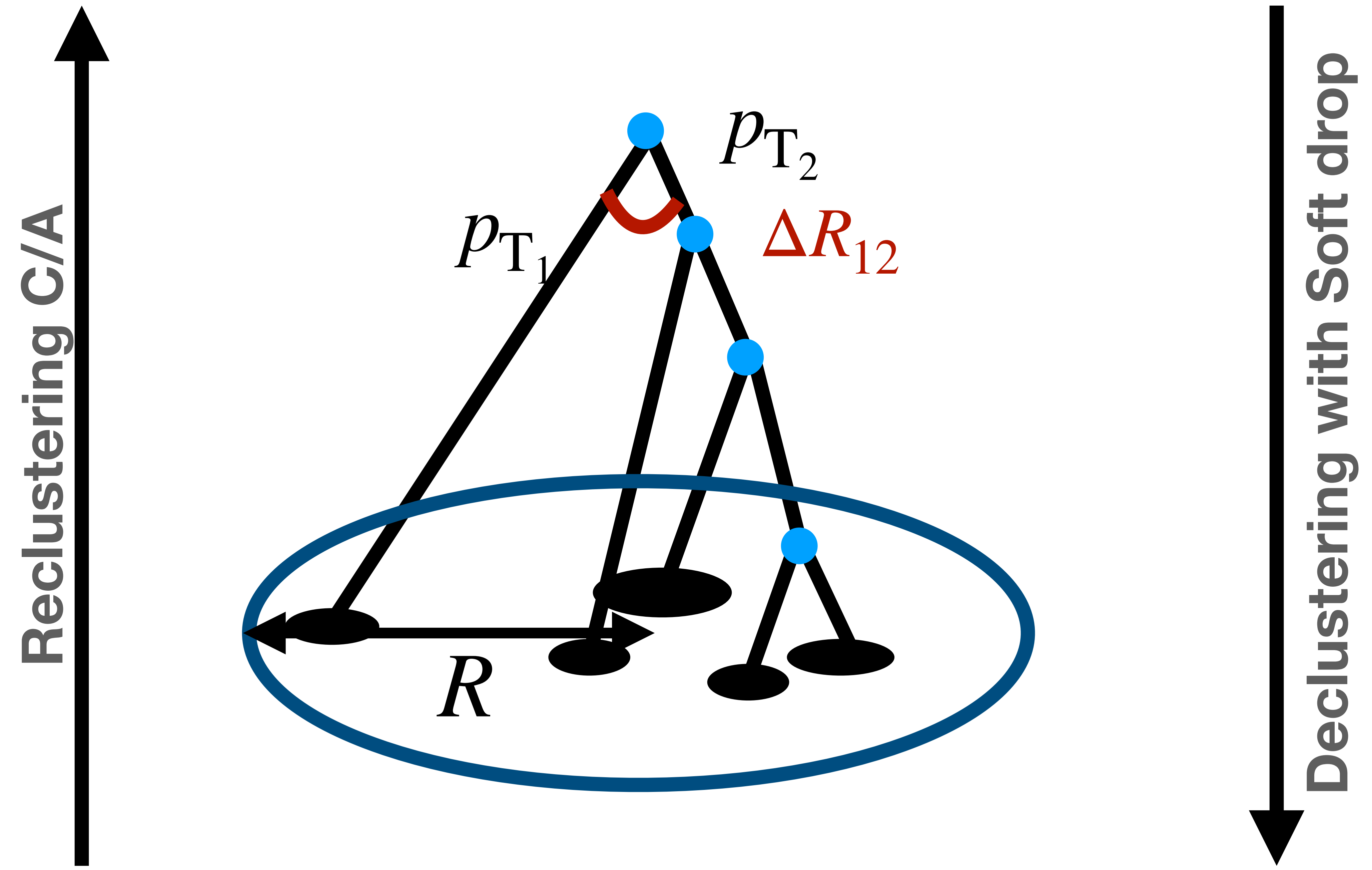

Groomed jet with the Soft Drop (SD) algorithm.

$$\frac{min(p_{T_1}, p_{T_2})}{p_{T_1} + p_{T_2}} > z_{cut}\left(\frac{\Delta R_{12}}{R}\right)^{\beta}$$

A. J. Larkoski et al. , JHEP 1405 (2014) 146

Accessing the c→cg splitting function

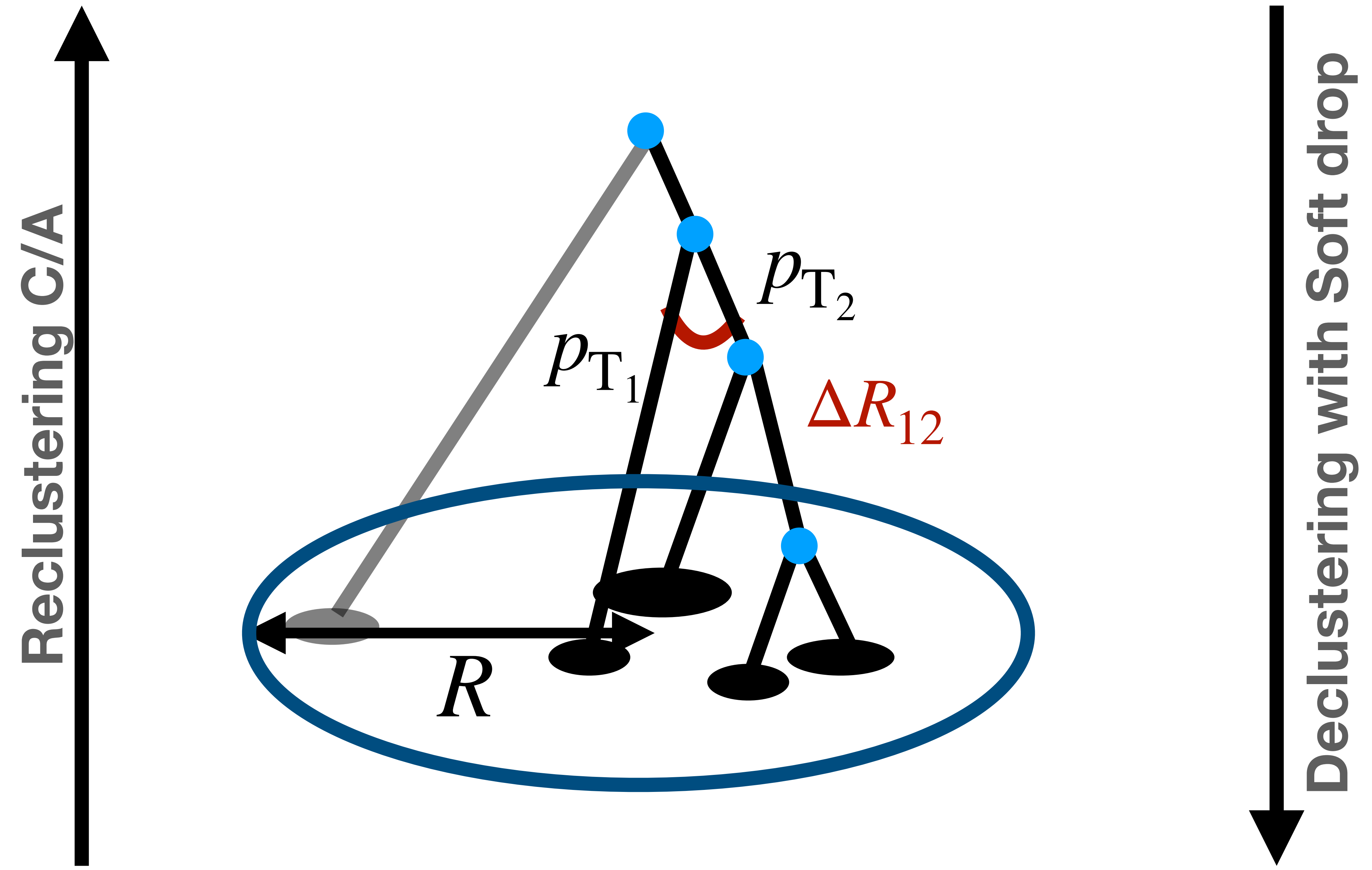

Groomed jet with the Soft Drop (SD) algorithm.

$$\frac{min(p_{T_1}, p_{T_2})}{p_{T_1} + p_{T_2}} > z_{cut}\left(\frac{\Delta R_{12}}{R}\right)^{\beta}$$

A. J. Larkoski et al. , JHEP 1405 (2014) 146

Accessing the c→cg splitting function

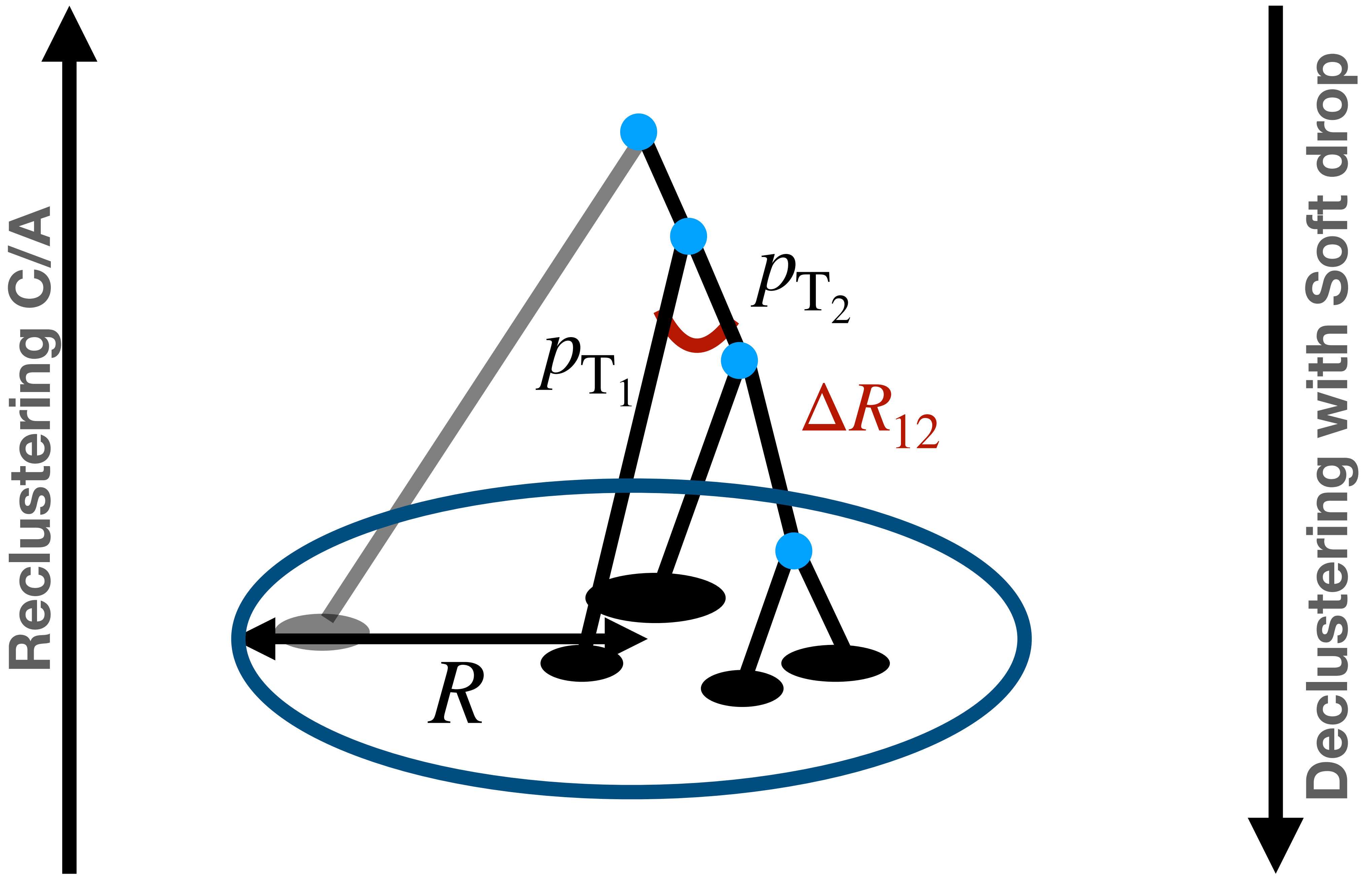

Groomed jet with the Soft Drop (SD) algorithm.

z_g R_g

$$\frac{min(p_{T_1}, p_{T_2})}{p_{T_1} + p_{T_2}} > z_{cut} \left(\frac{\Delta R_{12}}{R}\right)^{\beta}$$

A. J. Larkoski et al. , JHEP 1405 (2014) 146

Accessing the c→cg splitting function

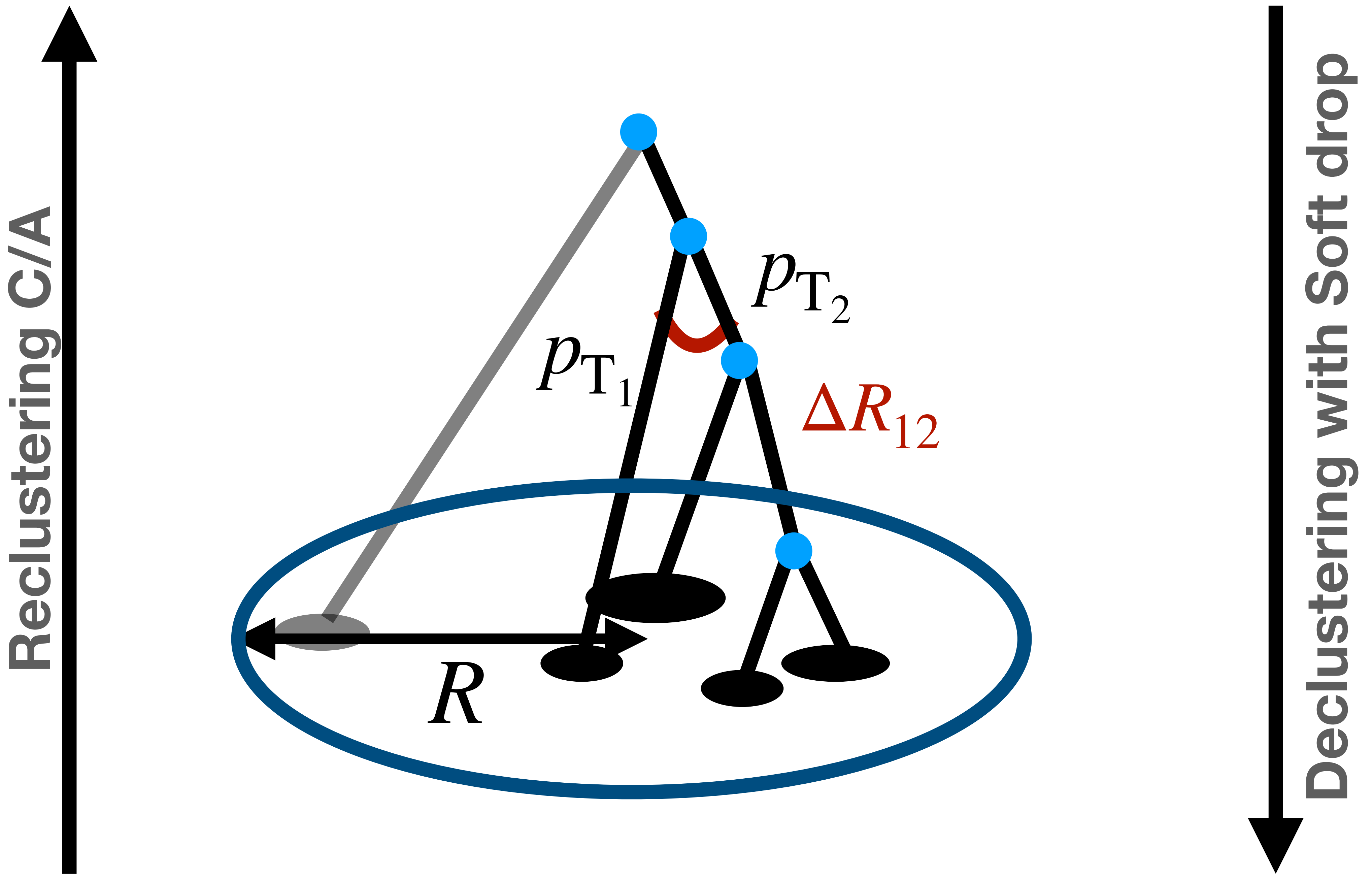

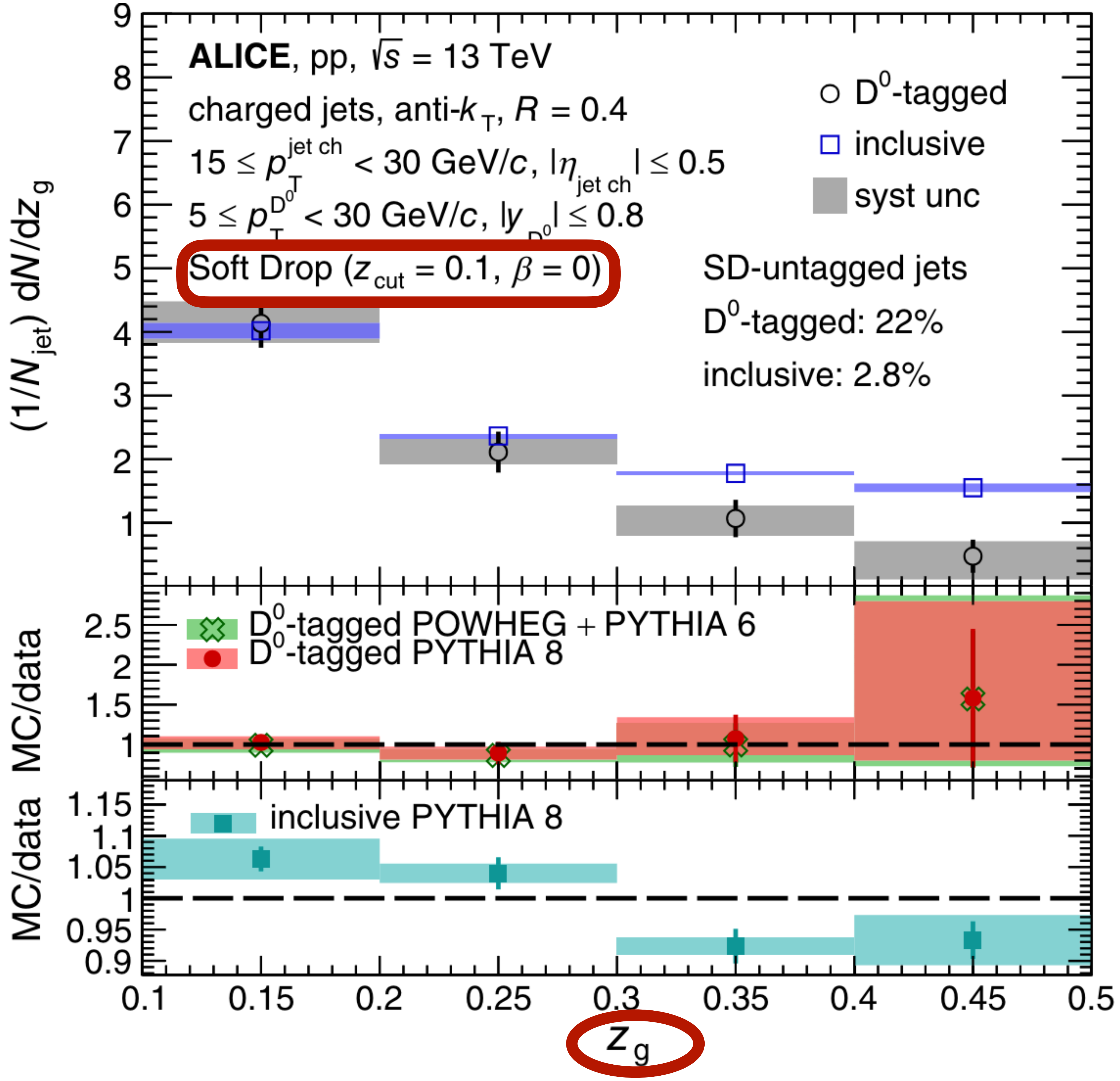

Groomed jet with the Soft Drop (SD) algorithm.

$$z_g = \frac{min(p_{T_1}, p_{T_2})}{p_{T_1} + p_{T_2}} > z_{cut} \left(\frac{\Delta R_{12}}{R} \right)^{\beta} \qquad R_g = \Delta R_{12}$$

A. J. Larkoski et al. , JHEP 1405 (2014) 146

- c→cg splittings have fewer symmetric splittings compared to splittings of light quarks and gluons

Accessing the c→cg splitting function

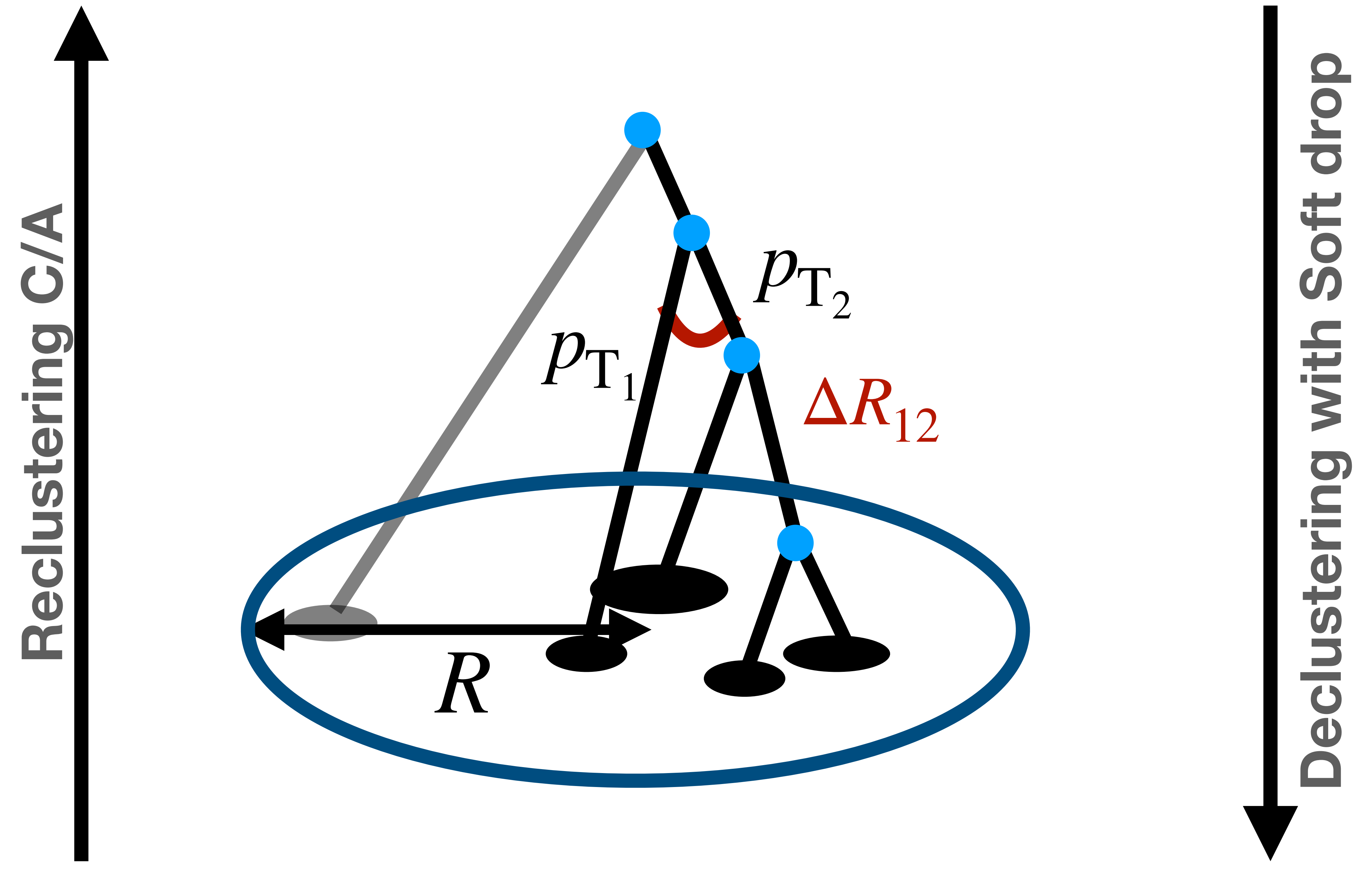

Groomed jet with the Soft Drop (SD) algorithm.

$$z_g: \quad \frac{min(p_{T_1}, p_{T_2})}{p_{T_1} + p_{T_2}} > z_{cut} \left(\frac{\Delta R_{12}}{R} \right)^{\beta} \quad R_g: \Delta R_{12}$$

A. J. Larkoski et al. , JHEP 1405 (2014) 146

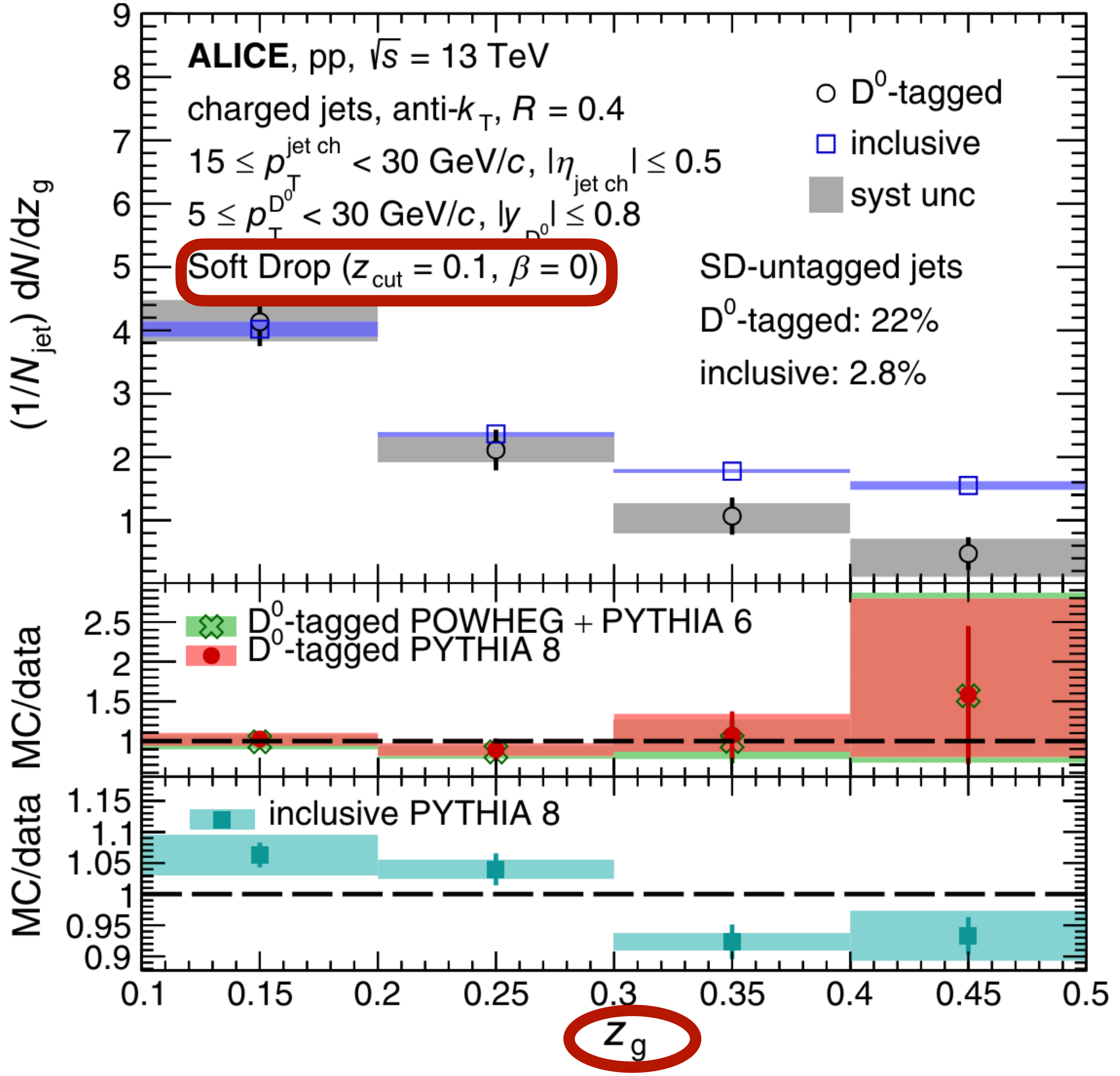

- c→cg splittings have fewer symmetric splittings compared to splittings of light quarks and gluons
  →dead cone of the charm quark

Accessing the c→cg splitting function

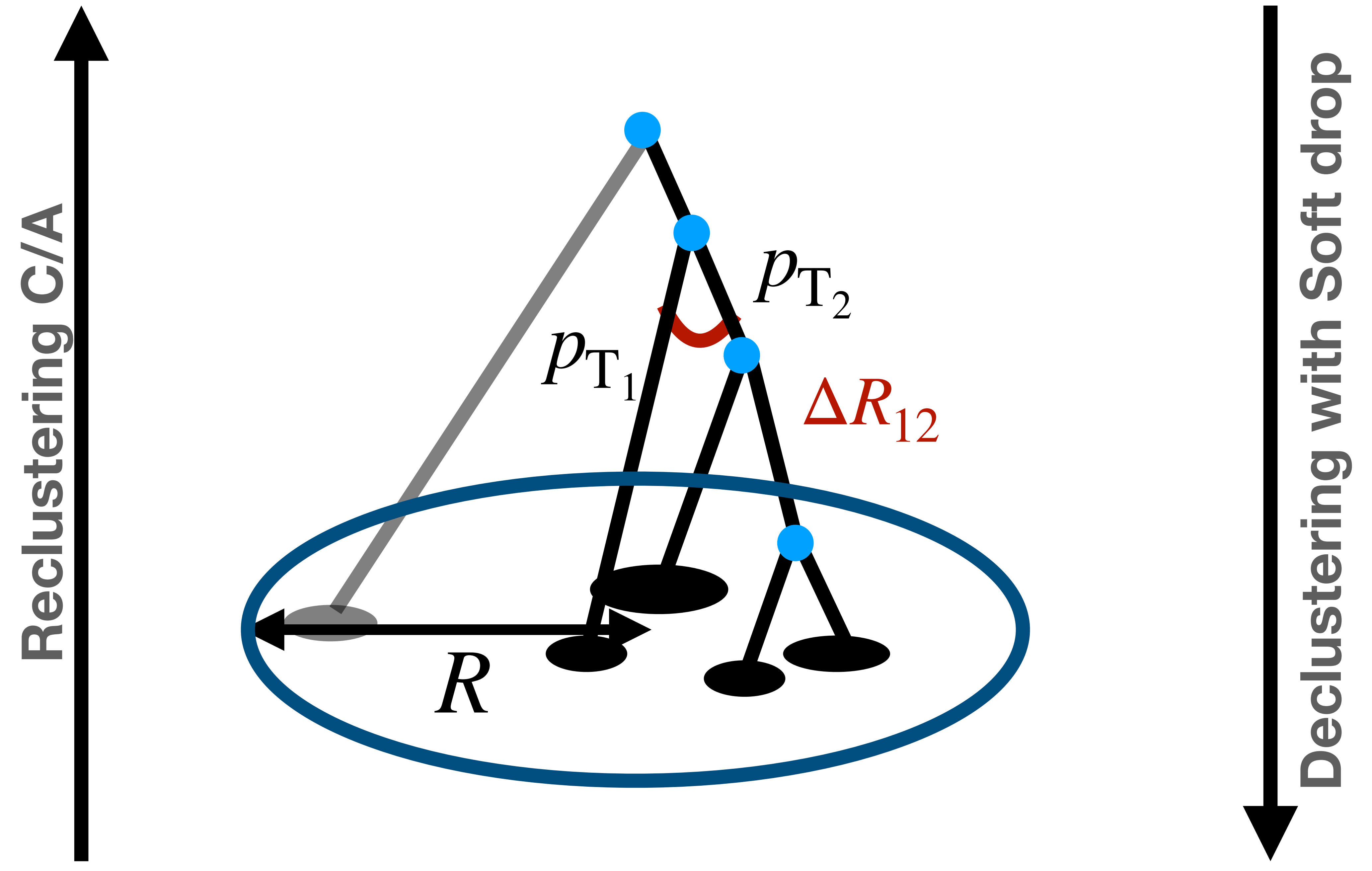

Groomed jet with the Soft Drop (SD) algorithm.

$$z_g \quad \frac{min(p_{T_1}, p_{T_2})}{p_{T_1} + p_{T_2}} > z_{cut} \left(\frac{\Delta R_{12}}{R}\right)^{\beta} \quad R_g$$

A. J. Larkoski et al. , JHEP 1405 (2014) 146

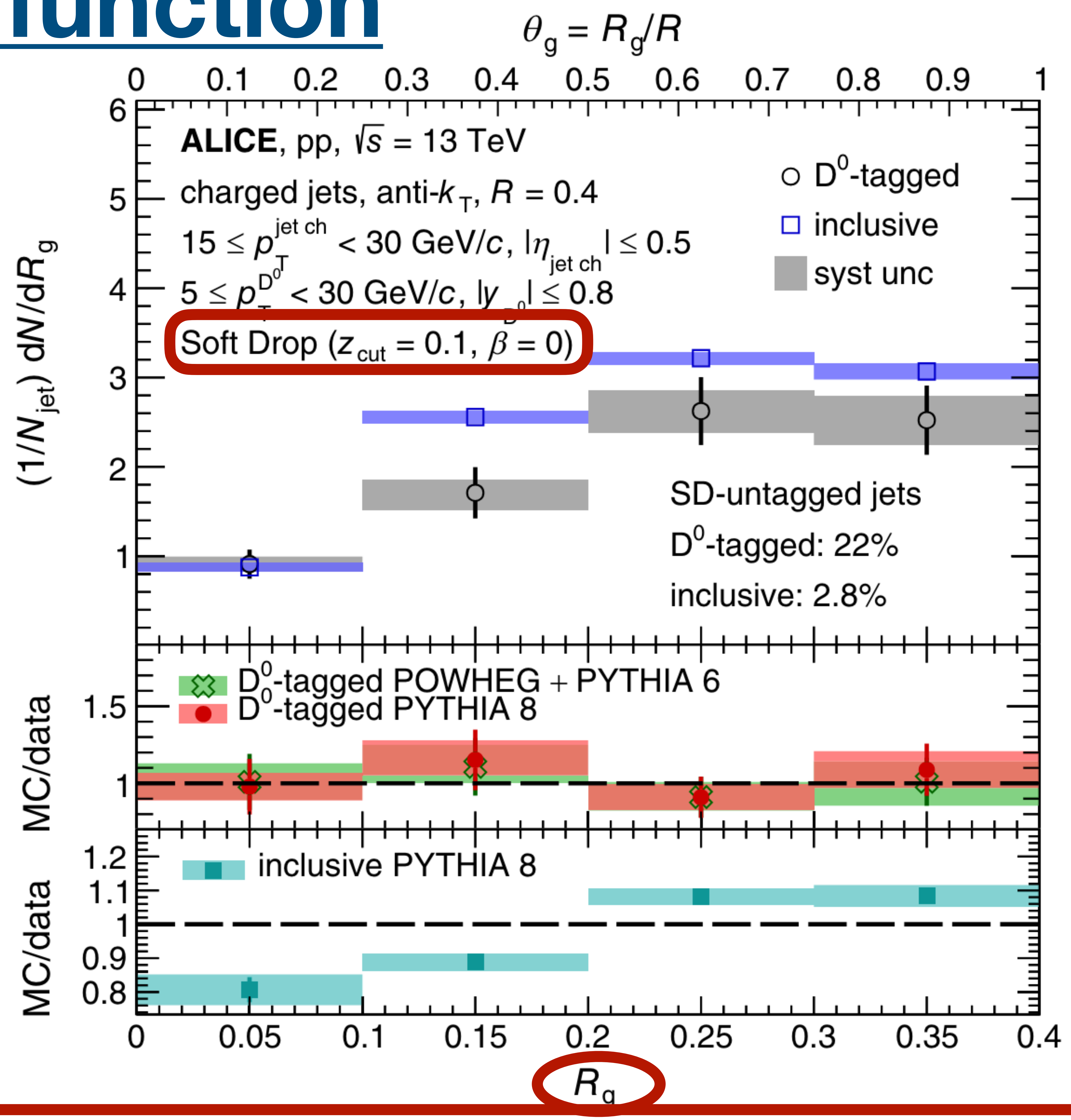

- c→cg splittings are narrower than splittings of the light quarks and gluons sample

Accessing the c→cg splitting function

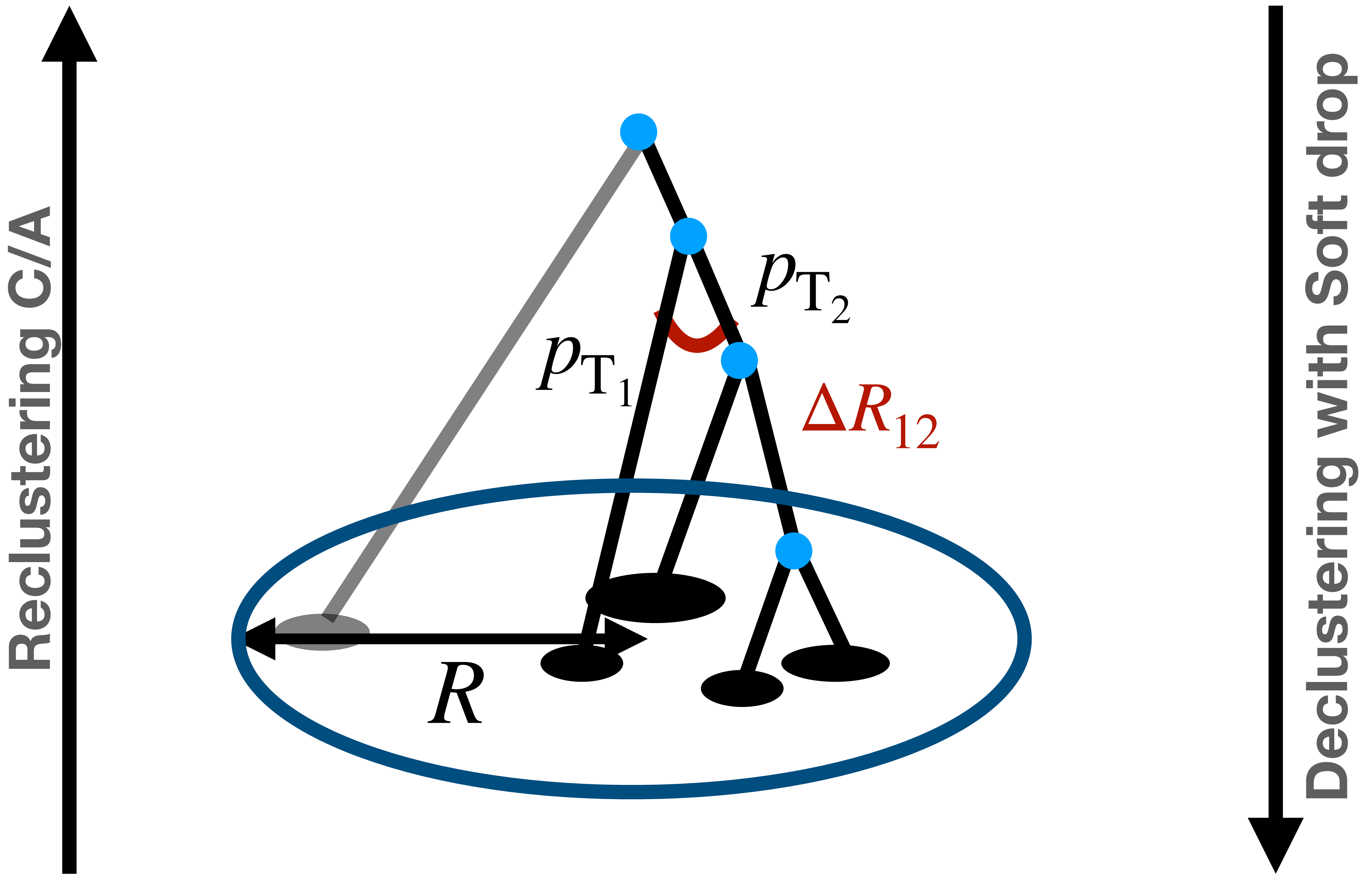

Groomed jet with the Soft Drop (SD) algorithm.

$$\underbrace{\frac{\min(p_{T_1}, p_{T_2})}{p_{T_1} + p_{T_2}}}_{z_g} > z_{cut} \left(\frac{\overbrace{\Delta R_{12}}^{R_g}}{R} \right)^{\beta}$$

A. J. Larkoski et al. , JHEP 1405 (2014) 146

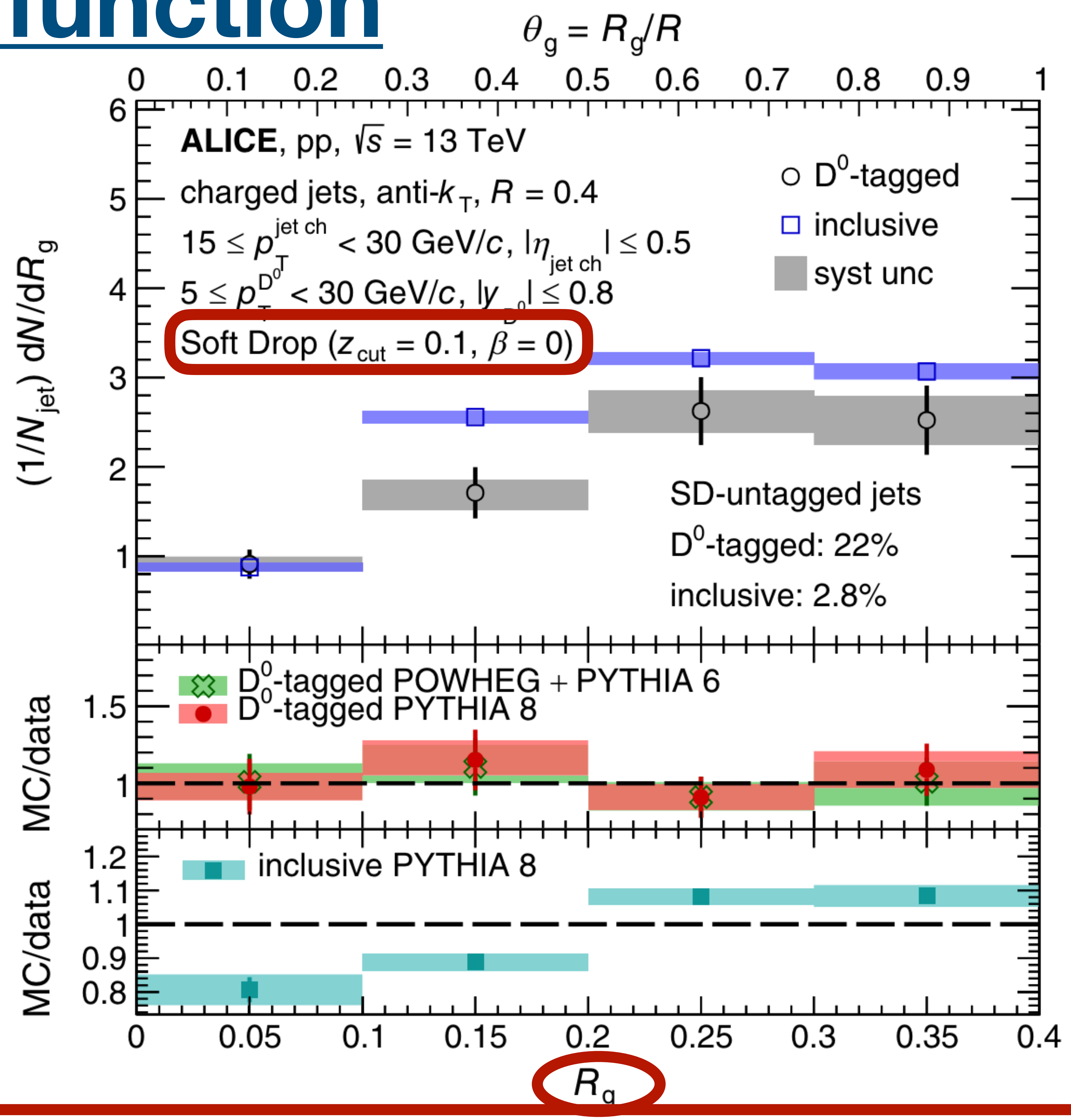

- c→cg splittings are narrower than splittings of the light quarks and gluons sample
  →larger Casimir color factor for gluons

Accessing the c→cg splitting function

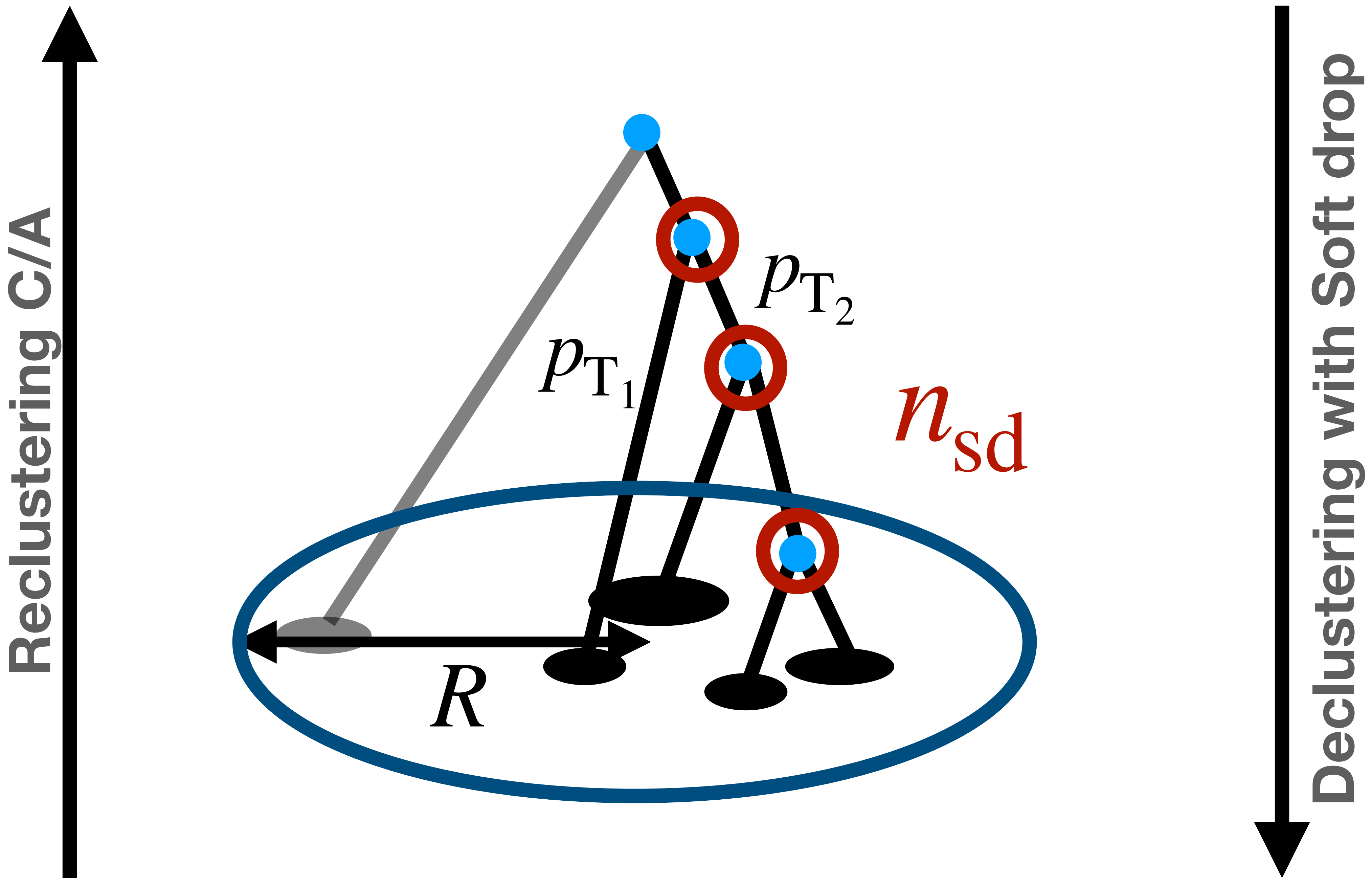

Groomed jet with the Soft Drop (SD) algorithm.

$$\frac{min(p_{T_1}, p_{T_2})}{p_{T_1} + p_{T_2}} > z_{cut} \left(\frac{\Delta R_{12}}{R} \right)^{\beta}$$

A. J. Larkoski et al. , JHEP 1405 (2014) 146

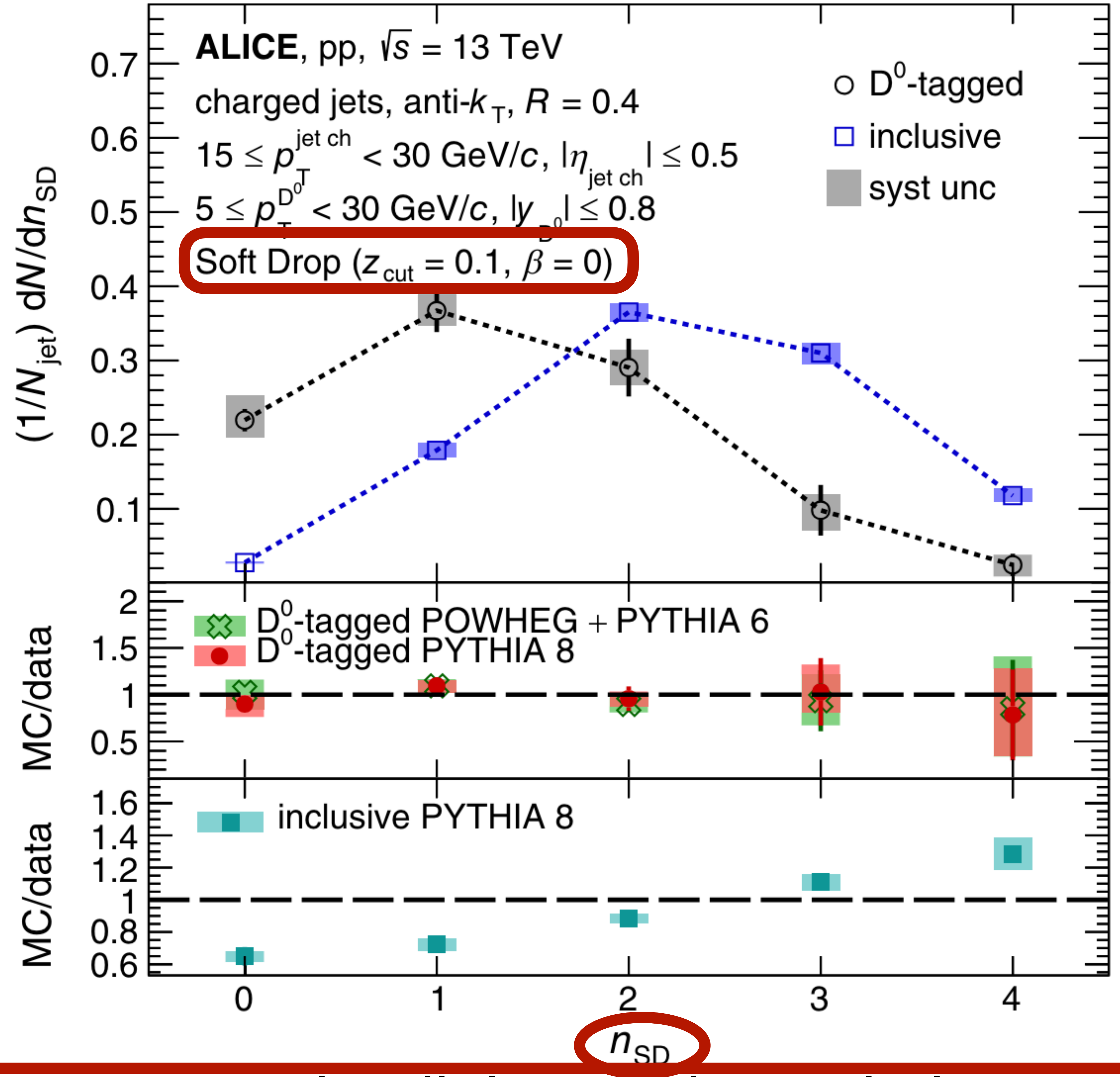

- Charm quarks have fewer perturbative emissions compared to light quarks and gluons

Results

Jet axes distribution

Jet Angularities

Groomed z_g and R_g

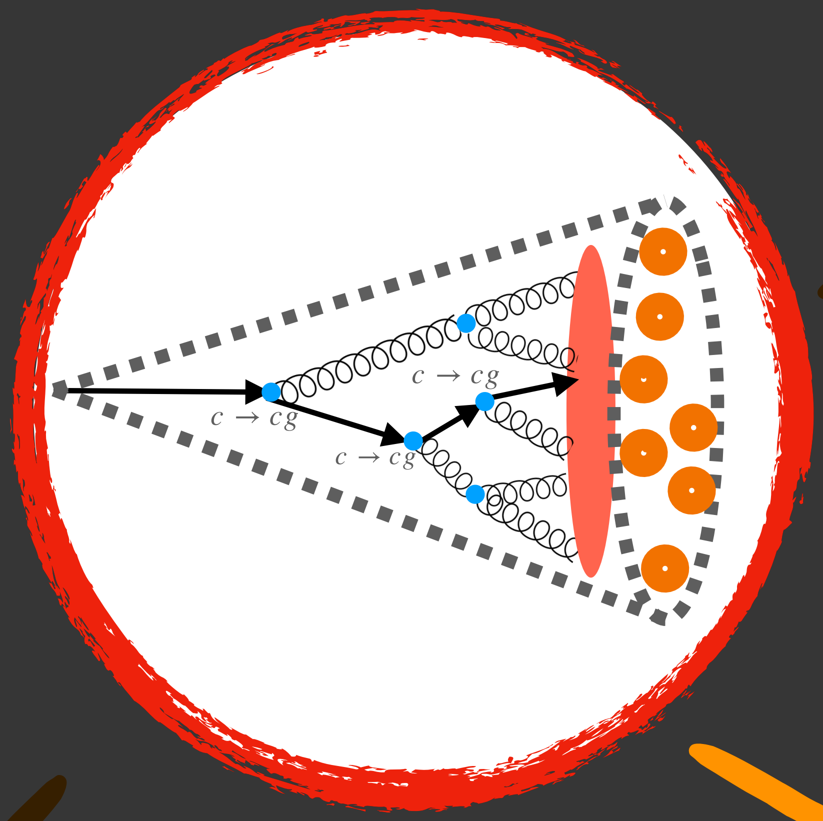

Dead-Cone Effect

Fragmentation function $z_{\parallel}$

Charm quark fragmentation

Fraction of longitudinal jet momentum carried by the charm hadron

$$z_{||}^{\mathrm{ch}} = \frac{\vec{p}_{\mathrm{ch\ jet}} \cdot \vec{p}_{\mathrm{D^0}}}{\vec{p}_{\mathrm{ch\ jet}} \cdot \vec{p}_{\mathrm{ch\ jet}}}$$

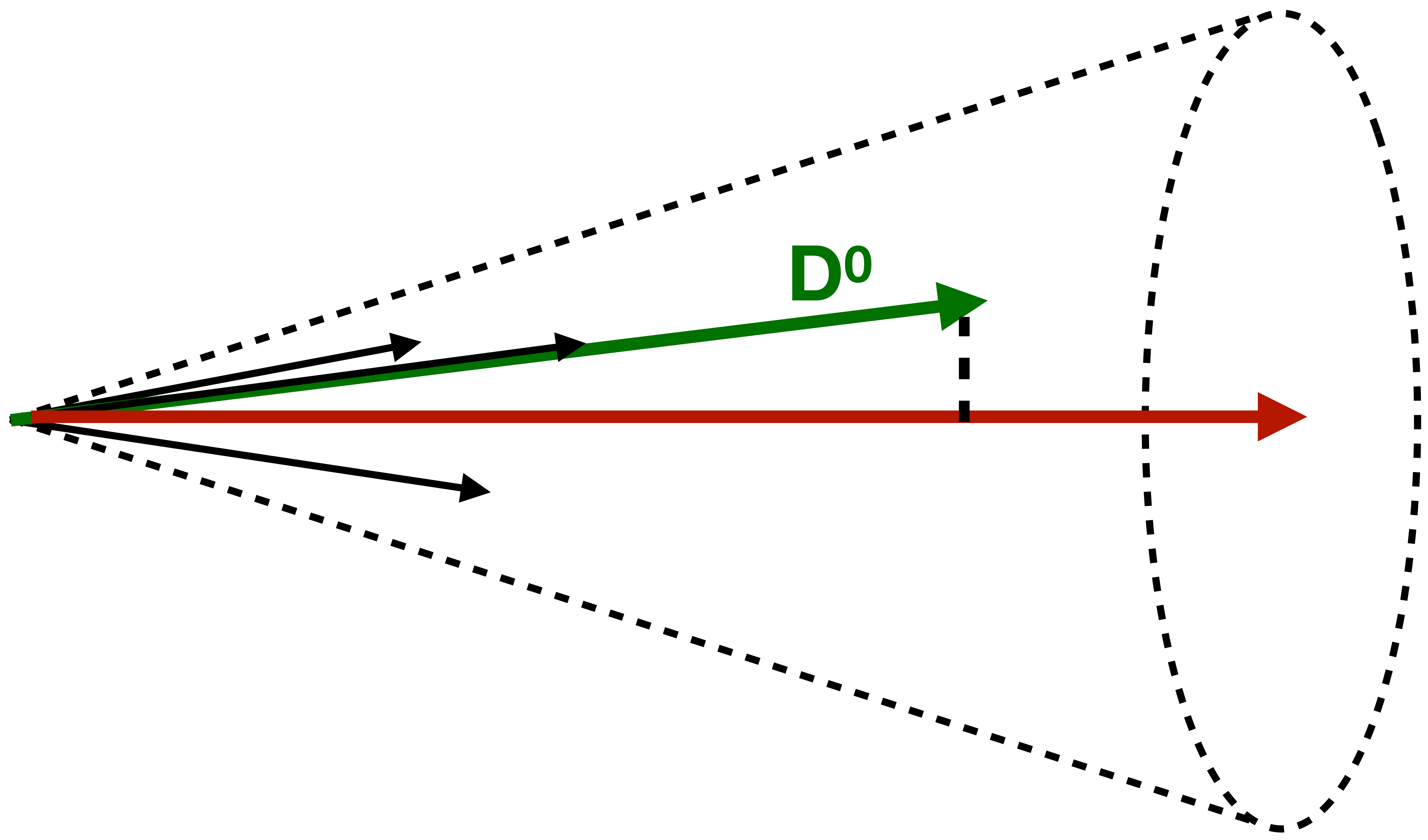

$\vec{p}_{\mathrm{D^0}}$ is the D^0-meson momentum

$\vec{p}_{\mathrm{ch\ jet}}$ is the total jet momentum

Charm quark fragmentation

$$z_{||}^{ch} = \frac{\vec{p}_{\text{ch jet}} \cdot \vec{p}_{D^0}}{\vec{p}_{\text{ch jet}} \cdot \vec{p}_{\text{ch jet}}}$$

$\vec{p}_{D^0}$ is the D^0-meson momentum

$\vec{p}_{\text{ch jet}}$ is the total jet momentum

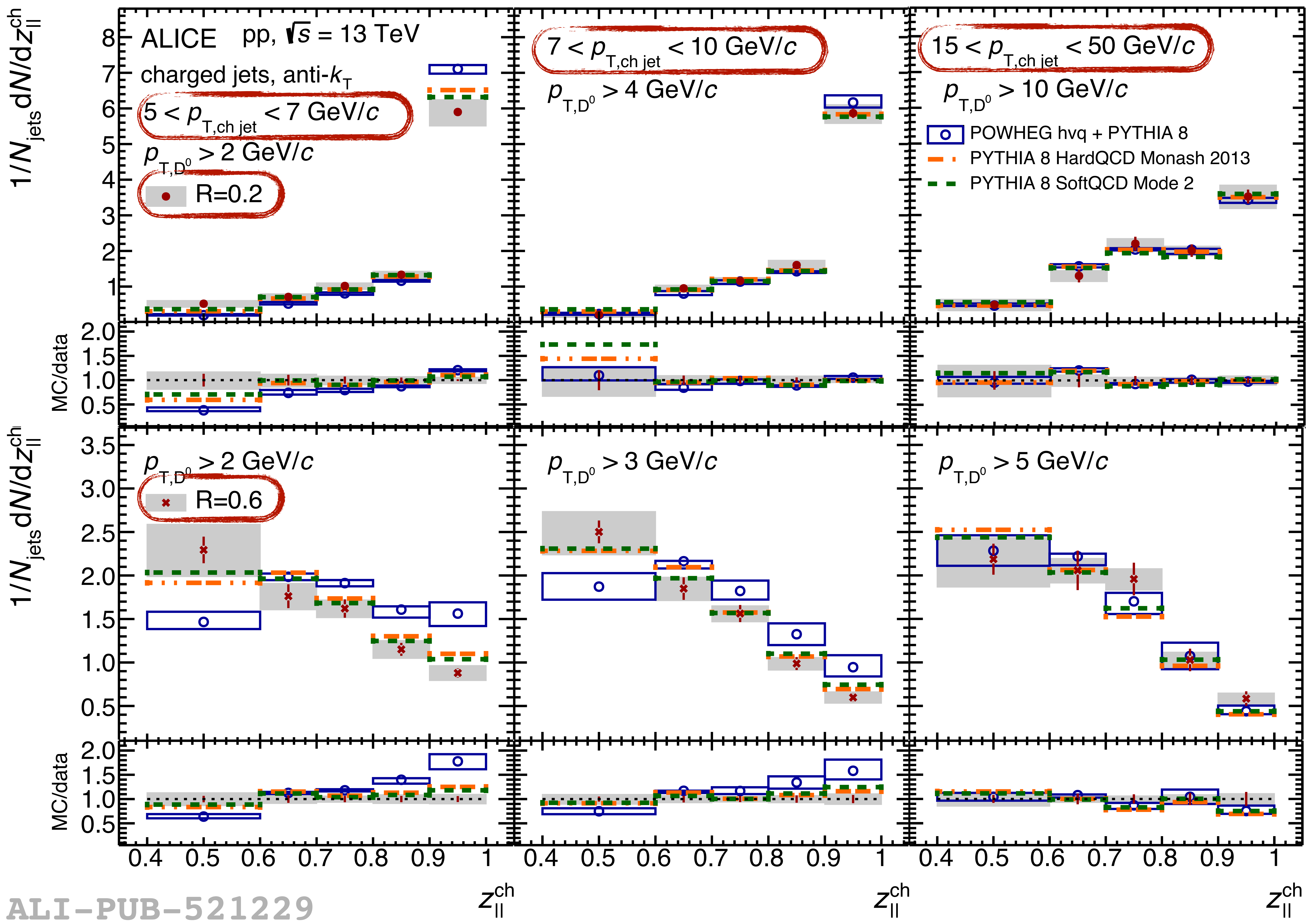

Charm quark fragmentation

$$z_{||}^{\mathrm{ch}} = \frac{\vec{p}_{\mathrm{ch\ jet}} \cdot \vec{p}_{\mathrm{D^0}}}{\vec{p}_{\mathrm{ch\ jet}} \cdot \vec{p}_{\mathrm{ch\ jet}}}$$

$\vec{p}_{\mathrm{D^0}}$ is the D^0-meson momentum

$\vec{p}_{\mathrm{ch\ jet}}$ is the total jet momentum

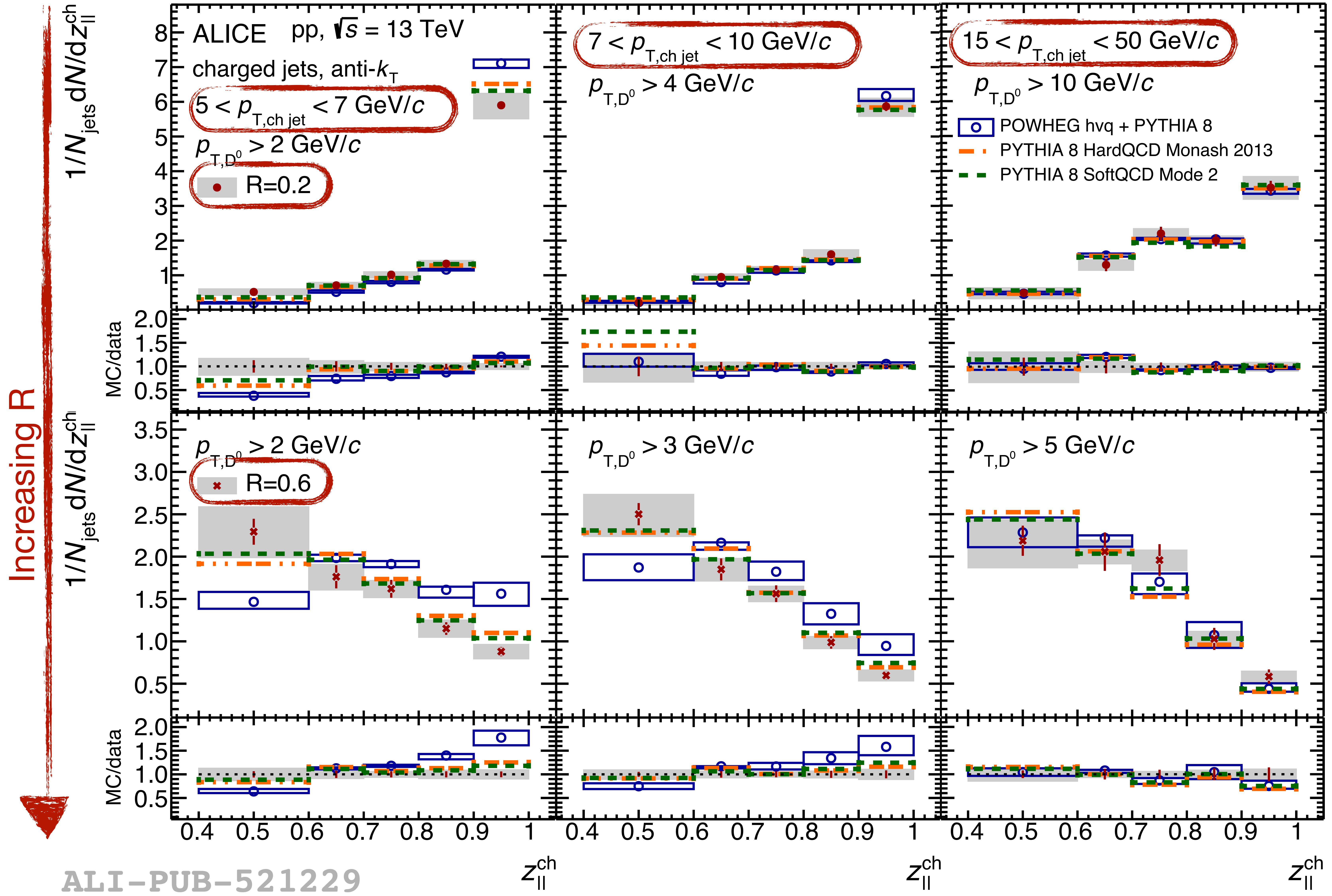

Charm quark fragmentation

$$z_{||}^{ch} = \frac{\vec{p}_{\rm ch\ jet} \cdot \vec{p}_{\rm D^0}}{\vec{p}_{\rm ch\ jet} \cdot \vec{p}_{\rm ch\ jet}}$$

$\vec{p}_{\rm D^0}$ is the D^0-meson momentum

$\vec{p}_{\rm ch\ jet}$ is the total jet momentum

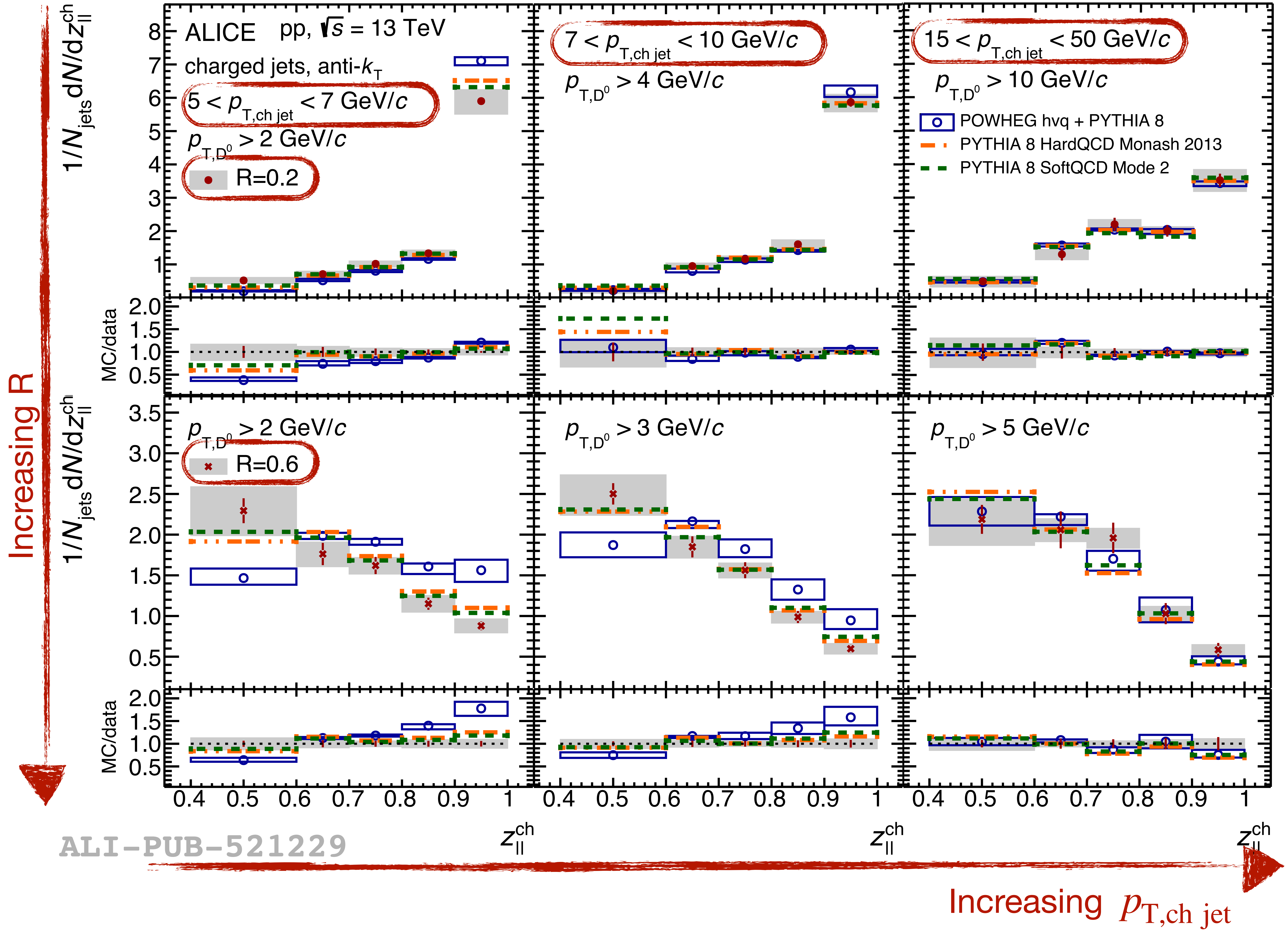

Charm quark fragmentation

- **Hint of a softer fragmentation** in data with respect to model predictions for low $p_{\mathrm{T,ch\,jet}}$ and larger *R*.

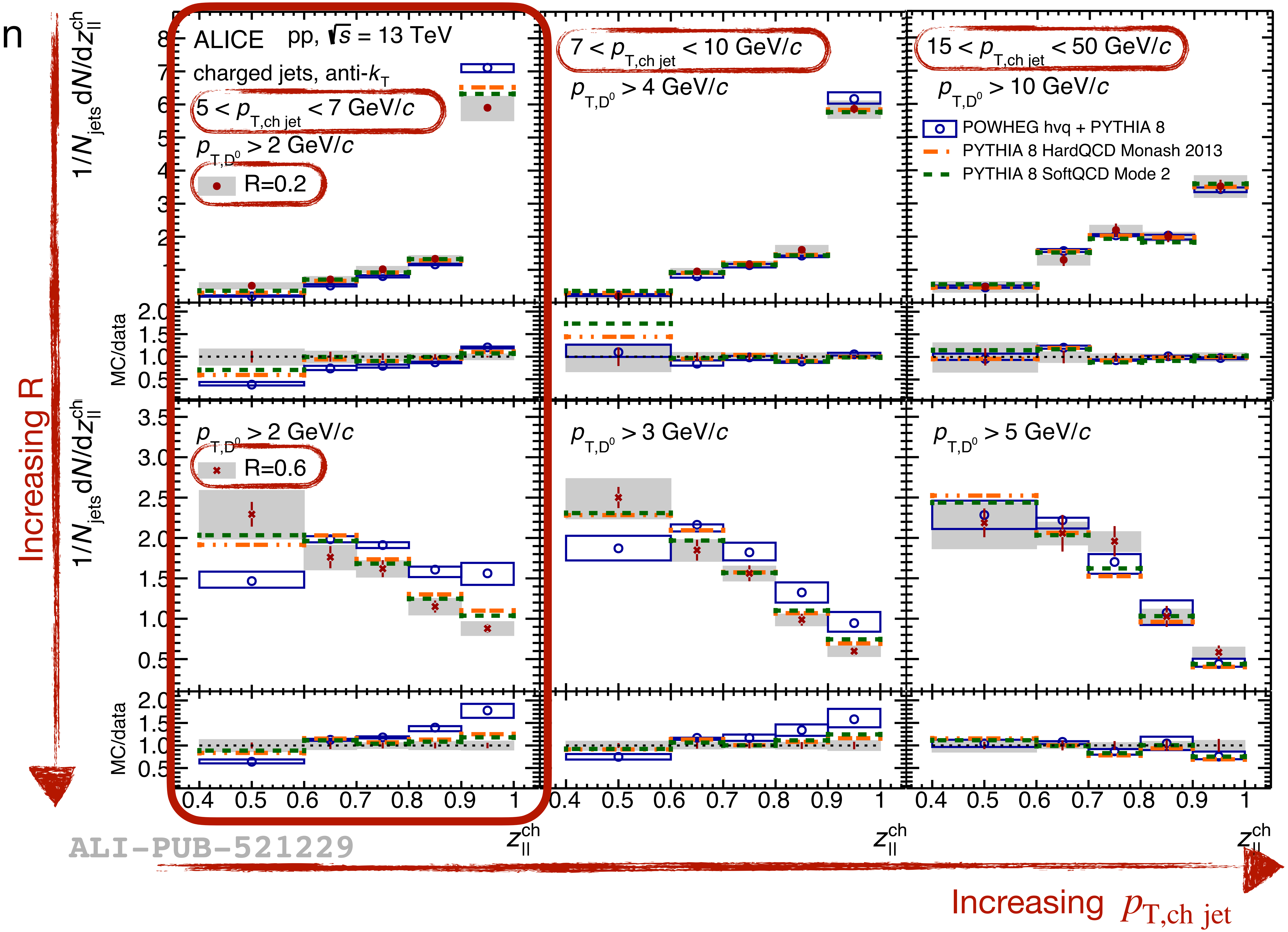

Charm quark fragmentation

- **Hint of a softer fragmentation** in data with respect to model predictions for low $p_{\mathrm{T,ch\ jet}}$ and larger *R*.

- For R = 0.2 and low $p_{\mathrm{T,ch\ jet}}$, D^0 carries a large fraction of $\overrightarrow{p}_{\mathrm{ch\ jet}}$

  →the core of the jet is dominated by the HF hadron.

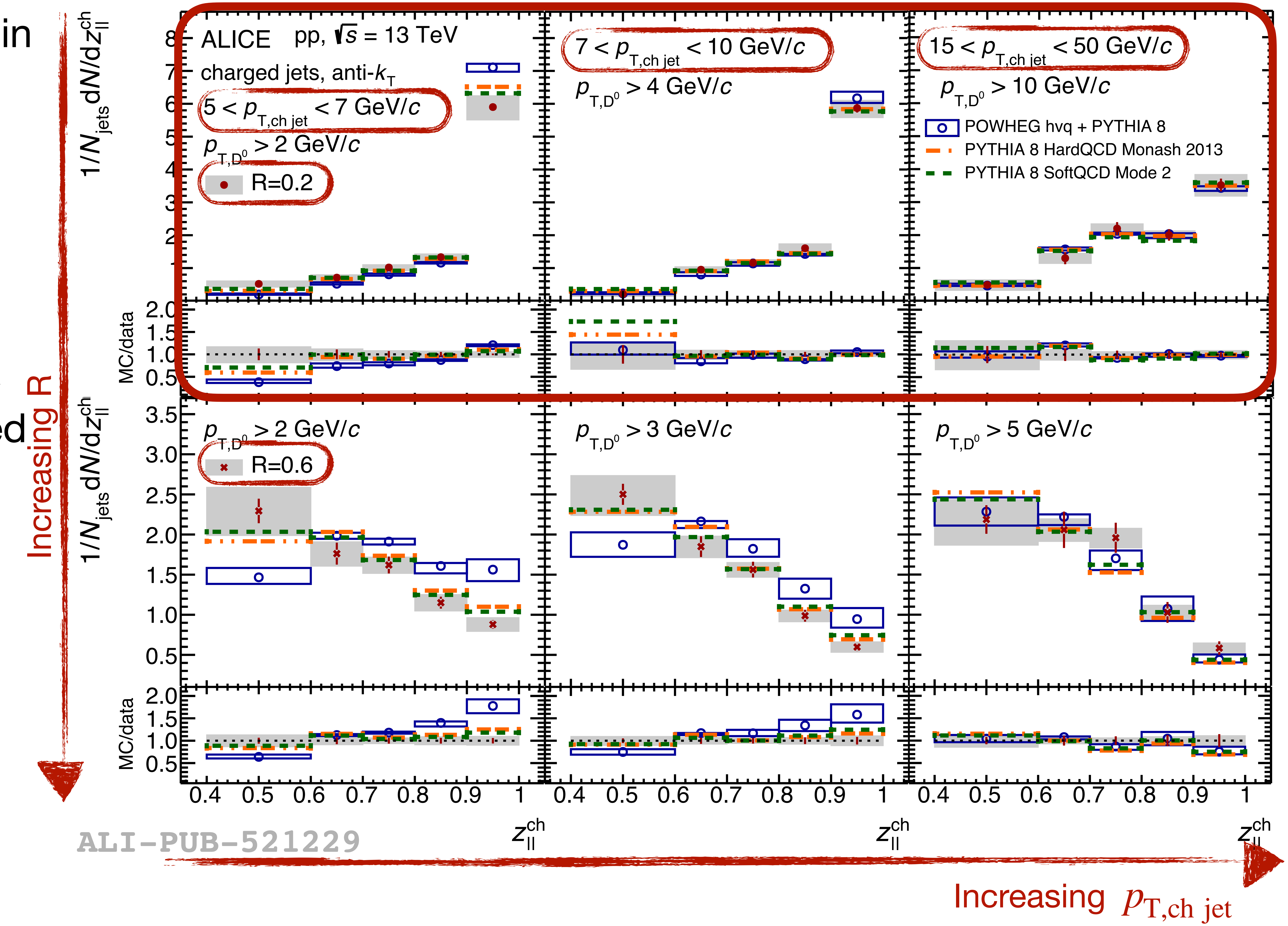

Charm quark fragmentation

- **Hint of a softer fragmentation** in data with respect to model predictions for low $p_{T,ch\ jet}$ and larger *R*.
- For R = 0.2 and low $p_{T,ch\ jet}$, D^0 carries a large fraction of $\overrightarrow{p}_{ch\ jet}$
  →the core of the jet is dominated by the HF hadron.
- At large angles (*R*>0.2) the charm quark emissions are recovered

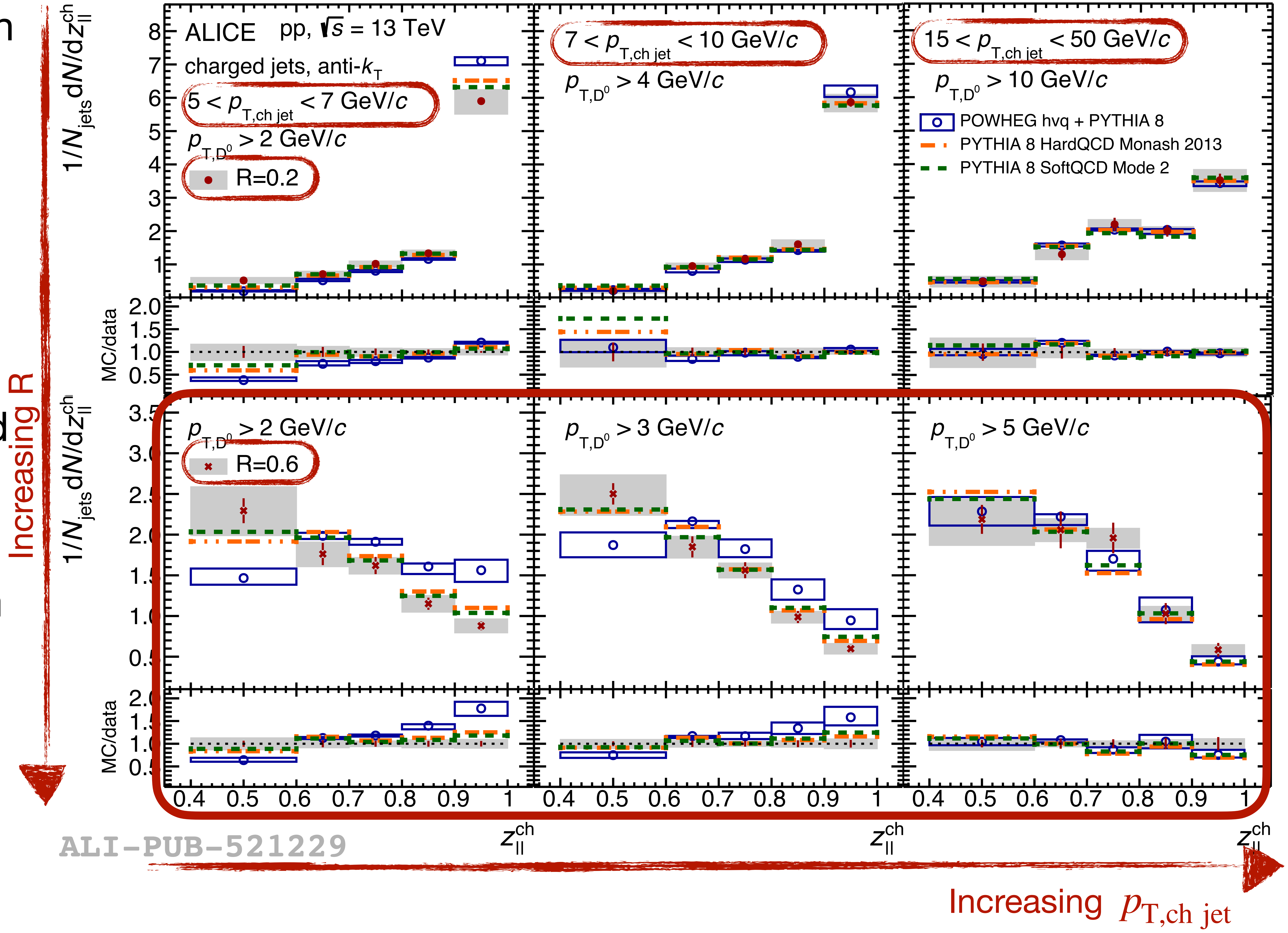

Charm quark fragmentation

Λ_c^+ baryon **softer** than D^0 meson?

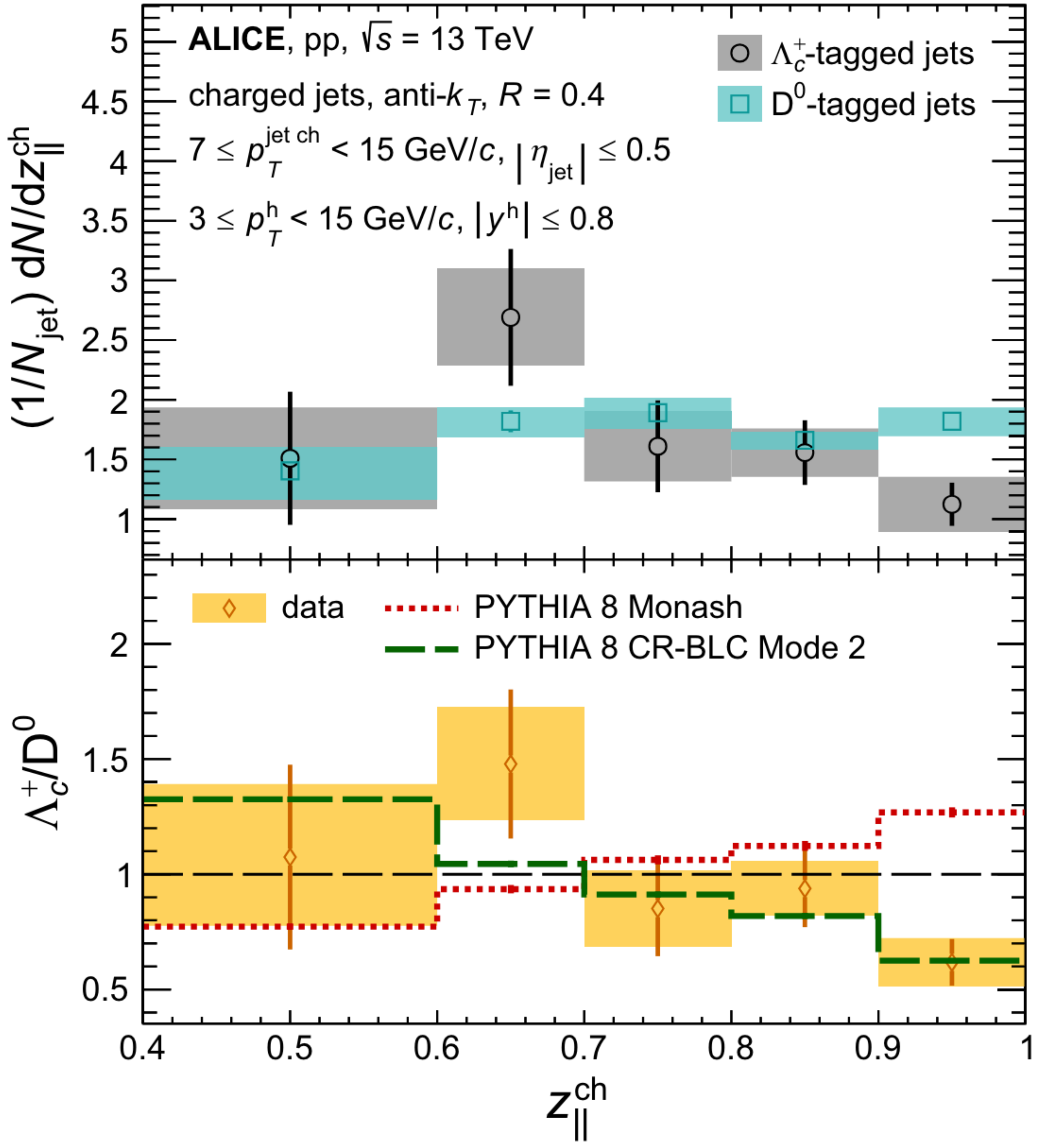

Phys. Rev. D 109 (2024) 072005

Charm quark fragmentation

Λ_c^+ baryon **softer** than D^0 meson?

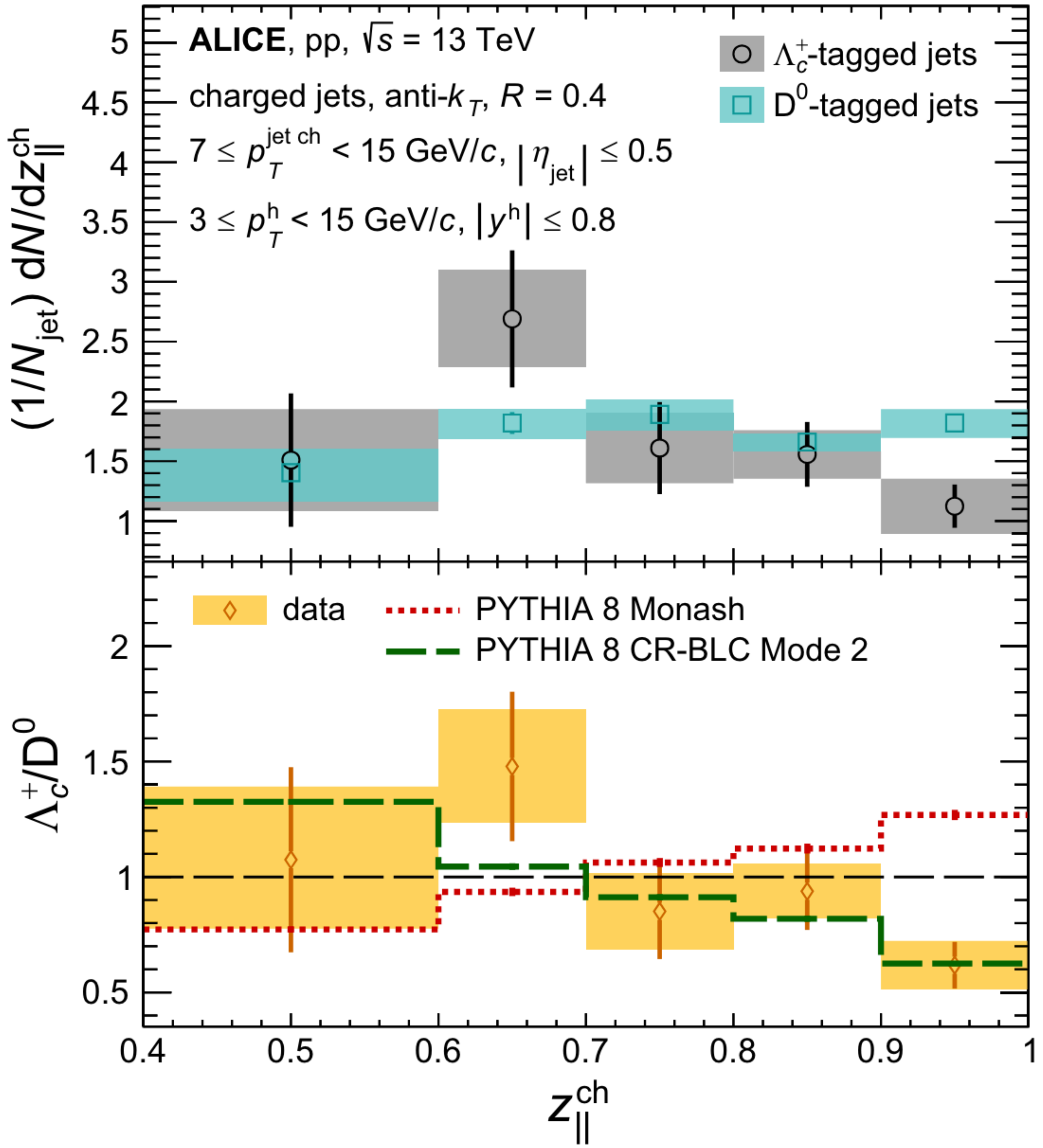

Phys. Rev. D 109 (2024) 072005

Ds^+ meson **harder** than D^0 meson?

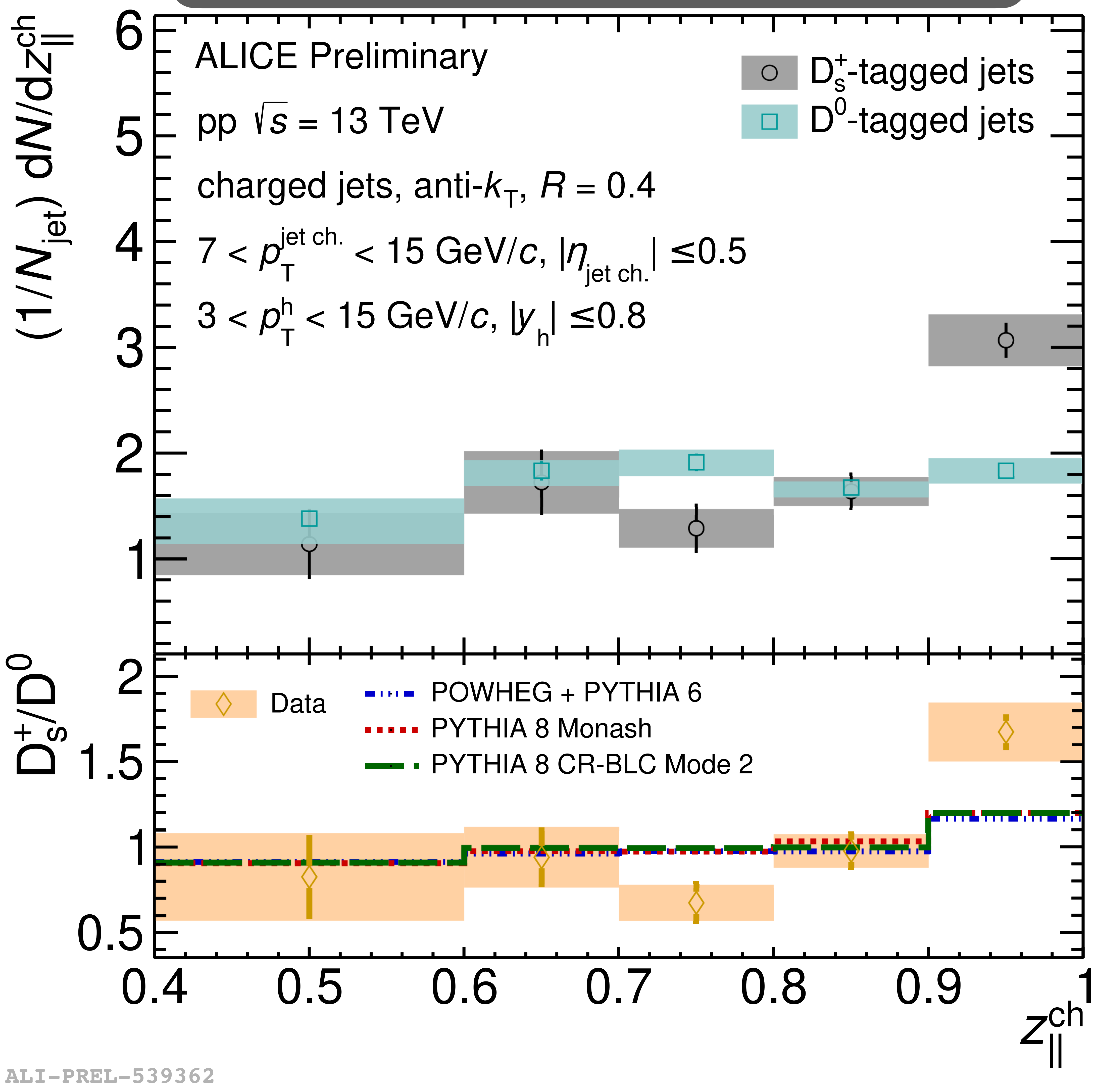

Results

Jet axes distribution

Jet Angularities

Groomed z_g and R_g

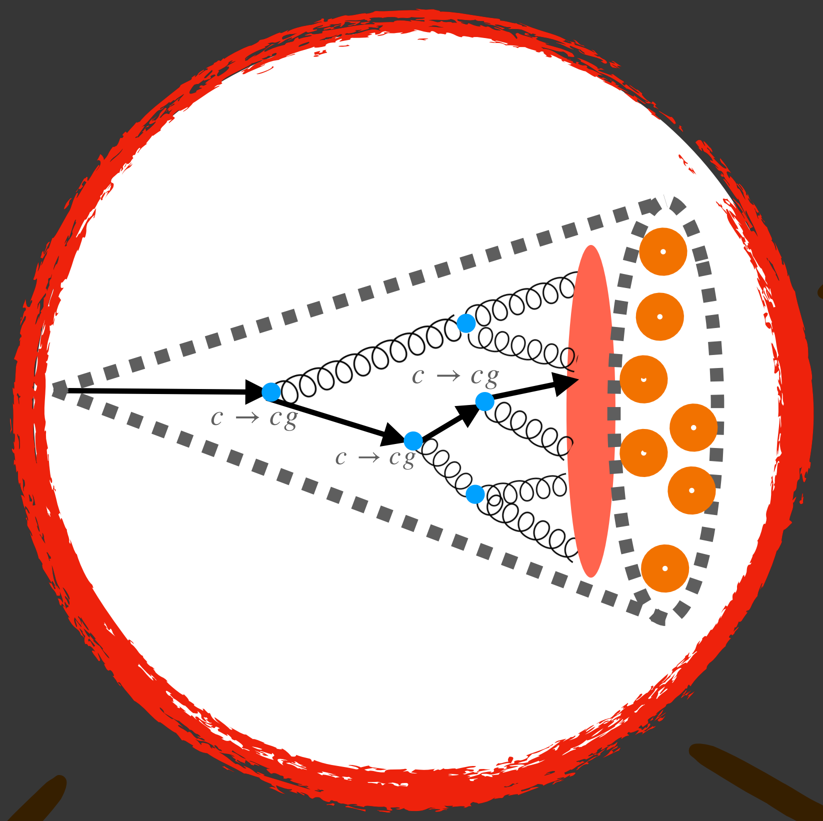

Dead-Cone Effect

Fragmentation function $z_{\parallel}$

Where is the p_T in the jet?

Jet Angularities :

$$\lambda_{\alpha} = \sum_{i \in \text{jet}} \ldots$$

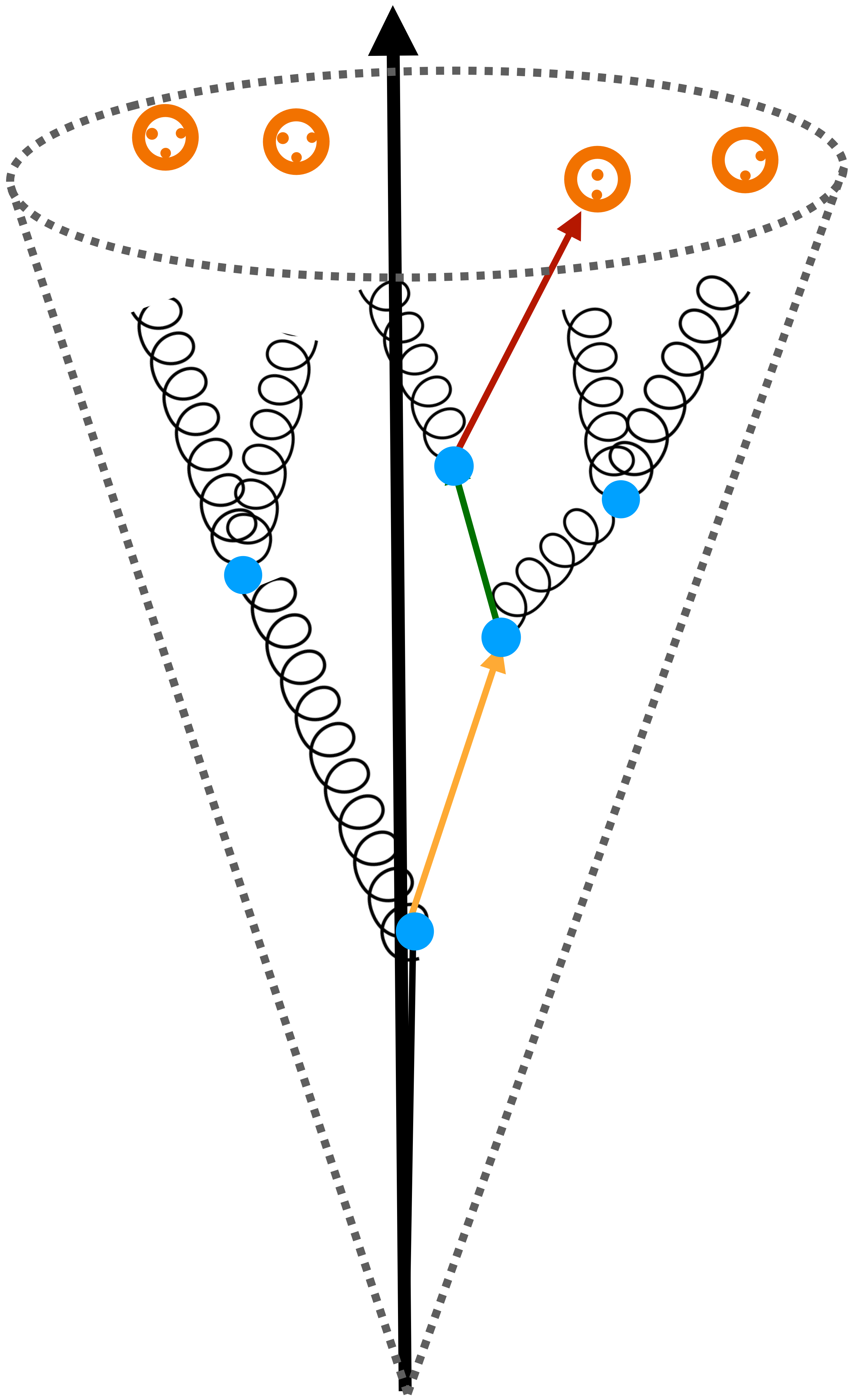

Where is the p_T in the jet?

Jet Angularities :

$$\lambda_\alpha = \sum_{i \in jet} \left(\frac{p_{T,i}}{p_{T,jet}} \right) \ldots$$

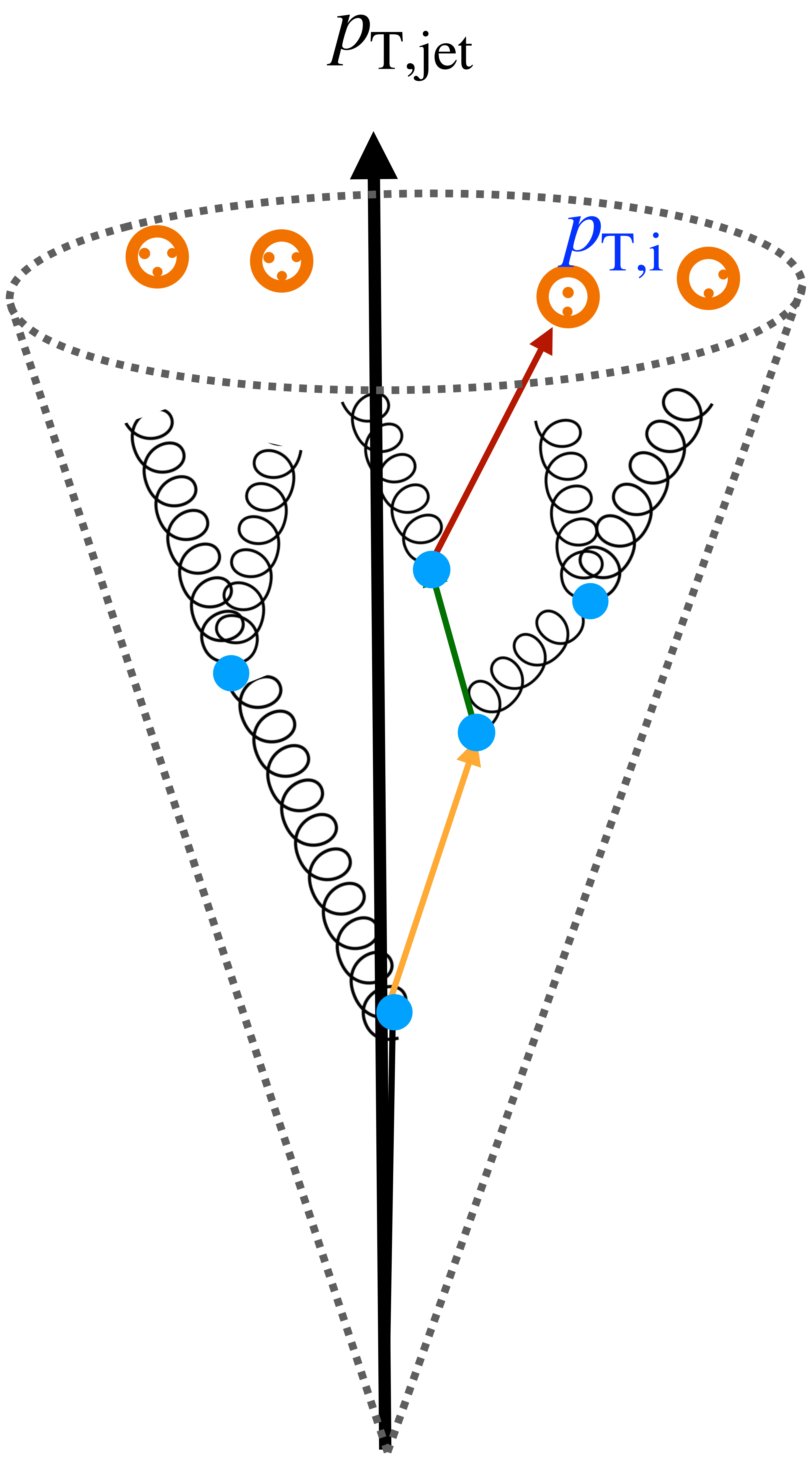

Where is the p_T in the jet?

Jet Angularities :

$$\lambda_\alpha = \sum_{i \in jet} \left(\frac{p_{T,i}}{p_{T,jet}}\right)\left(\frac{\Delta R_{jet,i}}{R_{jet}}\right)^\alpha$$

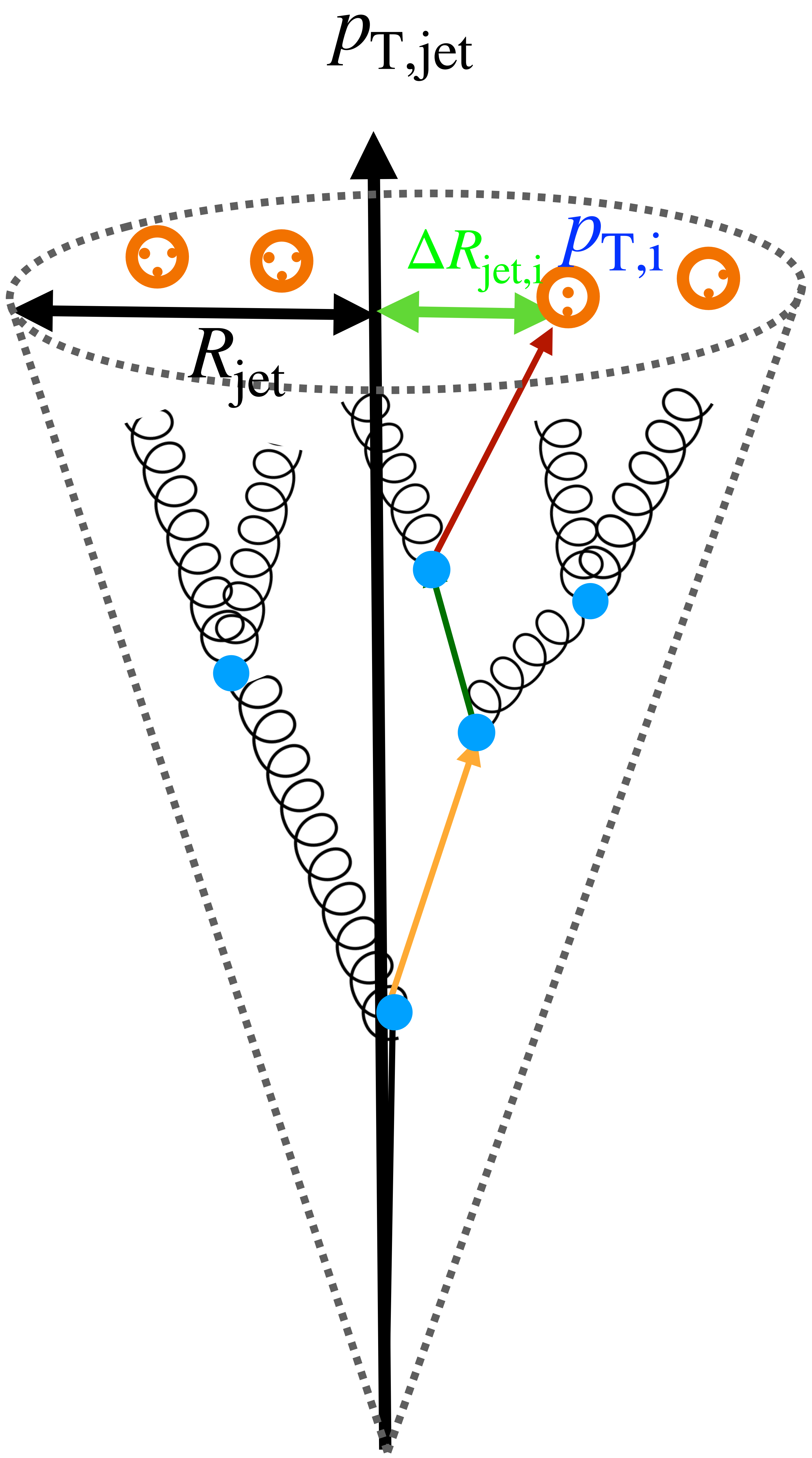

Where is the p_T in the jet?

Jet Angularities :

$$\lambda_\alpha = \sum_{i \in jet} \left(\frac{p_{T,i}}{p_{T,jet}}\right)\left(\frac{\Delta R_{jet,i}}{R_{jet}}\right)^\alpha$$

$$= \sum_{i \in jet} z_i \theta_i^\alpha$$

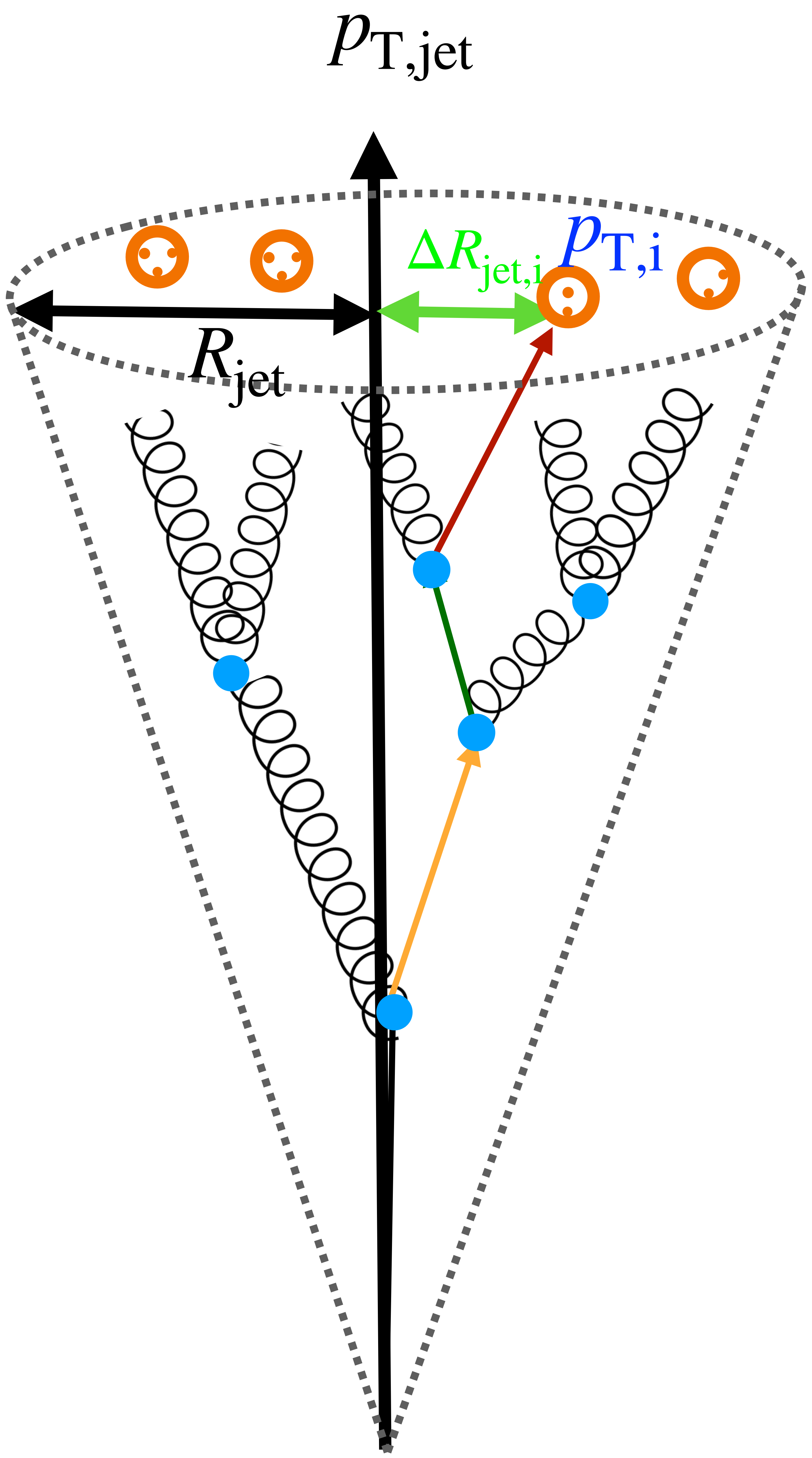

Jet angularities

Jet Angularities :

$$\lambda_{\alpha} = \sum_{i \in jet} \left(\frac{p_{T,i}}{p_{T,jet}}\right)\left(\frac{\Delta R_{jet,i}}{R_{jet}}\right)^{\alpha}$$

$$= \sum_{i \in jet} z_i \theta_i^{\alpha}$$

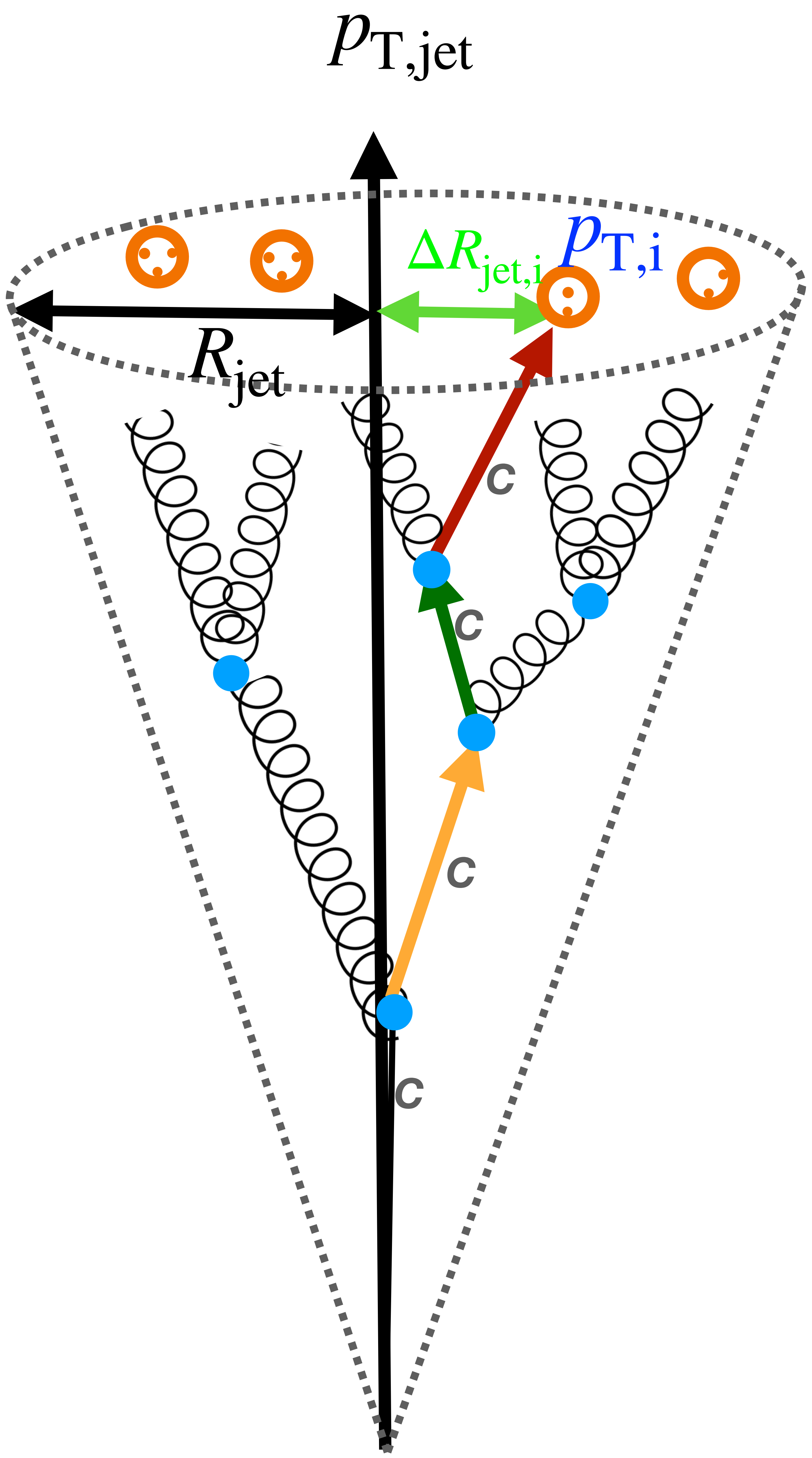

Jet angularities

Jet Angularities :

$$\lambda_{\alpha} = \sum_{i \in jet} \left(\frac{p_{T,i}}{p_{T,jet}}\right)\left(\frac{\Delta R_{jet,i}}{R_{jet}}\right)^{\alpha}$$

$$= \sum_{i \in jet} z_i \theta_i^{\alpha}$$

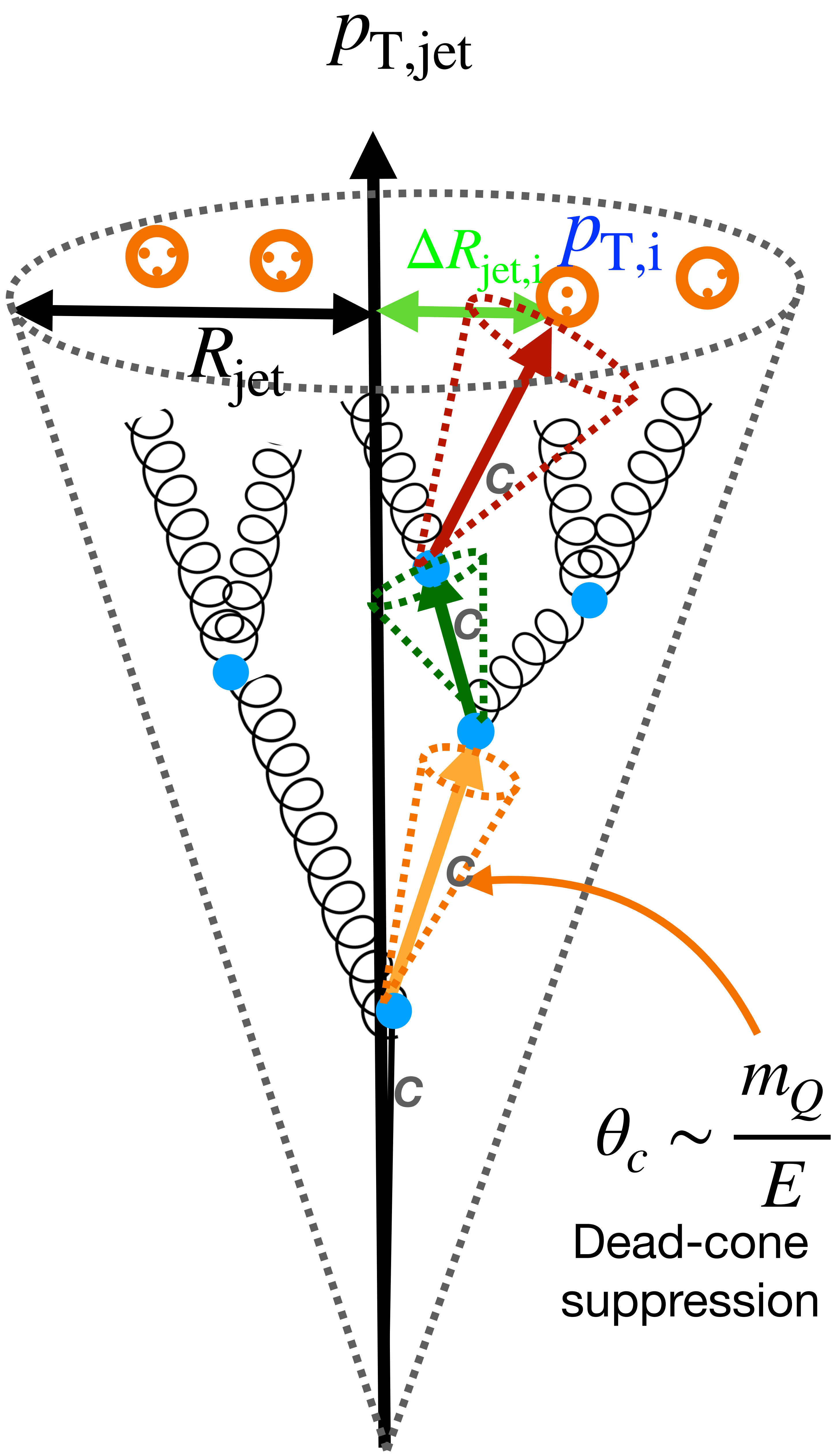

Jet angularities

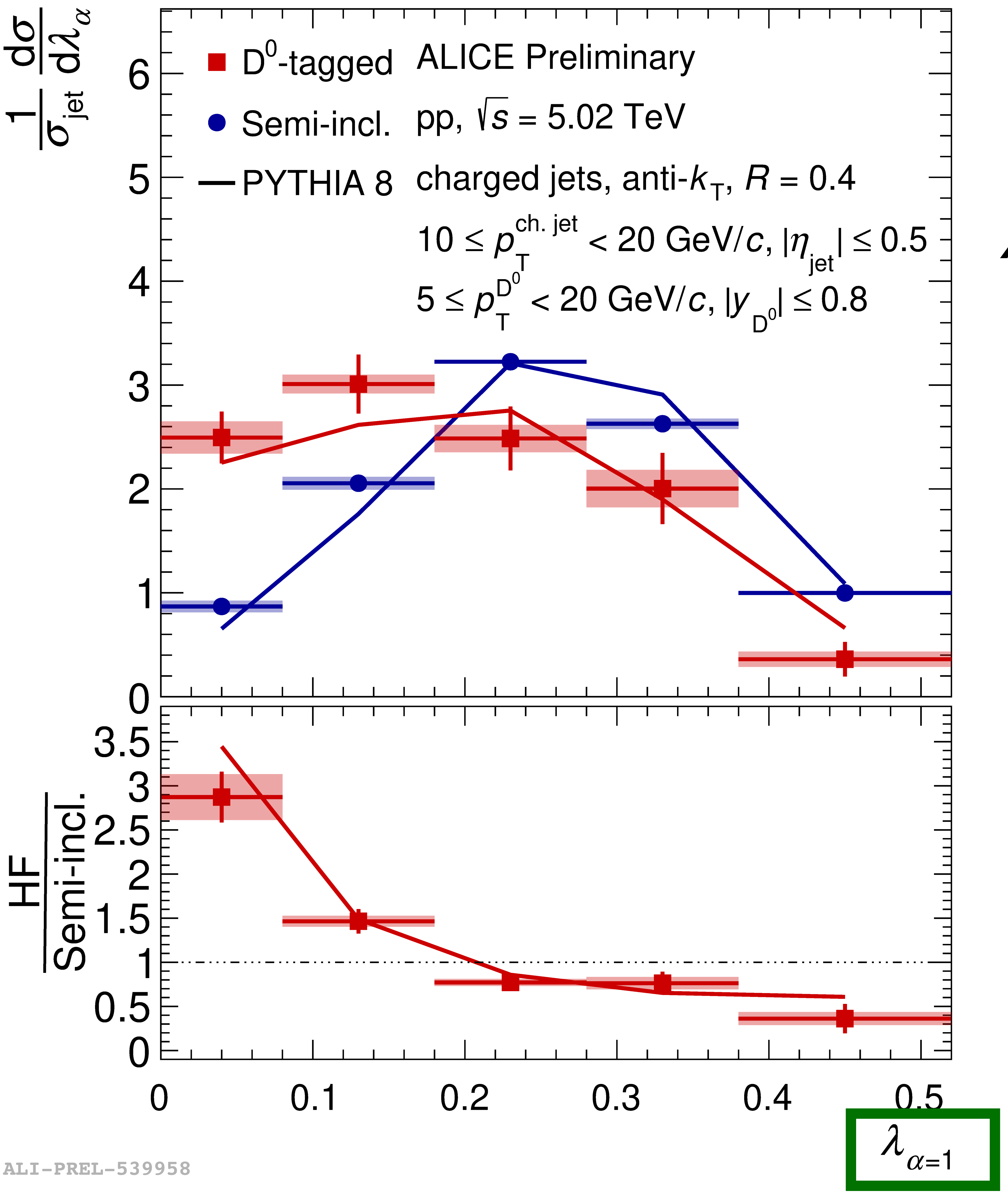

Jet Angularities :

$$\lambda_\alpha = \sum_{i \in jet} \left(\frac{p_{T,i}}{p_{T,jet}}\right)\left(\frac{\Delta R_{jet,i}}{R_{jet}}\right)^\alpha$$

$$= \sum_{i \in jet} z_i \theta_i^\alpha$$

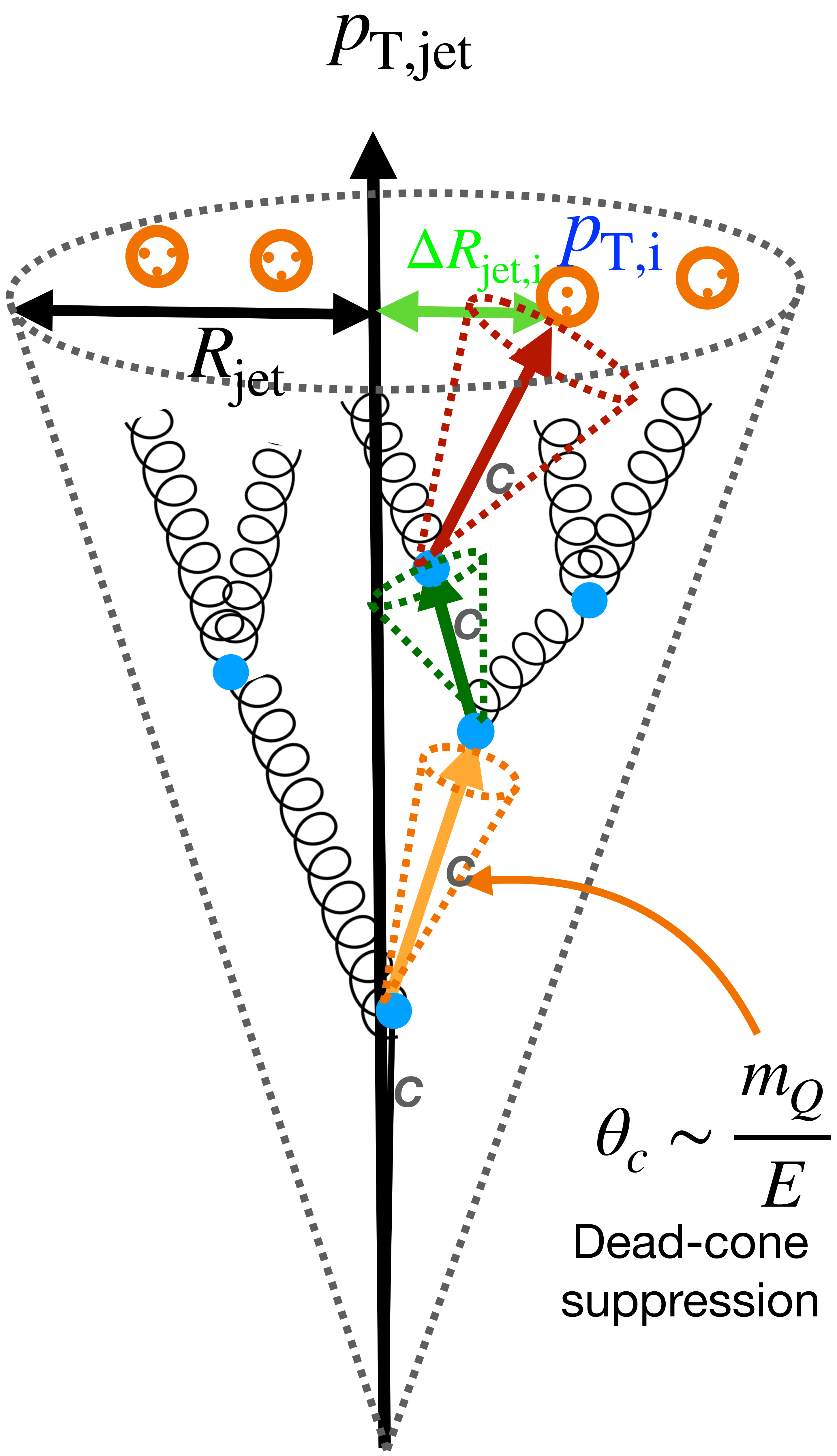

Jet angularities

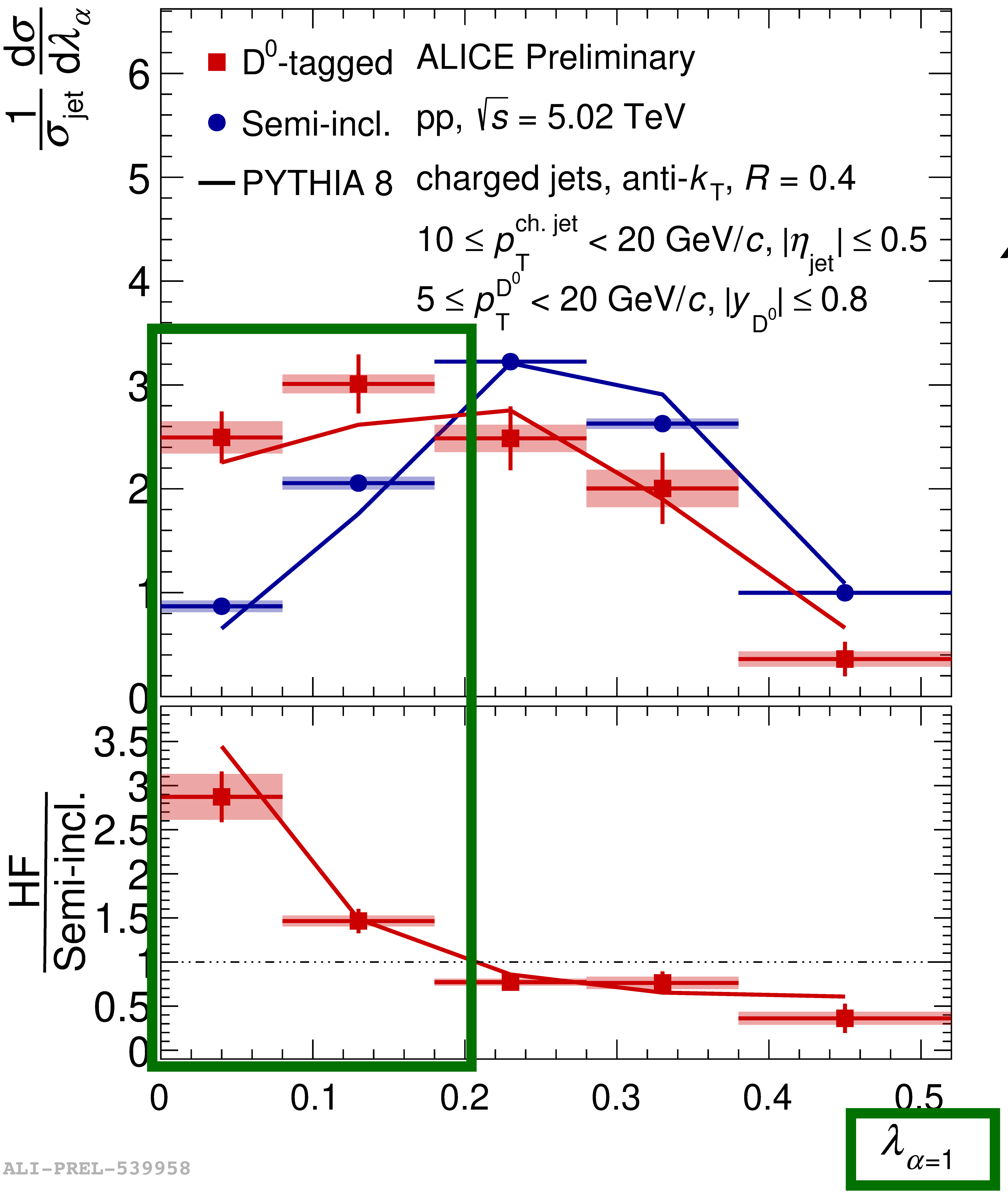

Jet Angularities :

$$\lambda_\alpha = \sum_{i \in jet} \left(\frac{p_{T,i}}{p_{T,jet}}\right)\left(\frac{\Delta R_{jet,i}}{R_{jet}}\right)^\alpha$$

$$= \sum_{i \in jet} z_i \theta_i^\alpha$$

charm distribution shifted to lower values of $\lambda_{\alpha=1}$
→Dead-cone/mass effects

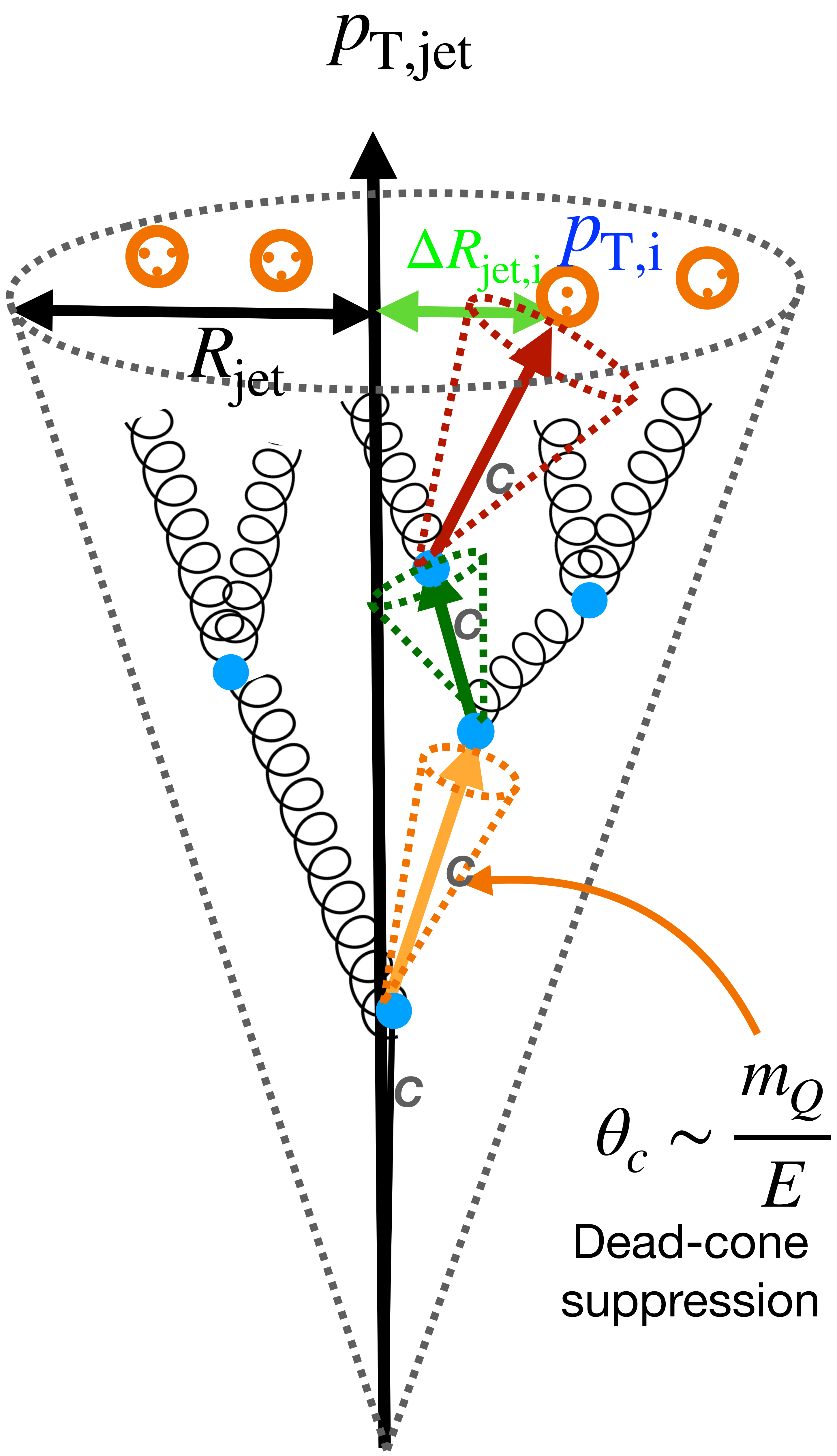

Jet angularities

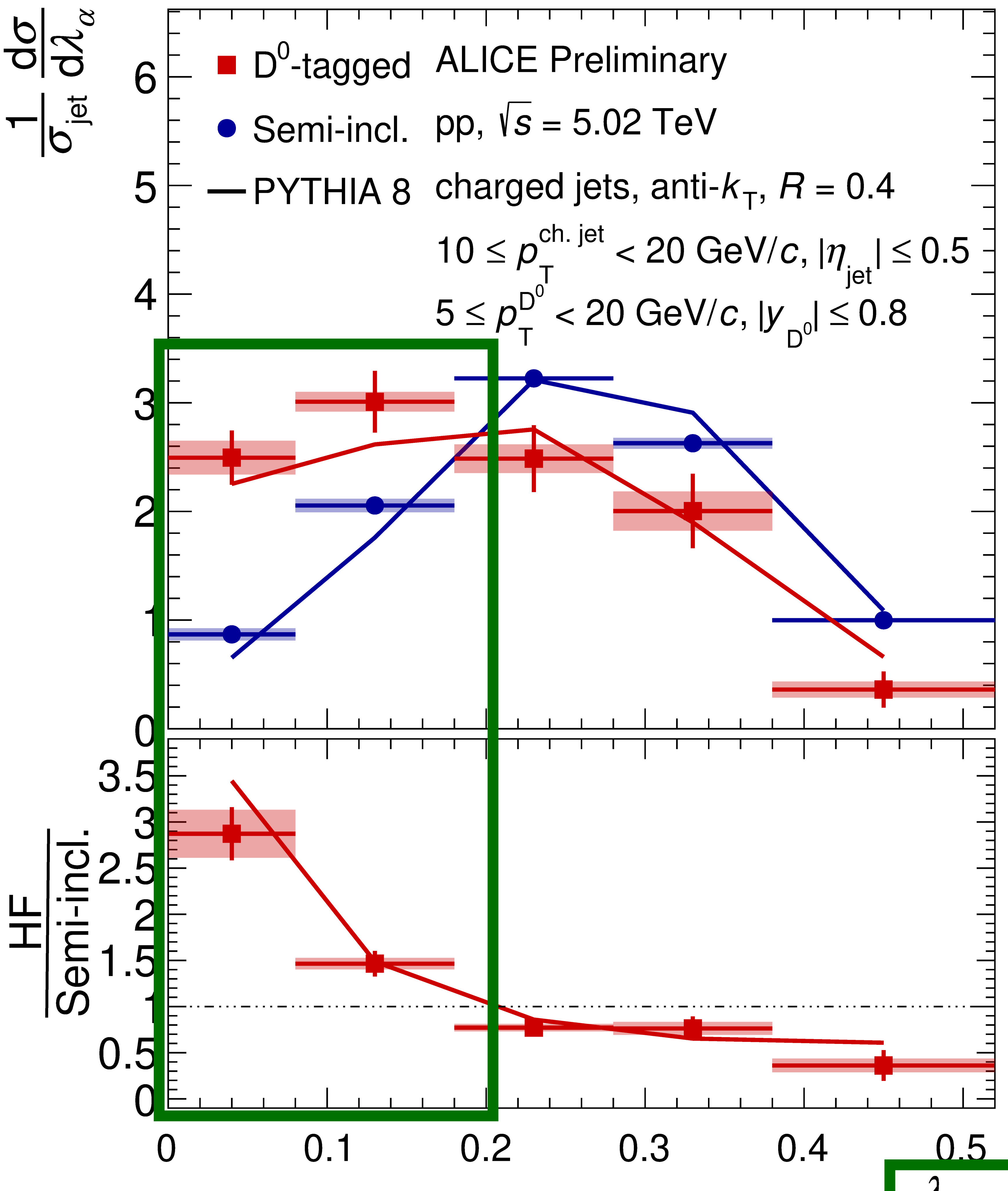

ALI-PREL-539958

$\lambda_{\alpha=1}$

Jet Angularities :

$$\lambda_\alpha = \sum_{i \in jet} \left(\frac{p_{T,i}}{p_{T,jet}}\right)\left(\frac{\Delta R_{jet,i}}{R_{jet}}\right)^\alpha$$

$$= \sum_{i \in jet} z_i \theta_i^\alpha$$

Higher α → more weight on wide angle emissions

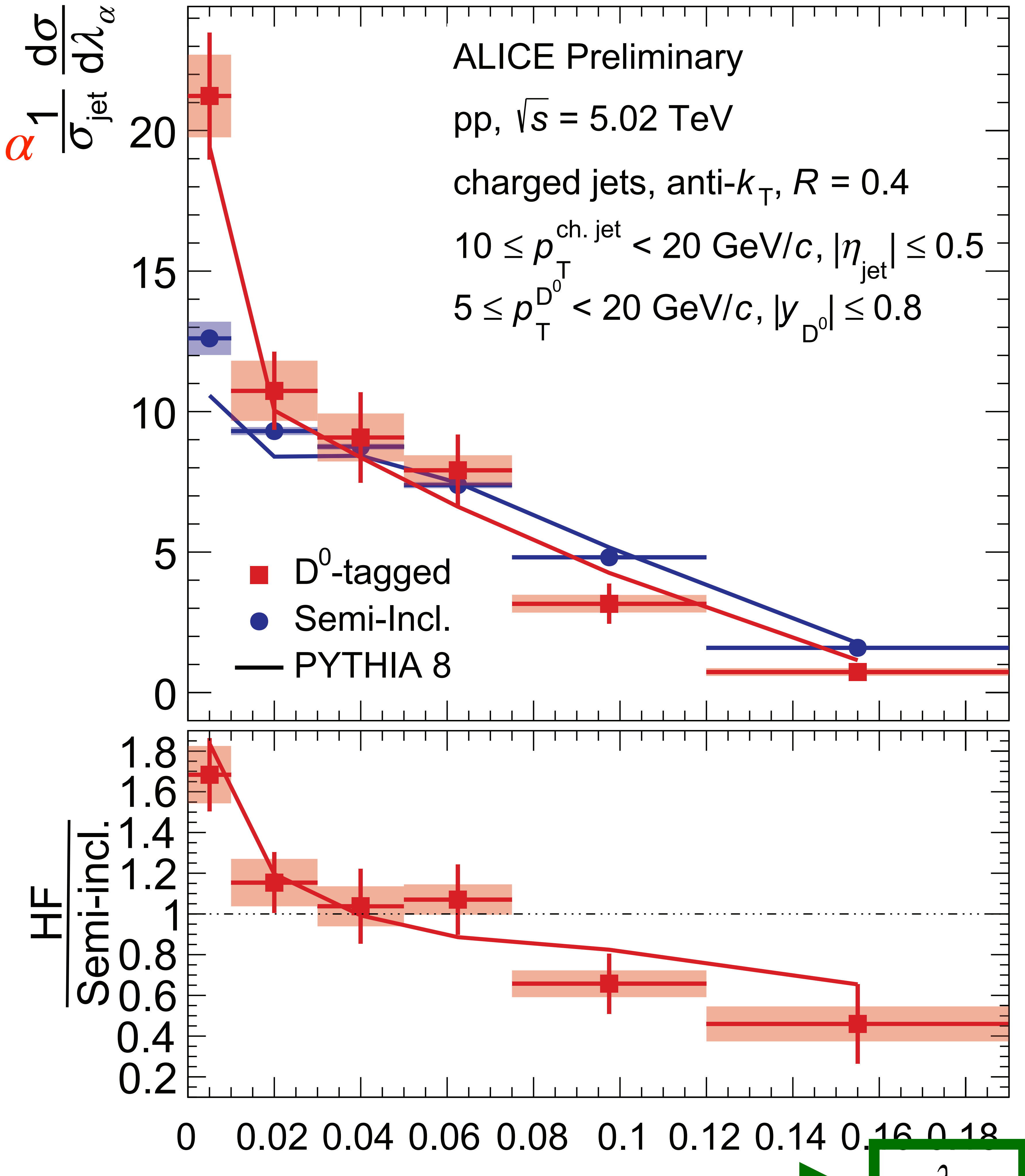

ALI-PREL-540855

$\lambda_{\alpha=3}$

Jet angularities

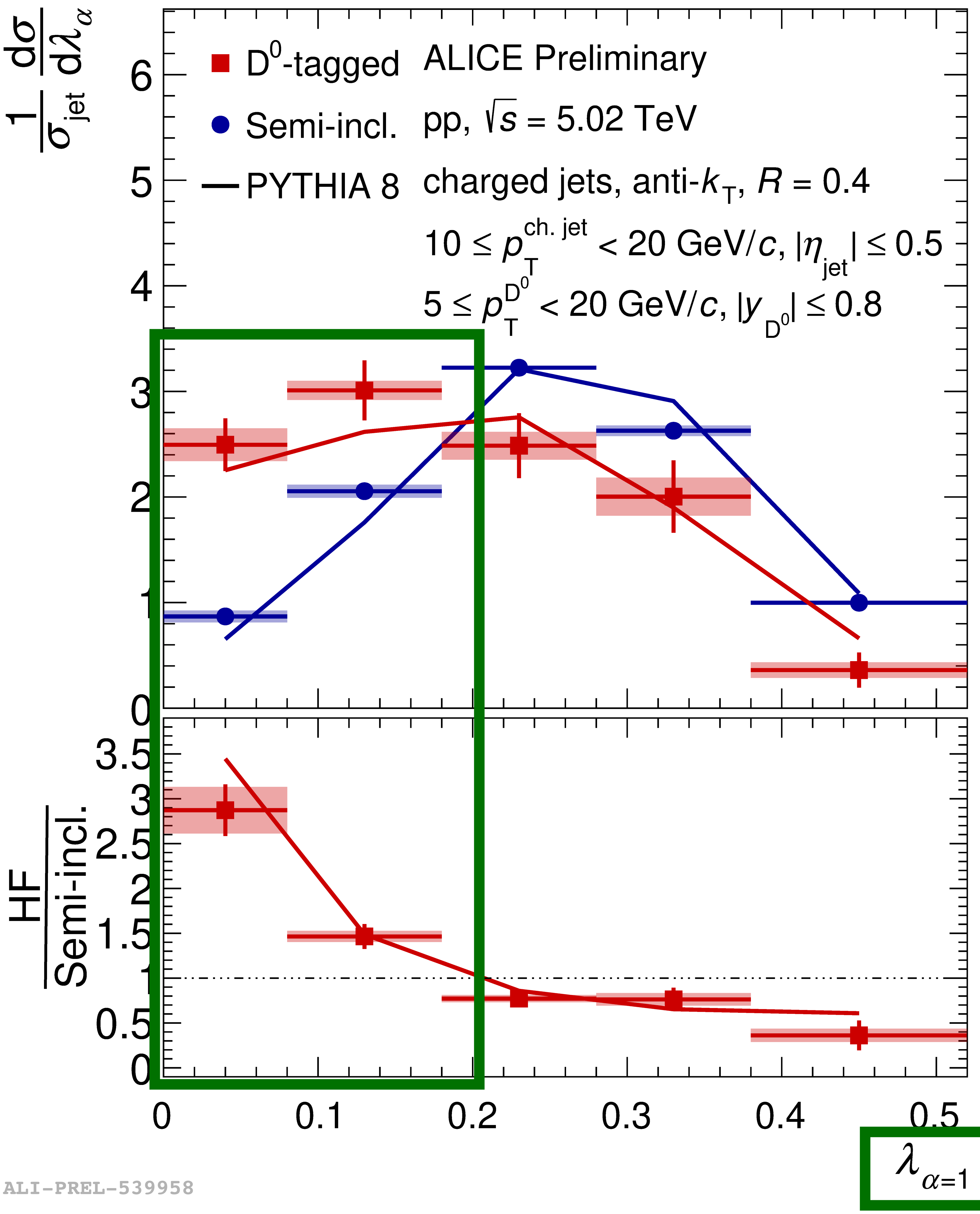

Jet Angularities :

$$\lambda_\alpha = \sum_{i \in jet} \left(\frac{p_{T,i}}{p_{T,jet}} \right) \left(\frac{\Delta R_{jet,i}}{R_{jet}} \right)^\alpha$$

$$= \sum_{i \in jet} z_i \theta_i^\alpha$$

Higher α → more weight on wide angle emissions

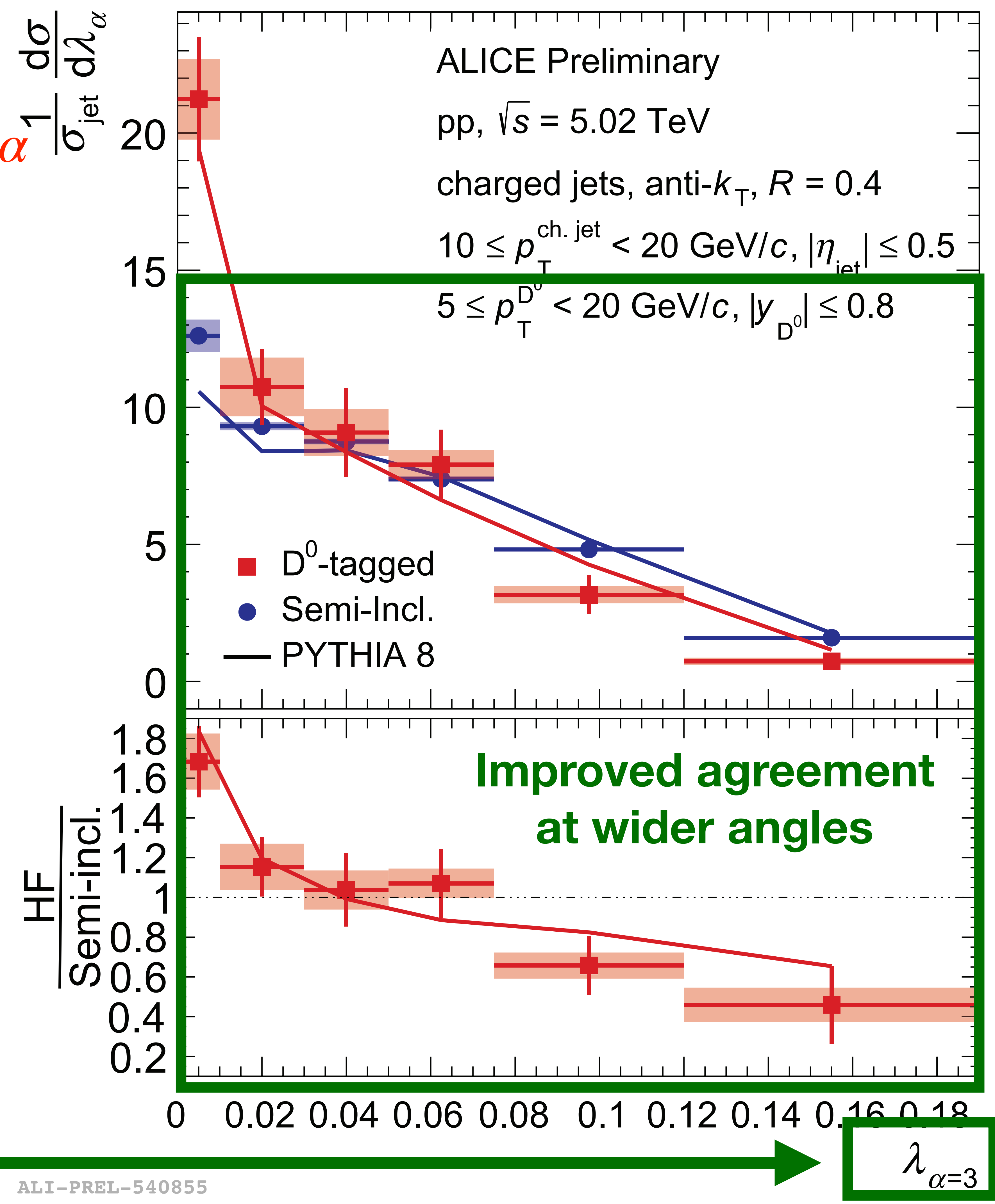

$\lambda_{\alpha=1}$ → $\lambda_{\alpha=3}$

Mass effects → **Casimir color effects**

Results

Jet axes distribution

Jet Angularities

Groomed z_g and R_g

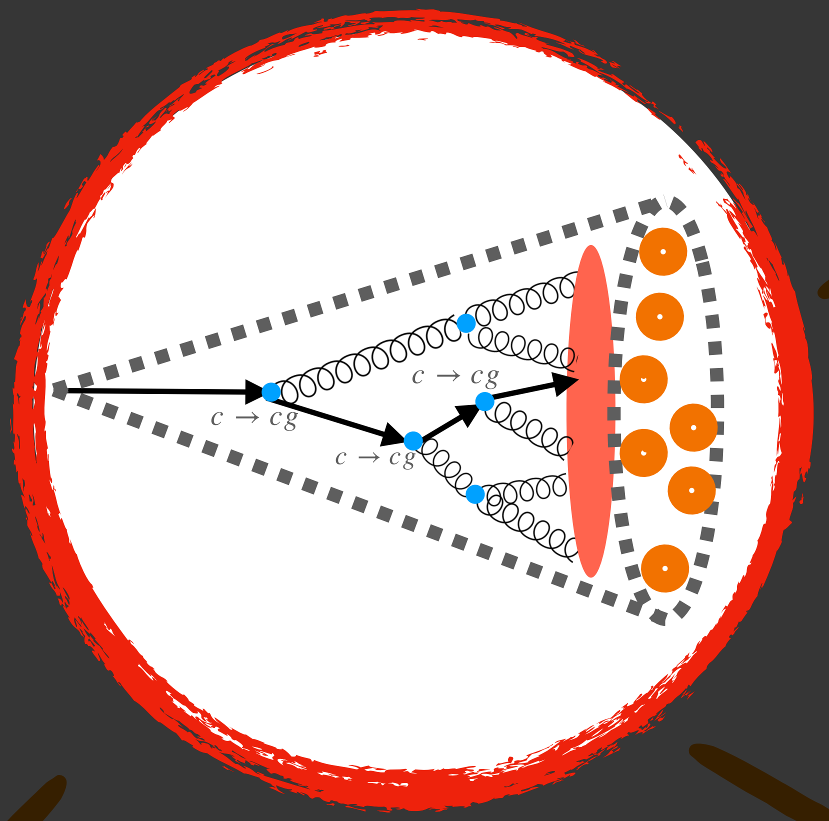

Dead-Cone Effect

Fragmentation function $z_{\parallel}$

Jet axes distribution: $\Delta R_{\mathrm{D}^0,\mathrm{jet}}$

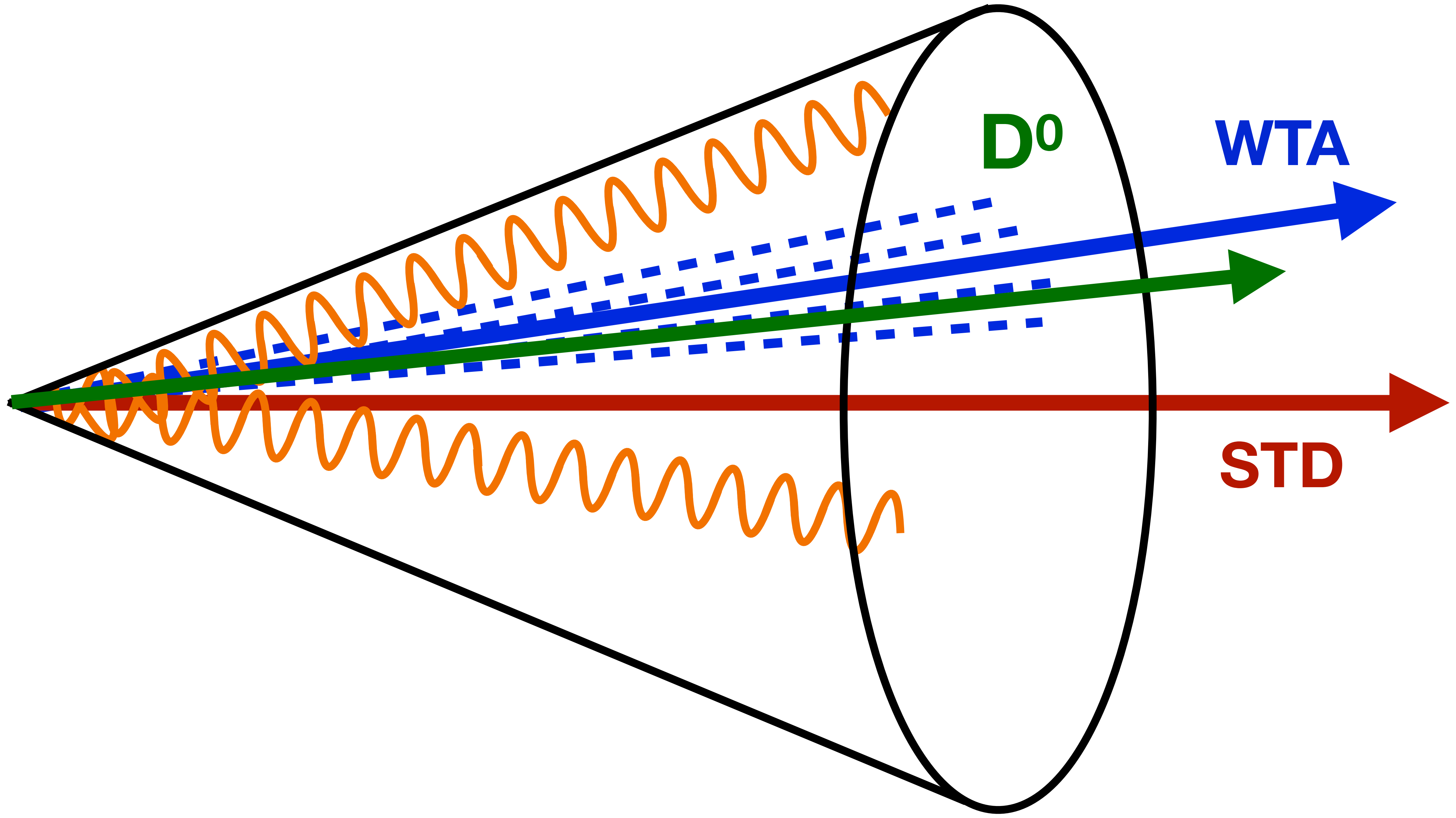

- $\Delta R_{\mathrm{D}^0,\mathrm{jet}}$ is difference between jet axis and D^0
- different sensitivity to soft radiation can be obtained by exploiting different definitions of the jet axis

Jet axes distribution: $\Delta R_{\mathrm{D}^0,\mathrm{jet}}$

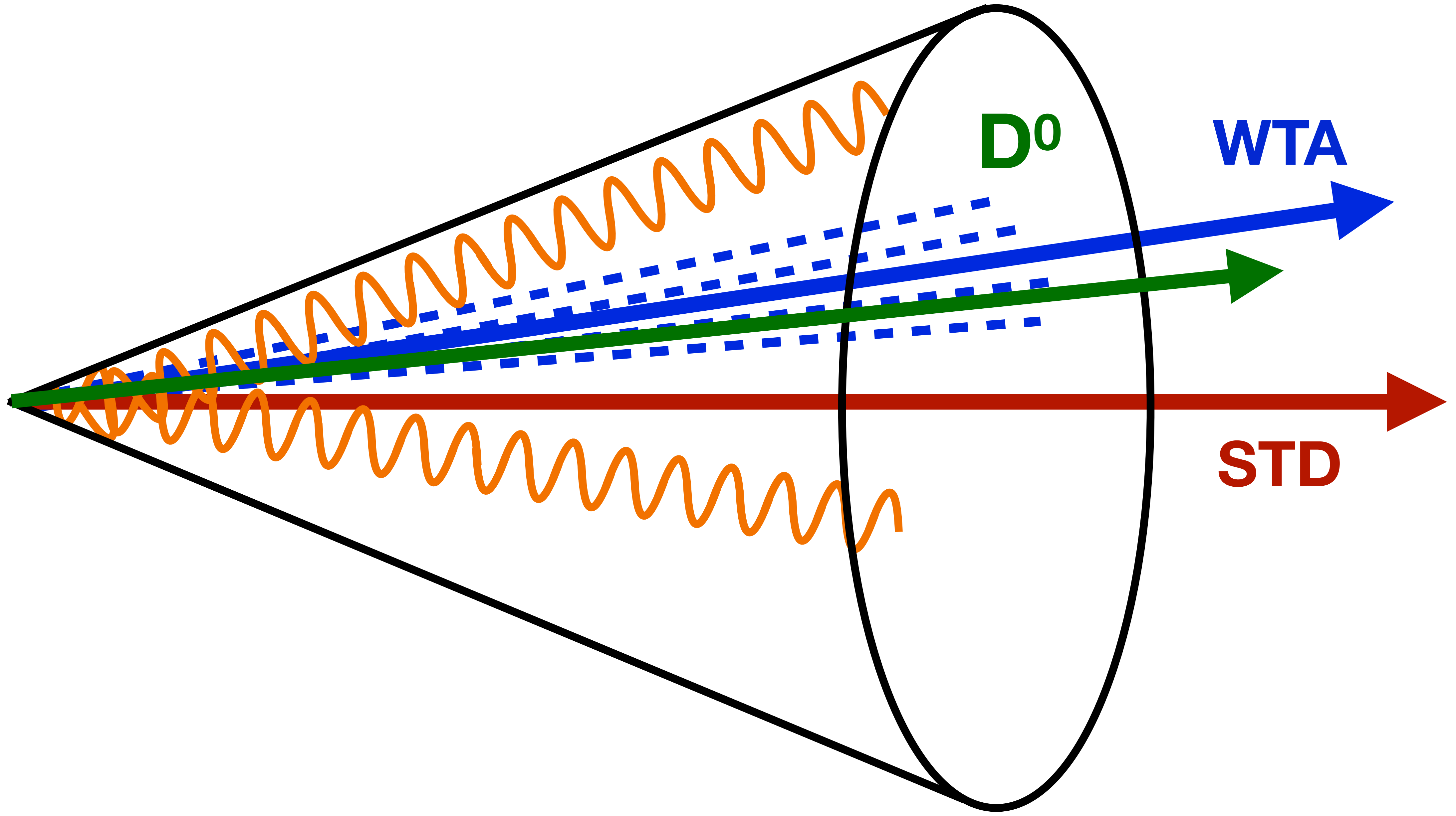

- $\Delta R_{\mathrm{D}^0,\mathrm{jet}}$ is difference between jet axis and D^0
- different sensitivity to soft radiation can be obtained by exploiting different definitions of the jet axis

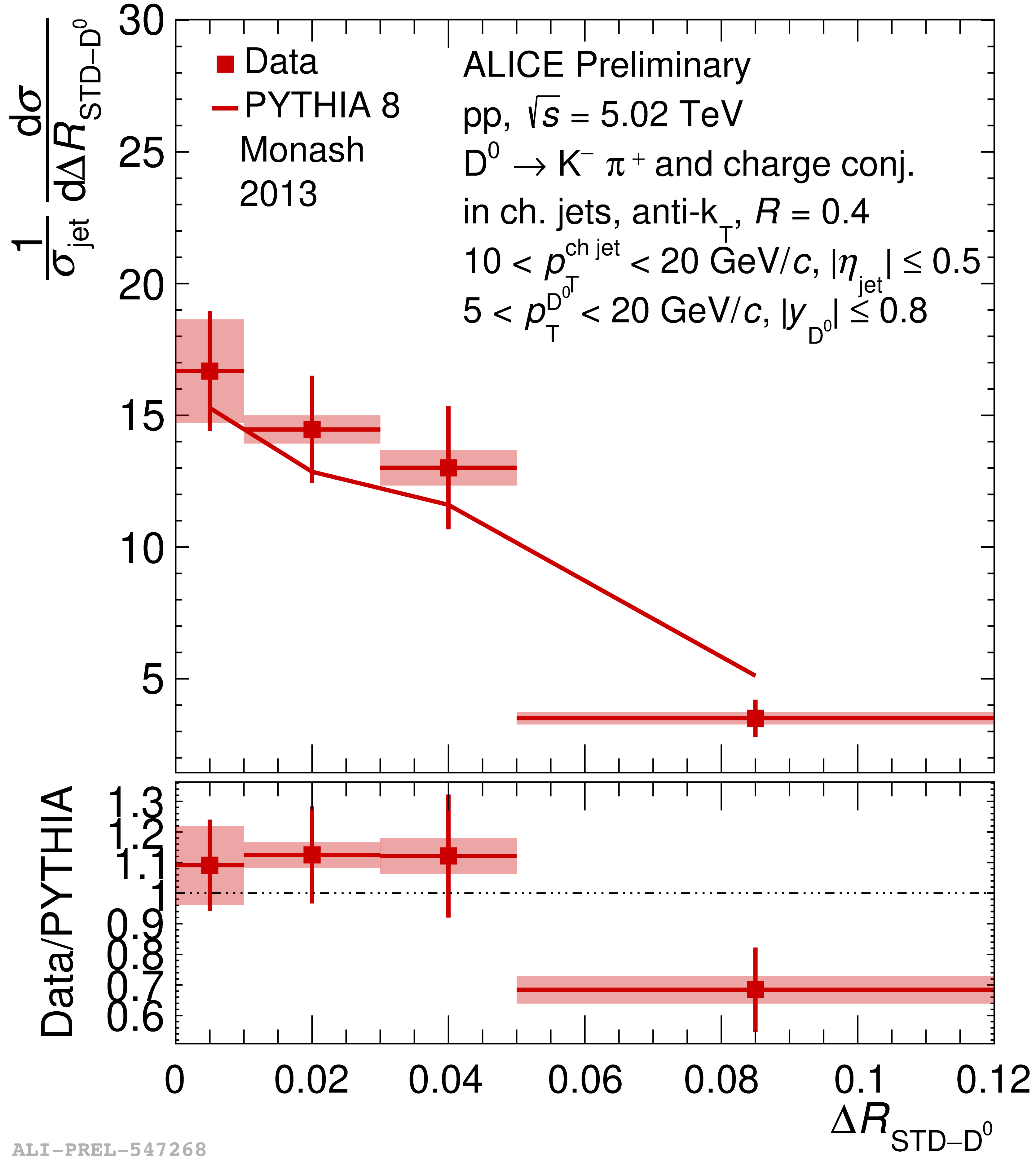

Standard jet (STD):
The jet axis resulting from a D^0-tagged sample of jets, clustered with anti-k_T algorithm, R = 0.4.

Jet axes distribution: $\Delta R_{D^0,jet}$

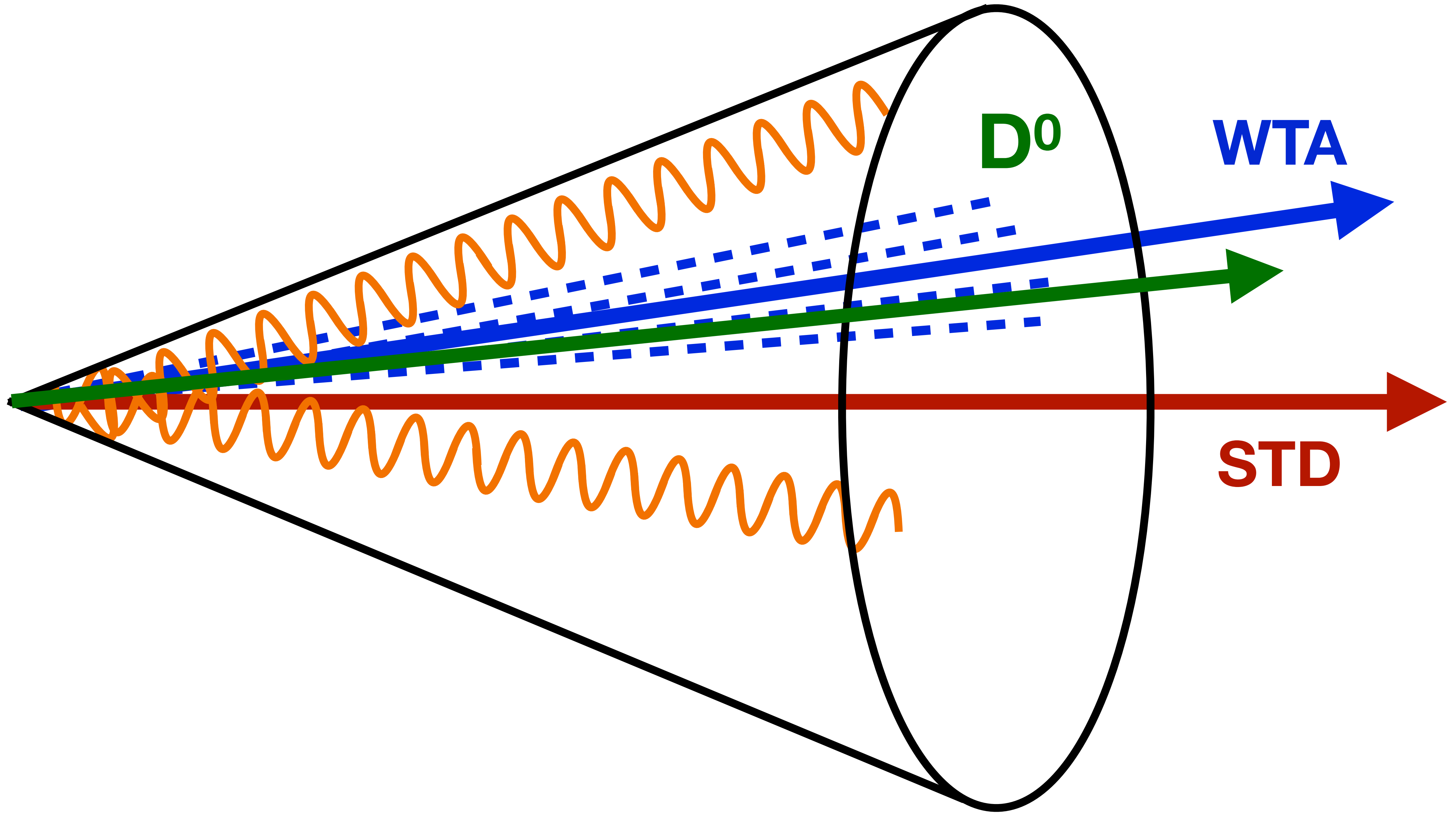

- $\Delta R_{D^0,jet}$ is difference between jet axis and D^0
- different sensitivity to soft radiation can be obtained by exploiting different definitions of the jet axis

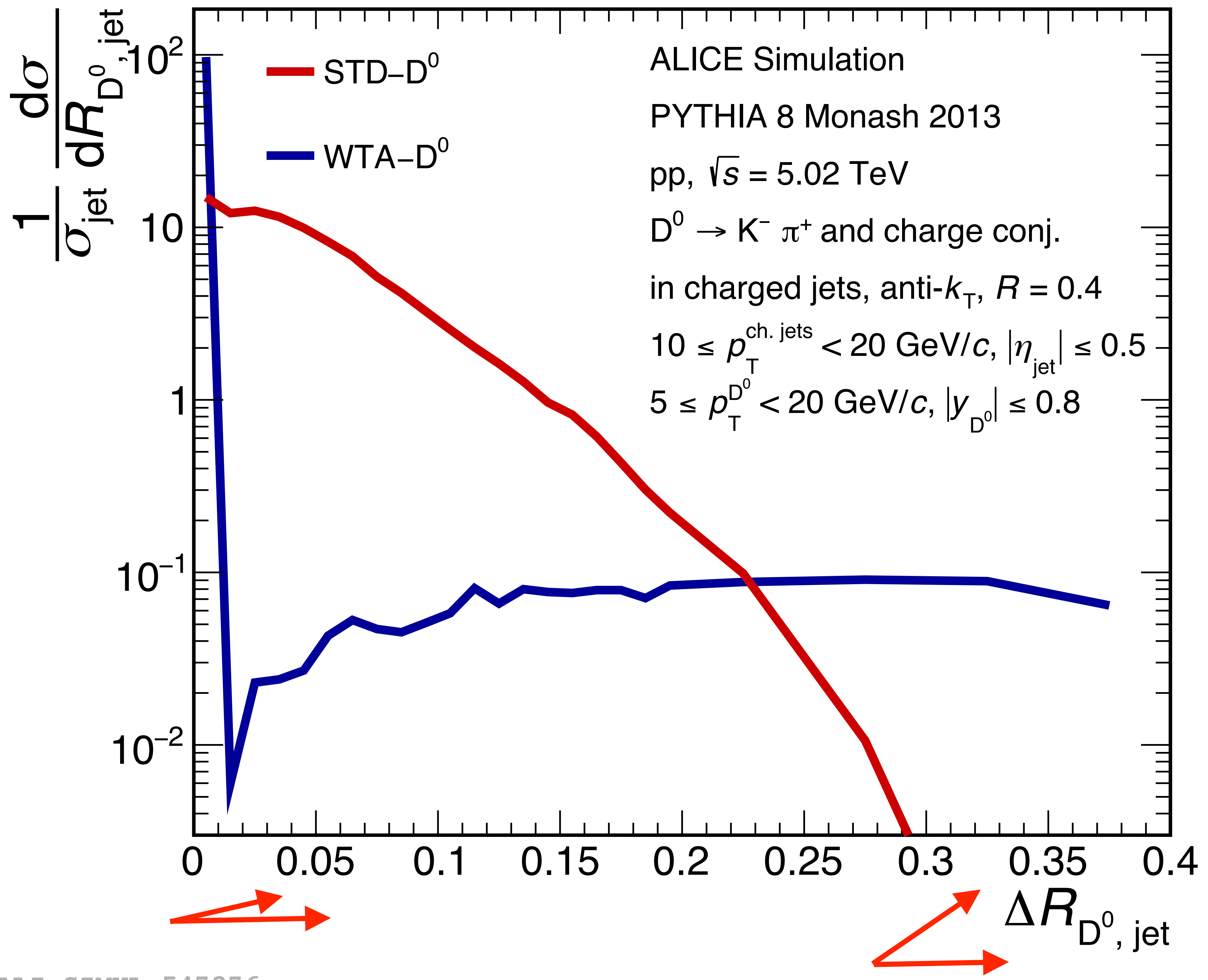

Standard jet (STD):
The jet axis resulting from a D^0-tagged sample of jets, clustered with anti-k_T algorithm, R = 0.4.

Winner-Take-all jet (WTA):
Original jet reclustered with Cambridge-Aachen algorithm and recombined using WTA recombination scheme.

Jet axes distribution: $\Delta R_{D^0,\mathrm{jet}}$

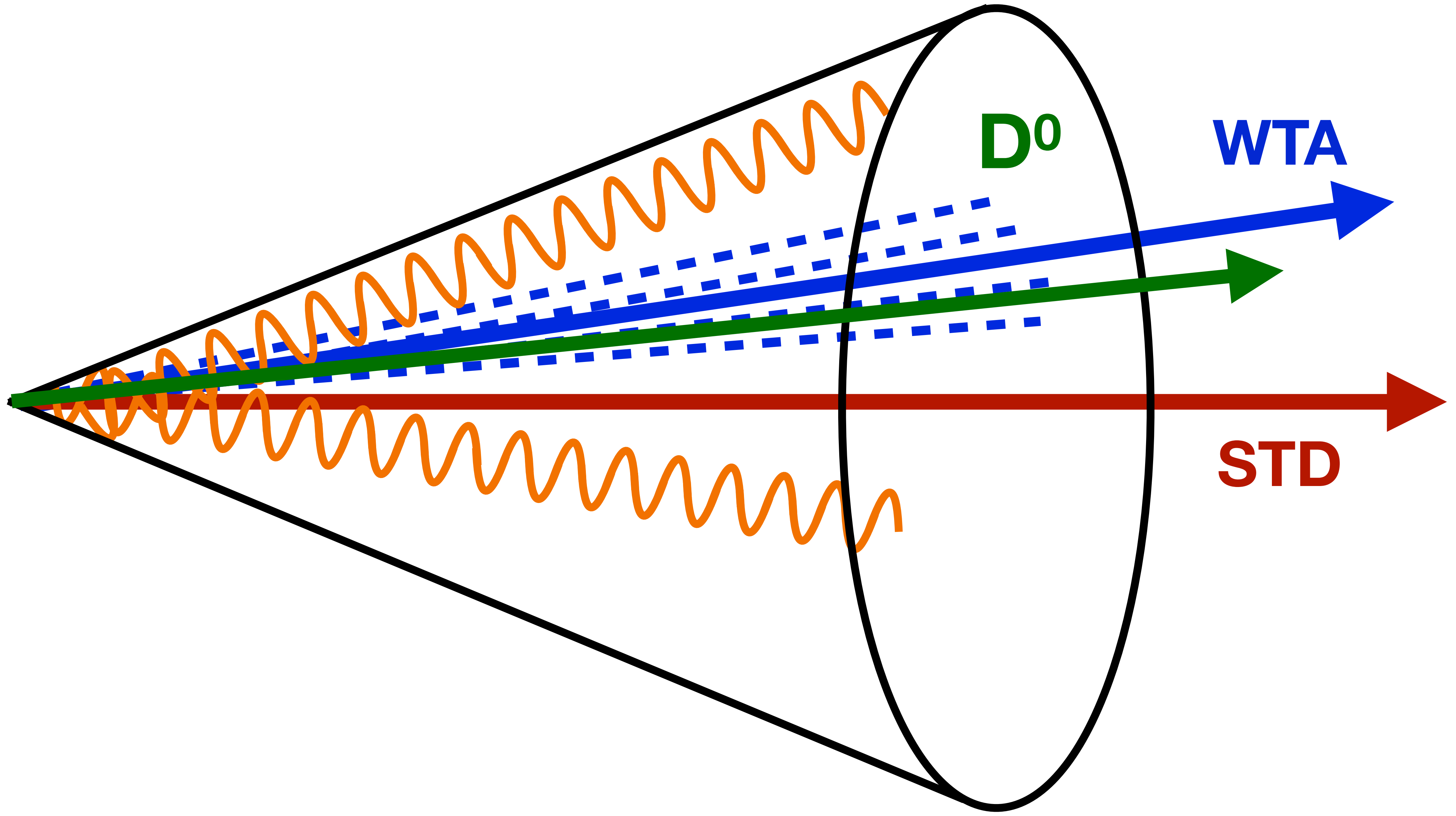

- $\Delta R_{D^0,\mathrm{jet}}$ is difference between jet axis and D^0
- different sensitivity to soft radiation can be obtained by exploiting different definitions of the jet axis

Standard jet (STD):
The jet axis resulting from a D⁰-tagged sample of jets, clustered with anti-k_T algorithm, R = 0.4.

Winner-Take-all jet (WTA):
Original jet reclustered with Cambridge-Aachen algorithm and recombined using WTA recombination scheme.

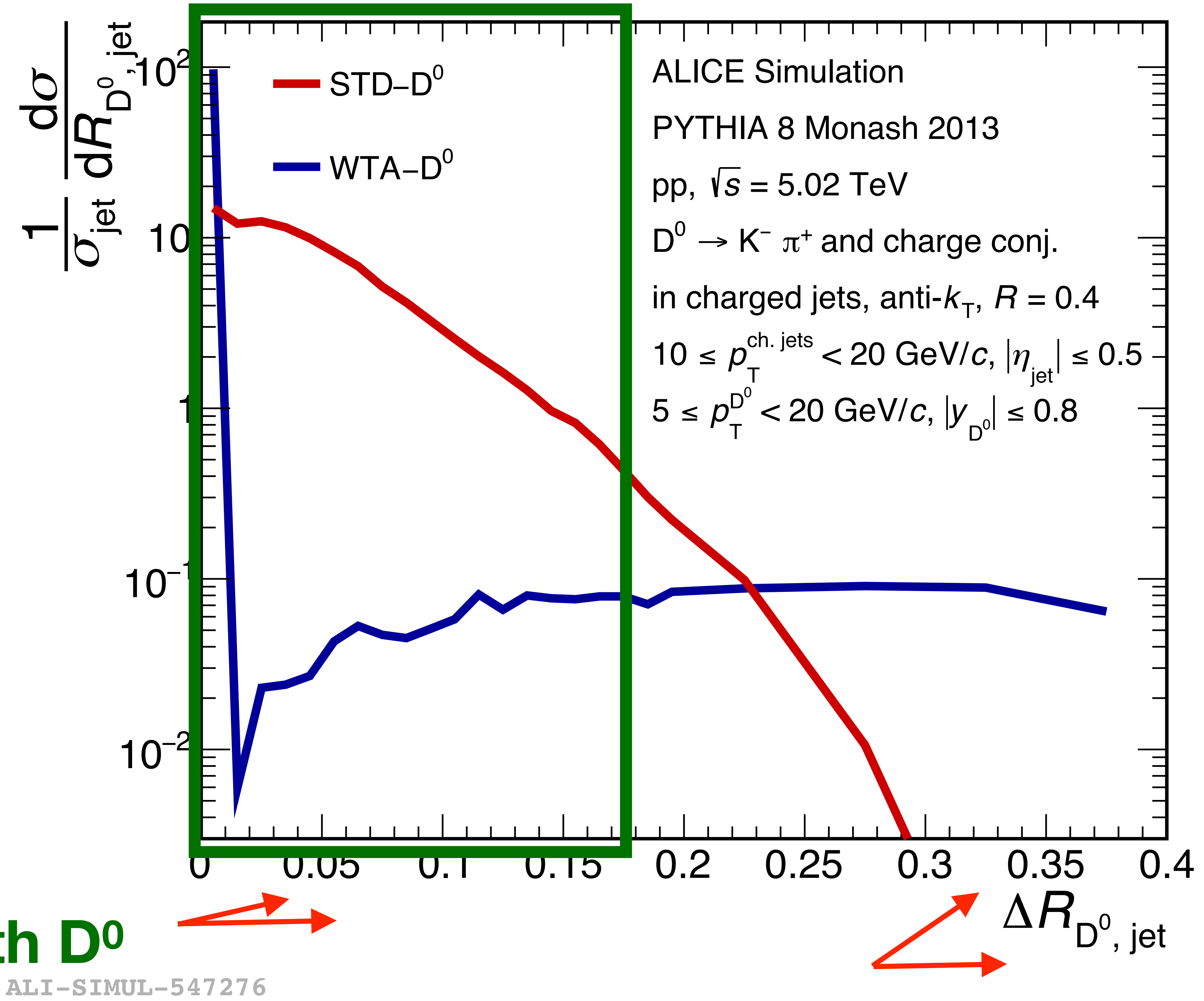

Winner-Take-all jet (WTA) is more strongly aligned with D⁰

Jet axes distribution

- $\Delta R_{\mathrm{D^0},\mathrm{jet}}$ vs $\Delta R_{\Lambda_c^+,\mathrm{jet}}$ to access possible modifications of the hadronization.

Jet axes distribution

- $\Delta R_{\mathrm{D}^0,\mathrm{jet}}$ vs $\Delta R_{\Lambda_c^+,\mathrm{jet}}$ to access possible modifications of the hadronization.

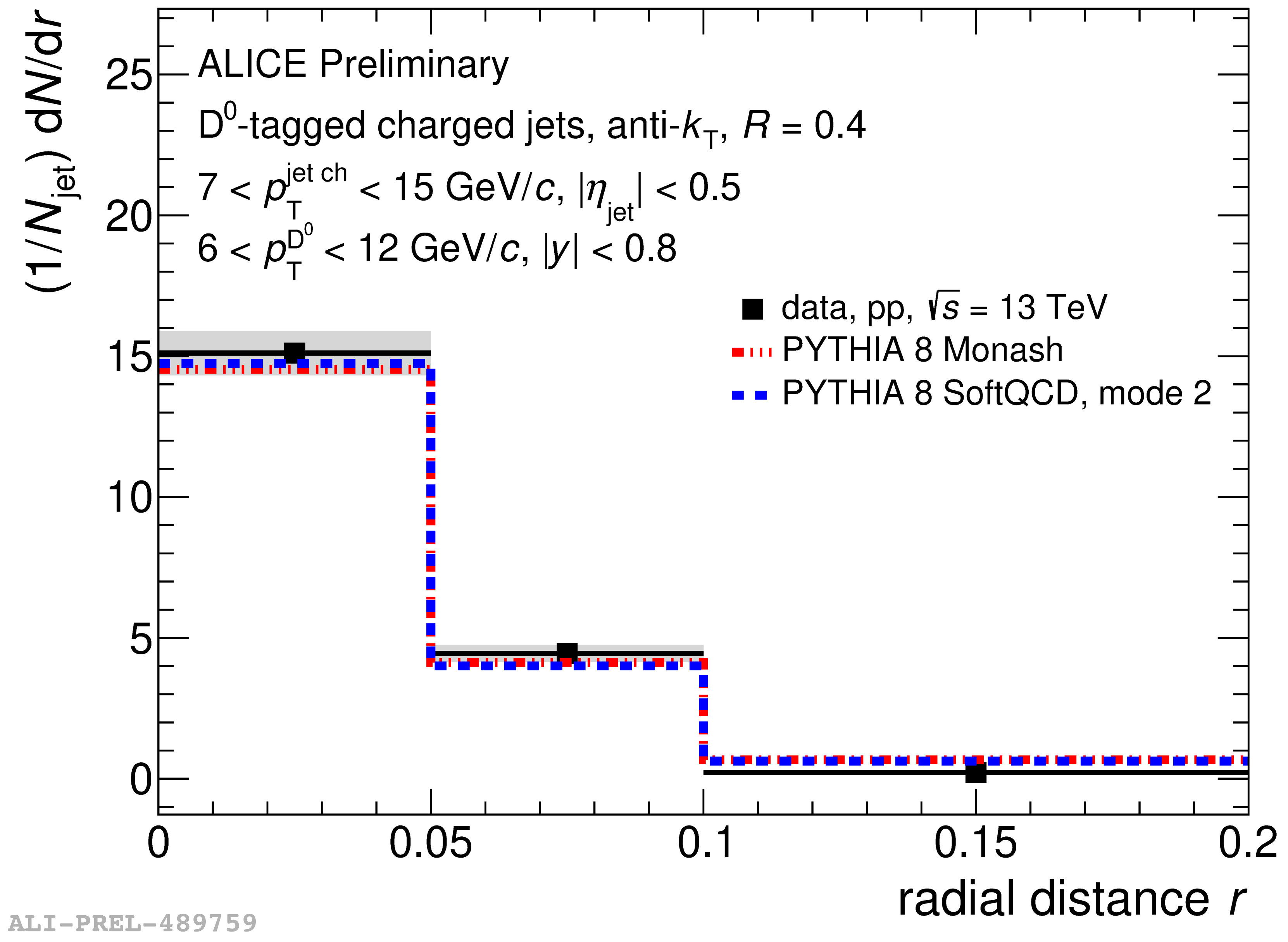

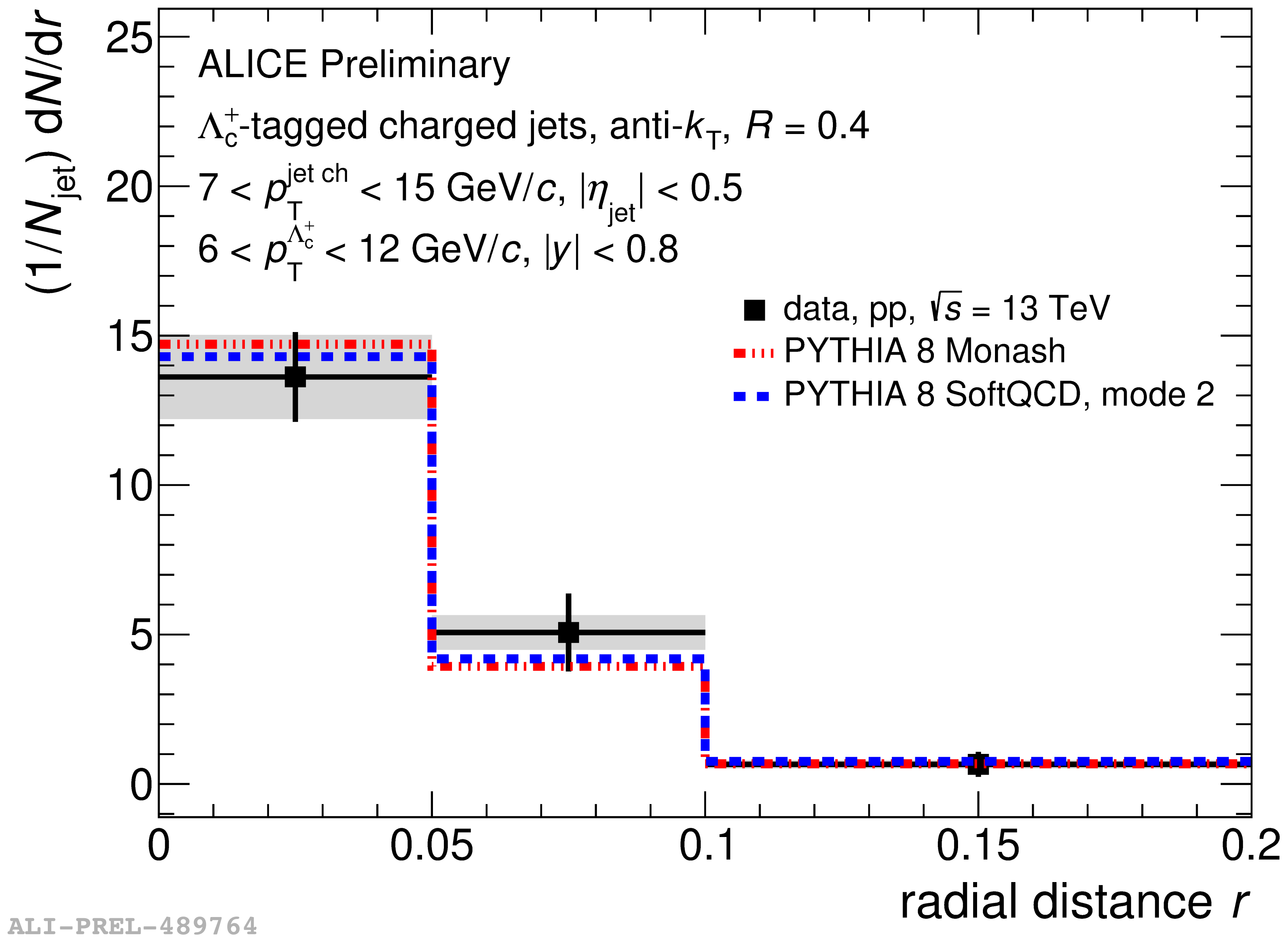

Jet axes distribution

- $\Delta R_{\mathrm{D^0,jet}}$ vs $\Delta R_{\Lambda_c^+,\mathrm{jet}}$ to access possible modifications of the hadronization.

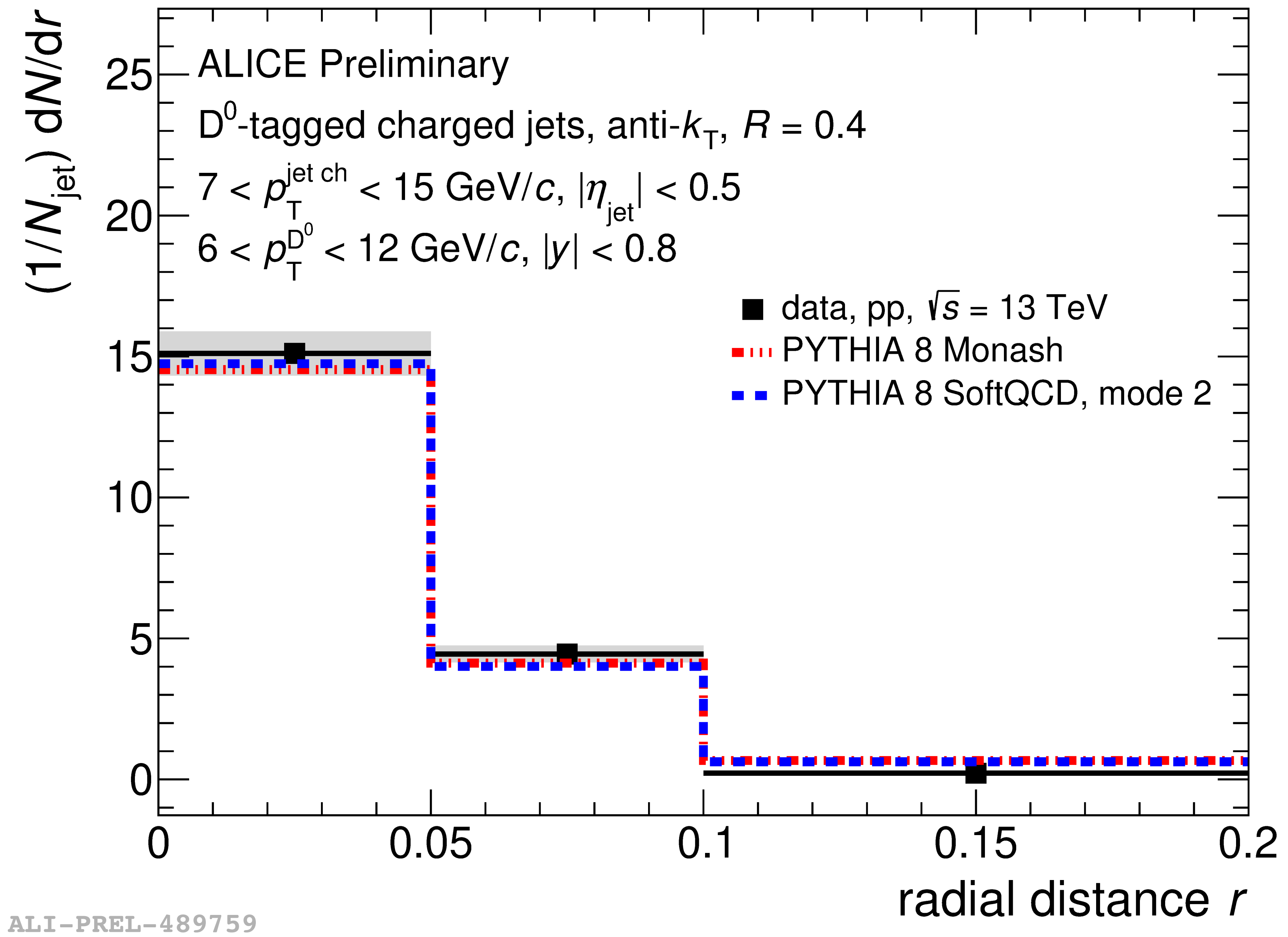

ALI-PREL-489759

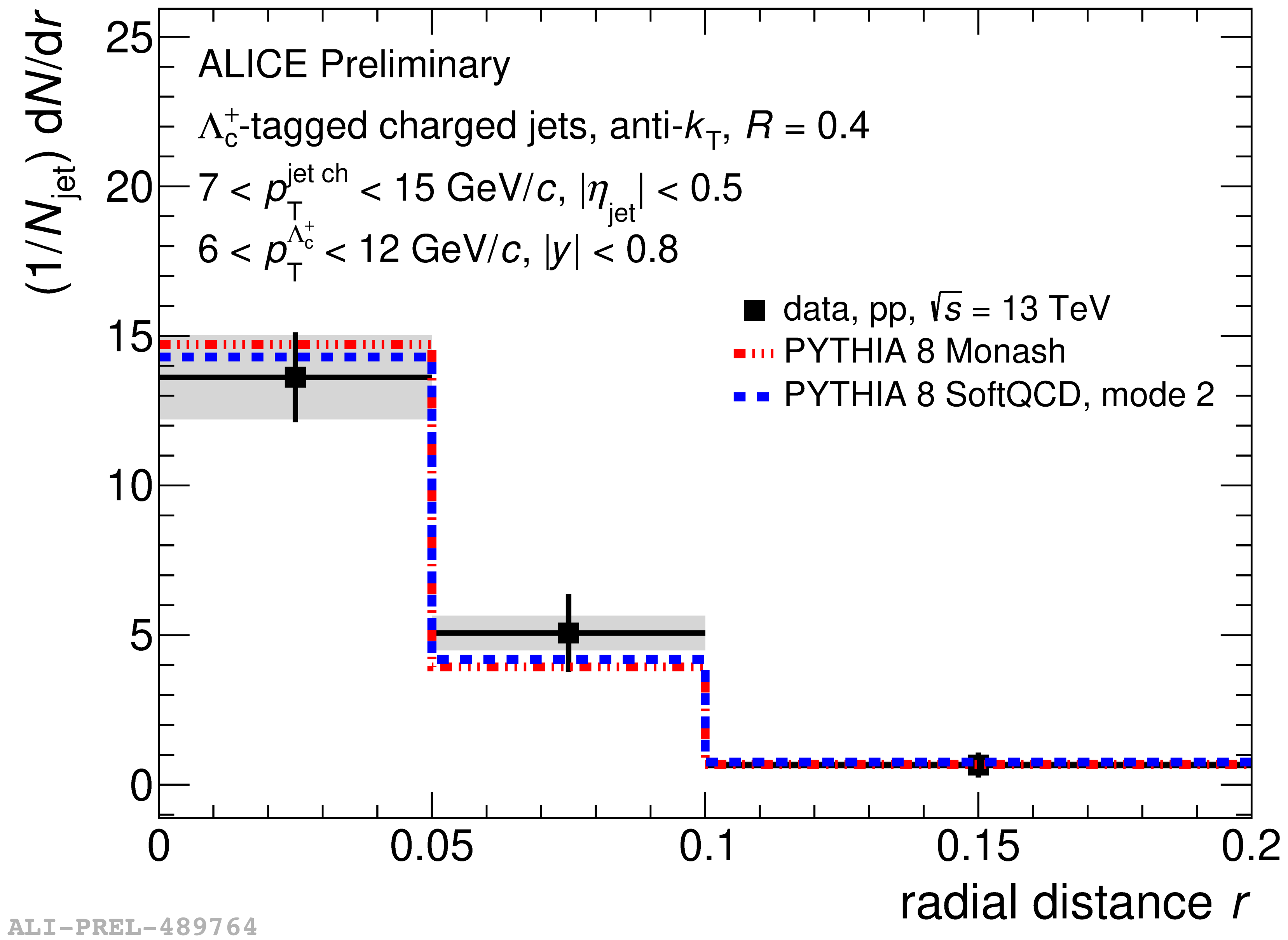

ALI-PREL-489764

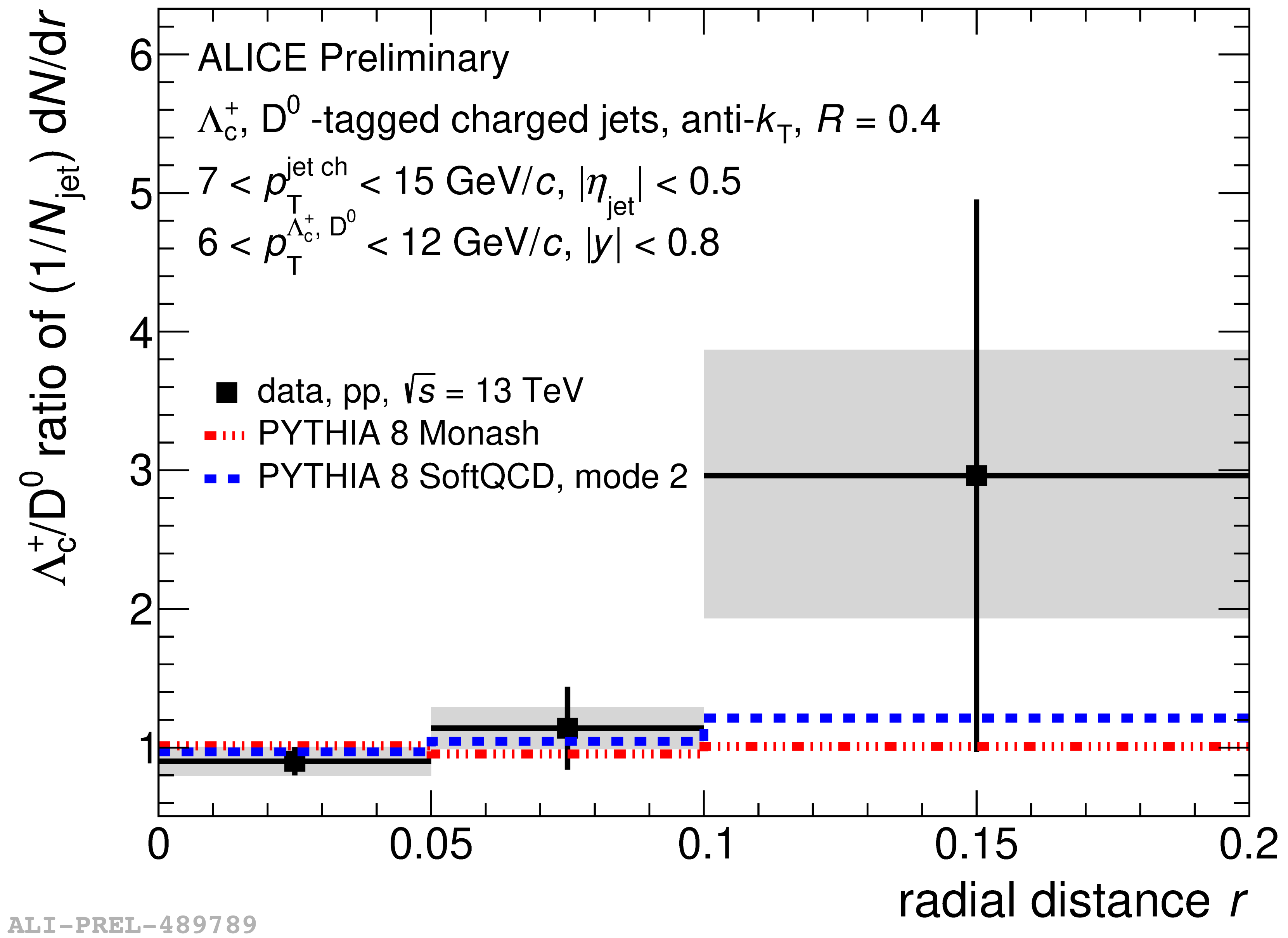

ALI-PREL-489789

Baryons produced **less collimated** than **mesons** w.r.t. the direction of the jet?

Jet axes distribution

- $\Delta R_{D^0,\text{jet}}$ vs $\Delta R_{\Lambda_c^+,\text{jet}}$ to access possible modifications of the hadronization.

Baryons produced **less collimated** than **mesons** w.r.t. the direction of the jet?
Would be Interesting to look at with the Run 3 data!

Summary

- Jets are **excellent** probes for QCD at all energy scales.
- Comparing charm-tagged jets with inclusive jets elucidates the flavor dependence of QCD showers.

Many open question still need to be addressed with Run 3 data.

- Push experimental tests of pQCD with higher precision charm-jet studies.
- Extend the studies to beauty-tagged jets and to higher jet p_{T}
- Systematically probe non-perturbative effects such as hadronization
- Extension of program to heavy-ion collisions to characterize in-medium interactions in the quark-gluon plasma formed in heavy-ion collisions and distinguish the QGP behavior from the in-vacuum QCD dynamics

Backup slides